



# Laser Desorption Ionisation of Forensically Significant Samples

An investigation into low mass analysis

By

**Rachel West**

*Thesis  
Submitted to Flinders University  
for the degree of*

**PhD**

College of Science and Engineering  
July 2021

---

## Declaration

I, Rachel Sarah West, certify that this thesis does not incorporate without acknowledgment any material previously submitted for a degree or diploma in any university; and that to the best of my knowledge and belief it does not contain any material previously published or written by another person except where due reference is made in the text.'

A handwritten signature in black ink, appearing to read 'Rachel Sarah West', written in a cursive style.

On 08/05/2019.

## Acknowledgements

The number of people I could acknowledge for just putting up with me while I was completing this thesis is endless. So, I'm going to try to narrow it down to the most important. Starting academically, and with the man without whom nothing would have ever been completed; Stewart Walker, my primary supervisor and elusive ninja. You have been through my impatience with the instrument, my confusion at many things, inability to decipher spectra and general questions as to where to go next. You met each issue with a sensible suggestion from your huge bank of knowledge, each question with an answer and punny side note, and each 2am email with a 3am reply. My co-supervisors, Paul Kirkbride and Mark Fitzgerald, thank you for many a timely insight and calm well thought out advice. The Walker research group, past and present, for your ideas and support and many a conversation spontaneously gathered in the lab or office. Especially Russell, with whom there were very many conversations about all parts of life. Especially for covering demonstrating shifts when needed. The Flinders Analytical Staff, primarily Jason Young, for being my MALDI sensei and teaching me everything I know, checking up on me every time I came in and giving me your thoughts and helping me with all your experience. Not so much for scaring me by accidentally sneaking up on me every half hour or so. Thank you for talking football, cricket and life experiences with me.

My Flinders family and co-conspirators, Karen Bruce, Caitlyn Rogers and Leigh Thredgold, one of you was always there to get me through. You guys were my inspiration to come in; you distracted me from my insanity, were always up for a timely cup of tea and a giggle and were the best thing to have come out of this PhD. Daniel Mangos, thank you for introducing me kindly to the world of nanoparticles, for your genuinely lovely presence and your hilarious inappropriateness. Our postgraduate suffering has bonded us forever and I am so grateful for what is sure to be a life-long friendship. To the people of the CAPS tea-room, for providing an escape from the office with ridiculous conversation and a different cast daily. Specifically, Jacqui Hull, without whom I'd still be locked out of my office and would never have made it past the first day, thank you for being my (and everyone else's) Uni mum!

The most emotionally fuelled thank yous are for the most important people in my life, my family. I dedicate this thesis to you, but especially to my mum. You were the strongest person that I have ever met, and you were my every day inspiration to keep going. You were my confidant, the person who grounded me and kept me calm and I miss you every day. I don't know how I made it over the massive hill of my thesis without you in my life. You have left a hole in my life that can never be filled but have also taught me to be the woman that I am today. I know you would have never made it past this page, but that you would have tried. I know you would have been so incredibly proud of

me, memorizing the title to brag to all your friends. I only regret that I didn't finish this in time to give you the opportunity to do this.

Dad your fortitude during the tough times encouraged me to mirror you and keep going about my days as normally as possible. Thank you for being my personal valet, chef, pastry consultant, tailor, hairdresser, advice giver and most wonderful, caring father ever to exist. Your strength and kindness inspire me every day. Thank you for putting up with my disorganisation, poor housework contributions and unexplained, inexplicable crying.

Kate: my sibling, my role model, my entertainer and my best friend. You've looked after and protected me to the best of your ability for the last 30 years. You've been my voice when I'm scared, my strength when I was weak and the second half to every quote I begin. Thank you for always being there for me, whatever I need. I promise this will be the last graduation you ever have to sit through.

To Cele Richardson, my sister from another mister and the best friend a girl could ever ask for. Thank you for being my outlet, for helping me escape my work, whether it was just for dinner, or sneakily to Europe, you helped maintain my normalcy and always make me smile.

This has been one of the hardest things I will ever have to do. It gave me all kinds of anxiety and some days I thought it would get the better of me, the people acknowledged here are the reason it didn't.

This thesis is brought to you by English Breakfast tea.

## Contents

Acknowledgements.....	ii
Contents .....	<b>iv</b>
List of Figures .....	vi
List of Tables .....	ix
List of abbreviations.....	xi
List of chemicals.....	xiii
<b>Conference Presentations .....</b>	<b>xiv</b>
<b>Summary .....</b>	<b>xv</b>
<b>Preface .....</b>	<b>1</b>
<b>Part One .....</b>	<b>2</b>
<b>1Introduction.....</b>	<b>2</b>
1.1 Laser Desorption Ionization Mass Spectrometry (LDI-MS).....	2
1.2 Matrix Assisted Laser Desorption Ionization (MALDI) .....	5
1.3 The History of LDI.....	6
1.4 Variations of LDI.....	8
1.5 Drug samples.....	20
<b>2Experimental .....</b>	<b>27</b>
2.1 Instrument settings.....	27
2.2 Sample Preparation .....	29
2.3 Alternative Matrices .....	31
2.4 Nanoparticles.....	32
<b>3Results and Discussion .....</b>	<b>36</b>
3.1 Alternative Matrices .....	36
3.2 Nanoparticles.....	50
<b>4Conclusions.....</b>	<b>66</b>
<b>Part Two – Propellant based Samples .....</b>	<b>69</b>
<b>5Introduction.....</b>	<b>69</b>
5.1 Propellants .....	69
5.2 Analysis .....	72
<b>6Experimental .....</b>	<b>77</b>
6.1 Samples.....	77
6.2 Solutions.....	83

6.3	High Pressure Liquid Chromatography .....	85
6.4	Gas Chromatography Mass Spectrometry.....	86
6.5	Mid-Far IR at the Australian Synchrotron .....	86
6.6	LDI Analysis .....	87
<b>7</b>	<b>Results and Discussion .....</b>	<b>89</b>
7.1	HPLC of FSSA propellant samples .....	89
7.2	GCMS of select propellant samples .....	91
7.3	Mid to Far IR of select propellant samples .....	93
7.4	LDI of all propellant samples.....	106
<b>8</b>	<b>Conclusions.....</b>	<b>120</b>
	<b>Overall Conclusions and Future Work .....</b>	<b>122</b>
	<b>Bibliography .....</b>	<b>125</b>

## List of Figures

Figure 1.1: Diagram of Desorption and Ionization process in MALDI <sup>[5]</sup> .....	2
Figure 1.2: Diagram of the basic design of Time of flight mass spectrometry <sup>[9]</sup> .....	4
<b>Figure 1.3: Schematic diagram of reflectron mode in ToF-MS <sup>[9]</sup> .....</b>	<b>5</b>
Figure 1.4: Molecular structure of CHCA .....	vi
<b>Figure 1.5: Molecular structure of DHB .....</b>	<b>vi</b>
Figure 1.6: Structure of 3-hydroxycoumarin.....	14
Figure 1.7: Structure of 6-aza-2-thiothymine .....	14
Figure 1.8: Molecular structure of 4-mercaptobenzoic acid .....	19
Figure 1.9: Molecular structure of thiosalicylic acid.....	19
Figure 1.10: Molecular structure of 3-mercaptobenzoic acid .....	19
Figure 1.11: Molecular structure of phenylethyl mercaptan.....	20
Figure 1.12: Molecular Structure of Morphine <sup>[142]</sup> .....	24
Figure 1.13: Molecular Structure of Codeine <sup>[142]</sup> .....	24
Figure 1.14: Molecular Structure of Heroin <sup>[142]</sup> .....	24
Figure 1.15: Molecular structure of 6-monoacetyl morphine <sup>[142]</sup> .....	24
Figure 1.16: Molecular structure of amphetamine .....	25
Figure 1.17: Molecular structure of methamphetamine .....	26
Figure 2.1: Spectrum of CsI calibrant from the MALDI plate .....	29
Figure 3.1: Spectrum of codeine from MALDI plate .....	36
Figure 3.2: Spectrum of codeine from carbon tape.....	38
Figure 3.3: Spectrum of carbon tape .....	38
Figure 3.4: Spectrum of codeine on copper tape .....	39
Figure 3.5: Spectrum of codeine fibres from copper tape.....	39
Figure 3.6: Spectrum of codeine fibres from double-sided tape.....	40
Figure 3.7: Spectrum of morphine fibres from copper tape.....	41
Figure 3.8: Spectrum of codeine with graphite from hole punch.....	42
Figure 3.9: Spectrum of 3-HC from MALDI plate .....	43
Figure 3.10: Spectrum of 6-ATT from MALDI plate.....	44
Figure 3.11: Spectrum of binary matrix from MALDI plate .....	44
Figure 3.12: Spectrum of 2:3 codeine: binary matrix from MALDI plate.....	45
Figure 3.13: Spectrum of 1:2 codeine: binary matrix from MALDI plate.....	46
Figure 3.14: Spectrum of 1:3 codeine: binary matrix from MALDI plate.....	46
Figure 3.15: Spectrum of 1:5 codeine: binary matrix from MALDI plate.....	47
Figure 3.16: Spectrum of 8:1 codeine: binary matrix from MALDI plate.....	47
Figure 3.17: Spectrum of 10:1 codeine: binary matrix from MALDI plate.....	48
Figure 3.18: Spectrum of 15:1 codeine: binary matrix from MALDI plate.....	48
Figure 3.19: Spectrum of 1:2 morphine: binary matrix from MALDI plate.....	49
Figure 3.20: SEM image of silicon nanoparticles distributed on filter paper fibres .....	50
Figure 3.21: Spectrum of mixed codeine SiNPs in ethanol .....	51
Figure 3.22: Spectrum of SiNPs in acetone on codeine .....	51
Figure 3.23: Spectrum of SiNPs in ethyl acetate on codeine .....	52
Figure 3.24: Spectrum of SiNPs in ethanol on codeine.....	52
Figure 3.25: Spectrum of SiNPs in water on codeine.....	52
Figure 3.26: Spectrum of codeine on SiNPs in ethanol.....	52

Figure 3.27: Spectrum of codeine with < 1 mg/mL SiNPs from plate.....	53
Figure 3.28: Spectrum of codeine and 1.5 mg/mL of SiNPs from plate.....	53
Figure 3.29: Spectrum of codeine and 4.75 mg/mL SiNPs from plate.....	53
Figure 3.30: Spectrum of Bare AuNPs.....	54
Figure 3.31: Spectrum of codeine with AuNPs diluted 1:4.....	56
Figure 3.32: Spectrum of codeine with AuNPs diluted 1:2.....	56
Figure 3.33: Spectrum of codeine with undiluted.....	56
Figure 3.34: Spectrum of codeine with undiluted AuNPs at 30% laser.....	56
Figure 3.35: Spectrum of sample indicating presence of methamphetamine with bare AuNPs from plate.....	57
Figure 3.36: Spectrum of TSA AuNPs from plate.....	58
Figure 3.37: Spectrum of codeine with TSA AuNPs from plate.....	58
Figure 3.38: Spectrum of 4-MBA AuNPs from plate.....	59
Figure 3.39: Spectrum of codeine with 4-MBA from plate.....	59
Figure 3.40: Spectrum of TSA AuNPs from fibre on copper tape.....	60
Figure 3.41: Spectrum of codeine with TSA AuNPs from fibres on copper tape.....	60
Figure 3.42: Spectrum of 4-MBA AuNPs on fibre from copper tape.....	61
Figure 3.43: Spectrum of codeine with 4-MBA AuNPs on fibre from copper tape.....	62
Figure 3.44: Older sample of 4-mercaptobenzoic acid gold nanoclusters on plate.....	62
Figure 3.45: Fresh sample of 4-mercaptobenzoic acid gold nanoclusters on plate.....	62
Figure 3.46: Spectrum of phenylethyl mercaptan gold nanoclusters from the plate.....	63
Figure 3.47: Spectrum of codeine with phenylethyl mercaptan gold nanoclusters from plate.....	64
Figure 3.48: Spectrum of codeine with 4-mercaptobenzoic acid attached gold nanoclusters from plate.....	64
Figure 6.1: Structure of Nitrocellulose.....	70
Figure 6.2: Structure of Nitroglycerin.....	70
Figure 6.3: Structure of Nitroguanidine.....	70
Figure 6.4: World war II era propellants provided by Victoria police.....	81
Figure 6.5: Winchester 760 ball powder propellants provided by Victoria Police.....	82
Figure 6.6: Hercules propellants provided by Victoria Police.....	83
Figure 8.1: Gas Chromatogram of FSSA Sample 2.....	91
Figure 8.2: Gas Chromatogram of FSSA Sample 4.....	92
Figure 8.3: Gas Chromatogram of FSSA Sample 6.....	93
Figure 8.4: Mid-far IR spectrum of 18 FSSA propellant samples.....	94
Figure 8.5: IR spectrum of 18 FSSA samples: 875-870 cm <sup>-1</sup> .....	95
Figure 8.6: IR spectrum of FSSA samples 2, 7, 8, 9, 12, 13 and 18.....	96
Figure 8.7: IR spectrum of FSSA samples 2, 7, 8, 9, 12, 13 and 18: 900-650 cm <sup>-1</sup> .....	96
Figure 8.8: IR spectrum of FSSA samples 2, 7, 8, 9, 12, 13 and 18: 700-400 cm <sup>-1</sup> .....	97
Figure 8.9: IR spectrum of FSSA samples 2 and 7.....	97
Figure 8.10: IR spectrum of FSSA samples 3, 4, 6, 17 and 19.....	98
Figure 8.11: IR spectrum of FSSA samples 3, 4, 6, 17 and 19: 860-760 cm <sup>-1</sup> .....	98
Figure 8.12: IR spectrum of FSSA samples 3, 4, 6, 17 and 19: 700-600 cm <sup>-1</sup> .....	99
Figure 8.13: IR spectrum of FSSA samples 1, 10, 11 and 16.....	99
Figure 8.14: IR spectrum of FSSA samples 1, 10, 11 and 16: 860-760 cm <sup>-1</sup> .....	100
Figure 8.15: IR spectrum of Victoria Police samples 91, 100, 103, 119, 126 and 146.....	101



Figure 8.16: IR spectrum of Victoria Police samples 91, 100, 103, 119, 126 and 146: 1000-750 cm <sup>-1</sup> .....	101
Figure 8.17: IR spectrum of Victoria Police samples 91, 100, 103, 119, 126 and 146: 780-450 cm <sup>-1</sup> .....	102
Figure 8.18: IR spectrum of Victoria Police samples 91, 100, 103, 119, 126 and 146: 460-50 cm <sup>-1</sup> ...	102
Figure 8.19: IR spectrum of Victoria Police samples 253, 256, 274, 279 and 285 .....	103
Figure 8.20: IR spectrum of Victoria Police samples 253, 256, 274, 279 and 285: 1000-780 cm <sup>-1</sup> .....	103
Figure 8.21: IR spectrum of Victoria Police samples 253, 256, 274, 279 and 285 780-400 cm <sup>-1</sup> .....	104
Figure 8.22: IR spectrum of Victoria Police samples 253, 256, 274, 279 and 285 500-50 cm <sup>-1</sup> .....	104
Figure 8.23: IR spectrum of Victoria Police samples 303, 304 and 305 .....	105
Figure 8.24: IR spectrum of Victoria Police samples 303, 304 and 305: 960-780 cm <sup>-1</sup> .....	105
Figure 8.25: IR spectrum of Victoria Police samples 303, 304 and 305: 800-550 cm <sup>-1</sup> .....	105
Figure 8.26: IR spectrum of Victoria Police samples 303, 304 and 305: 600-300 cm <sup>-1</sup> .....	106
Figure 8.27: IR spectrum of Victoria Police samples 303, 304 and 305: 500-50 cm <sup>-1</sup> .....	106
Figure 8.28: LDI spectrum of Victoria Police sample 119 .....	115
Figure 7.29: LDI spectrum of Victoria Police sample 146 .....	116
Figure 8.30: LDI spectrum of Victoria Police sample 253 .....	117
Figure 8.31: LDI spectrum of Victoria Police sample 256 .....	117
Figure 8.32: LDI spectrum of Victoria Police sample 274 .....	117
Figure 8.33: LDI spectrum of Victoria Police sample 279 .....	117
Figure 8.34: LDI spectrum of Victoria Police sample 285 .....	117
Figure 8.35: LDI spectrum of Victoria Police sample 303 solid .....	119
Figure 8.36: LDI spectrum of Victoria Police sample 304 .....	119
Figure 8.37: LDI spectrum of Victoria Police sample 305 .....	119

## List of Tables

Table 2.1: MALDI spectrometer settings .....	27
Table 2.2: MALDI detection settings.....	27
Table 2.3: MALDI setup settings .....	28
Table 2.4: Csl calibrant positive peaks .....	29
Table 2.5: Concentrations and molar masses of drug solutions.....	30
Table 3.1: Conductivities of a variety of double-sided tapes.....	37
Table 3.2: Calibration peaks for gold .....	54
Table 5.1: Common propellant additives and their properties .....	70
Table 6.1: Propellants sourced from FSSA.....	77
Table 6.2: Propellants provided by the DST group .....	79
Table 6.3: World War II era propellants provided by Victoria Police .....	80
Table 6.4: Winchester 760 ball powder propellants provided by Victoria Police.....	81
Table 6.5: Hercules propellants provided by Victoria Police .....	82
Table 6.6: Solvation of FSSA propellant samples.....	83
Table 6.7: Solvation of DST group propellant samples .....	84
Table 6.8: Solvation of Victoria Police propellant samples.....	84
Table 6.9: Standard preparation for LDI analysis.....	84
Table 6.10: Standard preparation for HPLC.....	85
Table 6.11: HPLC conditions.....	85
Table 6.12: Solvent composition.....	86
Table 6.13: Csl calibrant negative peaks.....	87
Table 7.1: Retention times (RT) of standards .....	89
Table 7.2: HPLC analysis of FSSA propellants, and the identification of standards.....	90
Table 7.3: List of possible propellant components for FSSA Sample 2 .....	92
Table 7.4: List of possible propellant components for FSSA Sample 4 .....	92
Table 7.5: List of possible propellant components for FSSA Sample 6 .....	93
Table 7.6: Peaks (m/z) from samples solvation in methanol - liquids .....	108
Table 7.7: Table of significant and minimal peaks (m/z) from solvation in methanol - solids .....	109
Table 7.8: Major LDI peaks (m/z) for DPA.....	110
Table 7.9: Major LDI peaks (m/z) for 2n-DPA .....	110
Table 7.10: Major LDI peaks (m/z) for 4n-DPA .....	111
Table 7.11: Major LDI peaks (m/z) for Nn-DPA.....	111
Table 7.12: Major LDI peaks (m/z) for Akardite II.....	111
Table 7.13: Major LDI peaks (m/z) for 2,4 DNT.....	111
Table 7.14: Major LDI peaks (m/z) for 2,6 DNT.....	112
Table 7.15: Major MALDI peaks (m/z) for MC .....	112
Table 7.16: Major LDI peaks (m/z) for EC .....	112
Table 7.17: Major LDI peaks (m/z) for DBP.....	112
Table 7.18: Major LDI peaks (m/z) for NC.....	113
Table 7.19: Major LDI peaks (m/z) of NG.....	113
Table 7.20: Major LDI peaks for DST Group propellants .....	113
Table 7.21: Major LDI peaks of Victoria Police sample 119.....	115
Table 7.22: Major LDI peaks of Victoria Police sample 146.....	116

Table 7.23: Peak summary of LDI samples Winchester 760 ball propellant..... 118  
Table 7.24: Peak summary of LDI samples Hercules..... 119

## List of abbreviations

<b>Abbreviation</b>	<b>Definition</b>
<b>2,4-DNT</b>	2,4-Dinitrotoluene
<b>2,6-DNT</b>	2,6-Dinitrotoluene
<b>2n-DPA</b>	2-Nitro-Diphenylamine
<b>3-HC</b>	3-hydroxycoumarin
<b>4-MBA</b>	4-mercaptobenzoic acid
<b>4n-DPA</b>	4-Nitro-Diphenylamine
<b>5-MSA</b>	5-methoxysalicylic acid
<b>6-ATT</b>	6-aza-2-thiothymine
<b>6-MAM</b>	6-monoacetyl morphine
<b>9-AA</b>	9-aminoacridine
<b>AAS</b>	Atomic Absorption Spectroscopy
<b>ADHD</b>	Attention deficit hyperactivity disorder
<b>AK II</b>	Akardite II
<b>AP-MALDI</b>	Atmospheric Pressure Matrix Assisted Laser Desorption Ionization
<b>ATR</b>	Attenuated Total Reflectance
<b>AuNPs</b>	Gold Nanoparticles
<b>CDR</b>	Cartridge discharge residue
<b>CE</b>	Capillary Electrophoresis
<b>CHCA</b>	$\alpha$ -cyano-4-hydroxycinnamic acid
<b>CMBT</b>	5-chloro-2-mercaptobenzothiazole
<b>CsI</b>	Caesium Iodide
<b>DART</b>	Direct Analysis in Real Time
<b>DBP</b>	Dibutyl phthalate
<b>DESI</b>	Desorption Electrospray Ionization
<b>DHB</b>	2,5-dihydroxybenzoic acid
<b>DIOS</b>	Desorption Ionization on Silicon
<b>DPA</b>	Diphenylamine
<b>DST</b>	Defence Science and Technology
<b>EC</b>	Ethyl centralite
<b>EDX</b>	Energy Dispersive X-ray spectroscopy
<b>ESI</b>	Electrospray Ionization
<b>FAB</b>	Fast Atom Bombardment
<b>FD</b>	Field Desorption
<b>FSSA</b>	Forensic Science South Australia
<b>GC</b>	Gas Chromatography
<b>GCMS</b>	Gas Chromatography Mass Spectrometry
<b>GSR</b>	Gunshot residue
<b>HAuCl<sub>4</sub></b>	Chloro-auric acid
<b>HPLC</b>	High Pressure Liquid Chromatography
<b>ICP</b>	Inductively Coupled Plasma
<b>IMS</b>	Ion Mobility Spectrometry
<b>IR</b>	Infrared

<b>LAMMA</b>	Laser Microprobe Mass Analysis
<b>LCMS</b>	Liquid Chromatography Mass Spectrometry
<b>LDI</b>	Laser Desorption Ionization
<b>LEMS</b>	Laser Electrospray Mass Spectrometry
<b>m/z</b>	mass to charge ratio (unit)
<b>MALDI</b>	Matrix Assisted Laser Desorption Ionization
<b>MC</b>	Methyl centralite
<b>MDMA</b>	Methylenedioxyamphetamine
<b>MS</b>	Mass Spectrometry
<b>NAA</b>	Neutron Activation Analysis
<b>NaBH<sub>4</sub></b>	Sodium borohydride
<b>nanoPALDI</b>	Nanoparticle Assisted Laser Desorption Ionization
<b>NaOH</b>	Sodium hydroxide
<b>NC</b>	Nitrocellulose
<b>NG</b>	Nitroglycerin
<b>NH<sub>4</sub></b>	Ammonium
<b>Nn-DPA</b>	N-nitroso-Diphenylamine
<b>NPs</b>	Nanoparticles
<b>OF</b>	Oral Fluid
<b>ROSITA</b>	Roadside testing assessment
<b>SALDI</b>	Surface Assisted Laser Desorption Ionization
<b>SEM</b>	Scanning Electron Microscopy
<b>SIMS</b>	Secondary Ion Mass Spectrometry
<b>SiNPs</b>	Silicon Nanoparticles
<b>SNPs</b>	Single Nucleotide Polymorphisms
<b>TDS</b>	Time Domain Spectroscopy
<b>THC</b>	Δ-9-tetrahydrocannabinol
<b>ToF</b>	Time of Flight
<b>TSA</b>	Thiosalicylic acid
<b>WW1/WW2</b>	World War 1/ World War 2

## List of chemicals

Chemical	Grade	Purity	Supplier
2,4-DNT	Analytical	97%	Ajax
AK II	Analytical	99%	Sigma Aldrich
DBP	Analytical	>99%	Sigma Aldrich
DPA	Analytical	>99%	Sigma Aldrich
EC	Analytical	99%	Sigma Aldrich
MC	Analytical	99%	Sigma Aldrich
Nn-DPA	Reagent	>97%	Sigma Aldrich
2,6-DNT	Analytical	97%	Ajax
Caesium Iodide	Analytical	99.9%	Sigma Aldrich
Phenylethyl Mercaptan	Food Grade	≥99%	Sigma Aldrich
3-Hydroxycoumarin			Sigma-Aldrich
4-mercaptobenzoic acid	>95%		Chem Supply
6-Aza-2-thiothymine	HPLC	>99%	Fluka
Acetonitrile	HPLC	>99.9%	Chem Supply
Chloroform	Analytical Reagent	99.8%	Chem Supply
Ethanol	Analytical Reagent	99.5%	Chem Supply
HAuCl <sub>4</sub>	ACS grade	>49%	Thermo Fisher
Methanol	HPLC	99.99%	Chem Supply
NaBH <sub>4</sub>	Reagent	>98%	Thermo Fisher
NaOH	Analytical	>98%	Chem Supply
Thiosalicylic acid		>90%	Chem Supply
Trifluoroacetic acid	Reagent	>99%	Sigma Aldrich
2n-DPA	Reagent	>98%	Merck
4n-DPA	Analytical	99%	Sigma Aldrich

# Conference Presentations

The research discussed in this thesis has been presented at a variety of conferences, in both poster and oral formats. See a summary of these below.

Poster: -RACI R&D Topics 2011, 2012,2013,2015

Oral: -RACI R&D Topics 2014

-Australian Energetic Materials Symposium 2012, 2014

Australia and New Zealand Forensic Science Symposium 2014

Pittcon 2015

# Summary

Forensically significant samples, such as drugs and propellants can be analysed using a range of standard techniques like High Performance Liquid Chromatography (HPLC) and Gas Chromatography Mass Spectrometry (GCMS). These methods can often be time-consuming, require complex sample preparation or extraction, with multiple steps and additional components. The drug samples investigated are those that have been inlaid in fibres, in this form to either mimic oral fluid based roadside drug tests or drug laden clothing and other fabrics used in smuggling cases. The analysis of these samples is important and can be complicated by the need for extraction of the analytes from the fibres and the possible destruction of evidence required to perform said analysis.

Laser Desorption Ionization (LDI) techniques are an intriguing alternative to these standard techniques as they can perform high throughput analysis with little sample preparation and often generate simple spectra. LDI is highly sensitive and specific and is compatible with less stable sample-types.

The initial issue for LDI analysis of drug samples was associated with low mass interference experienced when such low mass analytes encounter similar mass matrices. Several alternatives to traditional matrices were explored, and it was successfully overcome for on-plate and fibre-based analyses using a layer of gold nanomaterials which provided increased laser absorption without the low mass interference.

LDI was also explored as a method of analysing complex propellant samples. Propellants contain several different species, which vary among manufacturers and as samples age. They often require multiple techniques for their analysis with different sample preparation techniques. LDI was compared to standard techniques as well as some more interesting alternatives, to successfully differentiate several diverse propellant samples.



# Preface

Matrix Assisted Laser Desorption Ionization is a well-established and frequently used analytical technique. Used for analysis of samples ranging from biologicals to polymers, MALDI is a proposed option for forensic purposes to quality control, for high throughput analyses and for confirmation of results.

In this thesis the use of the laser desorption ionization is removed from the traditional matrix assisting format which analyses the standard larger molar mass samples. Instead the focus is on lower mass forensic samples, primarily oral fluid-based drug tests and firearm propellants. The first part will cover an introduction to laser desorption ionization and its application to the analysis of selected drugs, prepared as mentioned above. The different types of alternative matrices discussed in the introduction are applied and discussed for the application to low mass drug samples analysed from single fibres.

The second part of the thesis covers the analysis and differentiation of propellants via a range of different techniques but focussing on Laser Desorption Ionization in the low mass range. The introduction contains information regarding propellants, and other analysis techniques, information regarding LDI discussed in the introduction and experimental chapters of part one will still be relevant. Part two discusses the advantages of LDI for propellant analysis, as well as its shortcomings.

# Part One

## 1 Introduction

### **1.1 Laser Desorption Ionization Mass Spectrometry (LDI-MS)**

Laser Desorption Ionization (LDI) is a primarily qualitative analytical technique based on ionization by a laser and detection by mass spectrometry (MS) <sup>[1]</sup>. Unlike many other MS based techniques, LDI samples undergo analysis via soft ionization. In soft ionization samples are ionized with little fragmentation due to the energy of ionization being lower than the energy of dissociation and the molecular ion is maintained as a prominent product <sup>[2]</sup>. This decreased fragmentation results in a lower number of peaks per spectrum, which is particularly relevant for high mass or multiple component samples, as fragmentation of such samples greatly increases the complexity of the spectrum. Samples are dissolved and pipetted onto a steel target plate, and allowed to dry down before entering the high vacuum environment of the instrument <sup>[3]</sup>. A pulsed UV laser is fired at the sample, forcing molecules to be desorbed from the surface and ionized via a complex mechanism that is affected by various parameters <sup>[1]</sup>. Desorption and ionization, occur on a minute scale in terms of time and size and while desorption and ionization are separate processes, they are intrinsically connected, occur simultaneously and interdependent <sup>[4]</sup>.

This image has been removed due to copyright restriction. Available online from Laboratory, N.H.M.F. National High Magnetic Field Laboratory: Matrix Assisted Laser Desorption Ionization (MALDI). 2011 [cited 2011 18/10/2011]; Available from: [http://www.magnet.fsu.edu/education/tutorials/tools/ionization\\_maldi.html](http://www.magnet.fsu.edu/education/tutorials/tools/ionization_maldi.html).

**Figure 1.1: Diagram of Desorption and Ionization process in MALDI<sup>[5]</sup>**

The first process is desorption; in which particles of the sample are freed from the surface of the target plate by the laser, as illustrated in Figure 1.1. The second process is ionization, where a charge is established on the analyte particles, this charge enables their analysis via MS. Although the precise

mechanisms of neither process can be explained in their entirety, there have been many studies into the subject and some viable explanations have been proposed <sup>[4]</sup>. The desorption that occurs in LDI has also been described as ablation, ejection, sublimation, vaporisation, explosive boiling, or phase explosion <sup>[6]</sup>. It is a process in which molecules gain sufficient energy from a source, often a laser, to change phase from solid to gas, increasing their susceptibility to manipulation and analysis. The group of particles that is freed from the surface and changed into gas phase forms what is known as the 'MALDI plume'<sup>[7]</sup> and can be seen in Figure 1.1. In terms of ionization, it has been proposed that a range of different processes occur, some simultaneously <sup>[7]</sup>. Different processes will occur depending on the structure of the analyte, the preparation of the sample and the conditions of the analysis <sup>[7]</sup>. Ionization can be separated into two major classes; primary and secondary. Primary ionization refers to the initial ionization mechanisms, which occur on the plate, whereas secondary ionizations occur in the 'MALDI plume' <sup>[7]</sup>. Some primary ionization methods include Multiphoton ionization, energy pooling and multicentre models and thermal ionization <sup>[7]</sup>. Secondary methods include gas-phase proton transfer, gas-phase cationization and electron transfer <sup>[7]</sup>. The mechanisms involved are based on complex physics and occur in different combinations and sequences specific to each sample and energy source.

After desorption and ionization of the analyte, it can be analysed by Mass Spectrometry. Time of flight mass spectrometry (ToF-MS) is the primary detection technique coupled with LDI is a detection method which has more specific uses than the more common quadrupole based techniques <sup>[8]</sup>. While when it was initially created it was incompatible with the technology of the time, in the last 20 years its usage has become more widespread <sup>[8,9]</sup>. Technological advances resulting in high speed computing equipment, as well as the development of LDI, has allowed for the optimization of the time of flight analysis technique <sup>[8,9]</sup>. It is recognised as both a high speed technique, and one that produces results with high levels of mass resolution and accuracy <sup>[8]</sup>. As the LDI laser is pulsed it requires a detector that is also pulsed, ToF-MS is preferred over other mass spectrometric techniques that require a more continuous supply of sample <sup>[10]</sup>. The technique is based on the simple principle that ions of different masses and charges travel at different speeds when accelerated. The ions are characterised by their mass to charge ratio ( $m/z$ ) and peaks are displayed to reflect the relative abundance of each ion <sup>[8]</sup>. The simplest version of the process, displayed in Figure 1.2, begins with the acceleration of ions from a plane towards a detector. This is done with the application of one or two electric fields ( $E_1$  and  $E_2$ ) and the beginning of this process initiates a timer, which tracks the ion progress <sup>[9]</sup>. Whilst travelling through the electric fields, the ions gain kinetic energy which is used to propel them through the drift region, and they are separated due to differences in velocity. The ions with the lowest mass to charge ratio will travel through to the detector quicker than those with higher mass to charge ratios.

This image has been removed due to copyright restriction. Available online from Guilhaus, M., MASS SPECTROMETRY | Time-of-Flight, in Encyclopedia of Analytical Science (Second Edition), W. Editors-in-Chief: Paul, T. Alan, and P. Colin, Editors. 2005, Elsevier: Oxford. p. 412-423.

Figure 1.2: Diagram of the basic design of Time of flight mass spectrometry <sup>[9]</sup>

ToF-MS is a technique that is considered to be a comprehensive method of analysis, which differs from the more specific quadrupole methods in that it does not analyse for pre-selected ions, but delivers a spectrum of all ions <sup>[9, 11]</sup>. High-speed technology was so vital for the development of this technique due to the “blanket”-type analysis it performs. Despite the many advances in the speed of detection and quality of analysis, there were still issues linked with lag and inconsistent ion starting time and position associated with ToF analysis. These were addressed with a solution known as reflectron mode<sup>[9]</sup>. The reflectron or ion mirror was originally proposed by Mamyrin *et.al.*<sup>[12]</sup> in the 1970s and involves the use of an ion mirror, shown in Figure 1.3, which reflects ions back towards the detector. The ion mirror is essentially a gradient electric field <sup>[10, 13, 14]</sup>, which is produced by numerous ring electrodes <sup>[10]</sup>. The electric field slows the ions down and reverses their direction <sup>[10]</sup>. Ions of the same mass with different energies are unified as those of higher energy travel further into the mirror, in reflection they are released at the same time and energy as the slower ones. Of the various advantages associated with reflectron mode, it is important to note the increased resolution. This is achieved due to the unification of ions and the longer drift times. The longer drift times can also be accomplished in a smaller instrument; smaller instruments are often advantageous due to space considerations. Miniaturised instruments are in development, progressing towards more portable systems <sup>[15]</sup>. This would make LDI techniques more usable and accessible for future endeavours.

This image has been removed due to copyright restriction. Available online from Guilhaus, M., MASS SPECTROMETRY | Time-of-Flight, in Encyclopedia of Analytical Science (Second Edition), W. Editors-in-Chief: Paul, T. Alan, and P. Colin, Editors. 2005, Elsevier: Oxford. p. 412-423.

Figure 1.3: Schematic diagram of reflectron mode in ToF-MS <sup>[9]</sup>

## 1.2 Matrix Assisted Laser Desorption Ionization (MALDI)

Laser Desorption Ionization was not initially successful for many materials, as most samples were not able to absorb the inbound laser energy, and thus be desorbed from the surface<sup>[4]</sup>. An alternative substance able to absorb and transfer the laser energy was required, this led to the development and application of compounds that are now referred to as matrices and the concept of Matrix Assisted Laser Desorption Ionization (MALDI). MALDI is a technique which is useful for the analysis of large, often biological, molecules <sup>[16]</sup>. The size of these molecules leads to difficulties in analysis, due to a tendency towards high fragmentation. Thermal instability and low sensitivity also means standard techniques, which use extreme heat and energy conditions have limited success <sup>[4]</sup>. The purpose of the matrix is multifaceted; it is proposed that efficiency is increased merely through dilution of the samples, reducing the intensity of the effect of the laser on the analyte <sup>[1]</sup>. Matrices are essentially compounds which easily absorb laser light. Much like samples analysed by UV-Vis Spectrometry, many matrices have a similar structure based on conjugated double bonds. Matrices must be volatile enough to be vaporised by the laser, but not so volatile that evaporation occurs before vaporisation. Finally the ability to transfer charge is an essential property of all matrices <sup>[1]</sup>. There are many compounds capable of acting as a matrix, the most common are small organic molecules, all of which work well with specific samples. Thus, matrix selection is of high importance in the analysis process. The early organic matrices were developed in the 1980s <sup>[17]</sup>. The selection of a matrix expanded to include many desirable properties, such as stability in a vacuum, the adduct peaks generated<sup>[18]</sup>, resonant absorbance wavelength <sup>[18, 19]</sup> and tolerance to contamination <sup>[20]</sup>. Two of the most commonly used and broadly effective matrices are  $\alpha$ -cyano-4-hydroxycinnamic acid (CHCA), as seen in Figure 1.4, and 2,5-dihydroxybenzoic acid (DHB), Figure 1.5. Developed in the 1990s <sup>[21]</sup>, CHCA was developed, based on the use of other cinnamic acid derivatives, sinapinic acid, ferulic acid and caffeic acid, it was used

initially for peptide samples <sup>[21]</sup>. DHB was also first used in the 1990s and was found to have little contaminant sensitivity <sup>[22]</sup>.

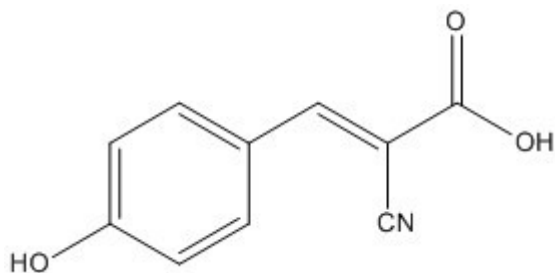


Figure 1.4: Molecular structure of CHCA

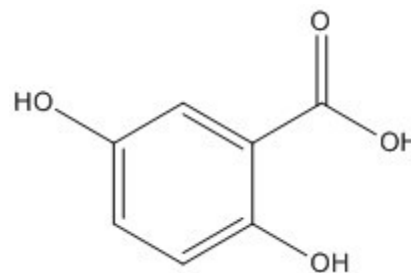


Figure 1.5: Molecular structure of DHB

The advantages of LDI, as an analytical technique are due to simple preparation, reliability and the low impact that contaminants have on results <sup>[3, 16, 23]</sup>. It is also favourable due to short data collection times<sup>[16]</sup>, ease of operation <sup>[24]</sup>, high sensitivity and ability to analyse solids <sup>[16]</sup>. In forensic investigations this technique is beginning to gain more recognition and has recently been used to analyse a range of samples. Mostly it has been used to look at biological style samples, such as Single Nucleotide Polymorphisms (SNPs) in DNA <sup>[25]</sup>, but it has also been used in tape adhesive identifying the different adhesive types <sup>[26]</sup> and questioned document investigations, which will be discussed in detail later in the chapter <sup>[27]</sup>. LDI analysis is also being developed for use in toxicological fields with some small molecule research extending to analysis of LSD with limited success<sup>[28]</sup>. Other LDI research has investigated the presence of amphetamines, one study was looking at analysis of blood <sup>[29]</sup> and others used alternative LDI techniques are discussed later in the chapter <sup>[30]</sup>.

### 1.3 The History of LDI

The LDI techniques used today were originally developed in the mid-1980s, derived from a combination of previously reputable techniques <sup>[4]</sup>. The earliest connection can be seen with Field Desorption (FD) <sup>[4]</sup>, a technique initially developed twenty years before LDI, in the 1960s <sup>[31]</sup>. FD was a mass spectrometric technique capable of analysing solids without necessitating their evaporation and using the, until then, typical high energies required. FD involved the adsorption of some of the sample onto what is known as the activated field anode, or emitter wire <sup>[31]</sup>. Molecules of the sample were adsorbed onto carbaceous microneedles situated on the surface of the wire which acted as the activated anode. Sample molecules were then desorbed using a strong electric field, which extracted ions from the compound of interest <sup>[31, 32]</sup>. Like LDI, FD was capable of the analysis of large molecules with little fragmentation and a strong signal corresponding to the molecular ion of the sample <sup>[31, 32]</sup>. FD has, however, been replaced by other techniques and is now obsolete, mainly due to the difficulty,

time and effort associated with manufacturing the anodes, as well as a limited number of analysers<sup>[32]</sup>.

The next technique to emerge in this field was Secondary Ion Mass Spectrometry (SIMS) in 1975<sup>[4]</sup>. SIMS uses high energy ion impact to remove some surface materials, some of which are ionized as the ejection occurs. These ions are representative of the sample surface<sup>[33]</sup>. The sputter (ejected) ions are referred to as being secondary as the ionization occurs during ejection driven by the primary ions. The primary ions can be atoms, atom clusters or even complete molecules<sup>[33]</sup> and is capable of detecting all elements, including Hydrogen and Helium. Unlike LDI, SIMS results in fractionated samples<sup>[33]</sup>, but is a technique in which a species is removed from the surface of a sample, or desorbed, and simultaneously ionized.

After SIMS, Fast Atom Bombardment (FAB) was developed in 1981<sup>[4]</sup>, a technique where the atoms fired at the sample are neutral, rather than ionized, and primarily consist of Argon. FAB results in a large amount of fragmentation and has also been used with the aid of a matrix, often a high boiling point solvent, such as glycerol, to dissolve the sample<sup>[34]</sup>. FAB was able to analyse a variety of materials including inks<sup>[35]</sup> and was the first to successfully tackle thermally instable solids. All other techniques developed prior required gas phase samples before ionization<sup>[34]</sup>. In Plasma Desorption, a technique which was introduced at a similar time, the sample was bombarded with nuclear decay products<sup>[4]</sup>. One example of Plasma Desorption used the energetic material Nitrocellulose for signal enhancement in a similar fashion to matrices<sup>[4]</sup>.

Shortly after the laser was invented the techniques previously mentioned were expanded on with Hillenkamp and Kauffman conducting experiments that replaced the use of atom bombardment with a laser<sup>[4]</sup>. The resulting technique, Laser Microprobe Mass Analysis (LAMMA)<sup>[36, 37]</sup> used both near and far UV lasers and the first major issue encountered was concerning sensitivity to the noise caused by the polymer used to set the sample<sup>[4]</sup>. In trying to correct this issue MALDI was developed in 1985 by Hillenkamp and Karas. Application of the LAMMA instrumentation with the assistance of a metal powder suspended in glycerol was used for the first time in the analysis of biopolymers<sup>[38]</sup>. The combination of metal powder and glycerol was the first iteration of the modern matrix. Applications of the new technique were extended to include protein analysis, this ground-breaking research was conducted in 1988. However a similar process was first performed by Tanaka, a chemical engineer working out of Japan<sup>[39]</sup>. The work performed by Karas and Hillenkamp took place a few months later and therefore the Nobel was awarded to Tanaka<sup>[17]</sup>.

The development of MALDI occurred concurrently with that of Electrospray Ionization (ESI), another technique that analyses large biological molecules, but operates differently to MALDI [4]. ESI is based on the principle of the nebulization of a solution in an electric field. The solution is pre-ionized via treatment with either an acid or a base, resulting in charged droplets [40]. Evaporation of the solvent used in ESI is unnecessary as it is analysed simultaneously with the sample. The advantage of having no evaporation step is decreased time spent in sample preparation, there is also no need for harsh treatments to speed up evaporation, or limitations to volatile solvents [40]. The disadvantage is that solvation is necessary, as solid samples cannot be analysed. ESI is also conducted at atmospheric pressure, saving operators time, energy and expense required for vacuum analysis and preventing evaporation of highly volatile samples [40]. An adaptation of ESI; Desorption Electrospray Ionization (DESI) has been used previously for the analysis of pharmaceuticals with strong concentrations [41]. In DESI the droplets are sprayed onto a surface, desorbing the analytes from the surface and forming secondary microdroplets that are further analysed [42]. There are many advantages that MALDI has over ESI, including that it is more sensitive [4], has less salt and buffer driven peak suppression [20, 43] and a broader range of detectable masses [44].

## 1.4 Variations of LDI

Matrix Assisted Laser Desorption Ionization is the most common variation of LDI but there are a variety of other alterations that can be made. In the following chapter these are explored. An overview of some common and complex variations will be discussed first, followed by a discussion of the techniques that are investigated in this thesis.

### *Other Variations to MALDI*

There are a range of variations to the MALDI technique. One example of which is Atmospheric Pressure MALDI (AP-MALDI) where the ionization occurs at higher or atmospheric pressure, as opposed to occurring in a vacuum [30, 44]. Results for this method generally have even less fragmentation than those from the regular vacuum method [44], although some samples, such as carbohydrates, undergo more fragmentation [1]. AP-MALDI is useful for the analysis of sensitive samples, which are stabilized in this method [1]. The total ion yield associated with AP-MALDI, is considered to be higher than that of the traditional vacuum based methods, indicating more analyte is desorbed [3]. A modification of AP-MALDI is ambient pressure MALDI, it is a further simplification to the ambient pressure system, in that the entire system is open [45]. Ambient mass spectrometry techniques are more simplistic to run and can be continuously monitored throughout an experiment. This simplifies analysis and improves efficiency [45]. When used in combination with vacuum based detectors, such as ToF-MS or ion trap MS, higher pressure ionization systems encounter transition issues which are believed to cause low detection limits [3, 44]. Therefore, the technique has been adapted to be used with ion mobility



spectrometry (IMS) a detector that can be used at higher pressures, leading to further developments in LDI <sup>[44]</sup>. IMS uses a drift tube and uses size to charge ratios, rather than mass to charge<sup>[30]</sup>. An advantage of IMS is that it is not used under vacuum and therefore avoids the time and expenses associated with vacuum environment. IMS also generates less fragmented results, however, this is coupled with lower detection limits due to the absence of the vacuum environment <sup>[46]</sup>.

MALDI imaging is another more complex technique used primarily for biological system samples, where a thin section of what is normally a tissue sample sprayed with a matrix, is analysed in detail <sup>[47]</sup>. This analysis involves mapping the molecular spread and, providing a more detailed understanding of the physical nature of a sample <sup>[47]</sup>. This application of MALDI is performed in conjunction with multichannel MS measurements and allows for the analysis of unknown samples. Previously visualisation of samples required knowledge of the sample in order to use chemical taggants for detection <sup>[47]</sup>. Imaging MALDI is able to identify molecules ranging from small drugs and their metabolites <sup>[48]</sup> to proteins and is often used to track biological systems in disease and pharmaceutical studies <sup>[47]</sup>.

MALDI has also been found to have quantitative abilities, however the sample preparation, instrumental setup and spectral analysis are much more complex than other quantitative techniques <sup>[49]</sup>. They require complex calibrations based on peak intensities, which requires the same laser strength and number of shots for each sample <sup>[50, 51]</sup>. This is something that is difficult to do due to few MALDI samples being homogenous <sup>[52]</sup>. This issue is sometimes known as shot-to-shot reproducibility and occurs when some areas have more concentrated sample or better ratios of matrix to analyte, making them more easily analysed and able to produce strong spectra <sup>[52]</sup>. Other areas may have little to no sample or too much matrix or calibrant, meaning they require harsher conditions for analysis <sup>[53]</sup>. While MALDI is typically associated with qualitative analysis, quantitation of various samples has been reported on. Examples of which include low molecular mass samples, the products of enzyme catalysed reactions <sup>[54]</sup> and small pharmaceuticals in a complex extension of the instrument requiring quadrupole analysis and an altered laser <sup>[20]</sup>.

### *Matrix Free Analysis*

MALDI is a highly useful technique, the advantages associated with it include high specificity and sensitivity, simple sample preparation; high throughput and soft ionization. It is, however, limited, primarily to higher mass samples, those above 500 gmol<sup>-1</sup>, including an array of biological samples and polymers. The use of MALDI is seen less frequently in low mass samples due to a phenomenon called matrix interference <sup>[10, 11]</sup>. Matrix interference occurs during the analysis of low mass samples when matrices are analysed competitively with the analytes, as the matrices are similar mass to the samples

<sup>[55]</sup>. A quality of matrices that dictate their selection in these MALDI experiments is high absorption of laser energy, therefore the laser affects them in the same way as any sample, leading to desorption and ionization and subsequent analysis of the matrix. The ideal matrix: analyte ratio of 1000:1 <sup>[11, 56]</sup> indicates that little matrix is required to absorb and transfer laser energy, therefore analysis of such compounds results in spectra with very strong peaks, stronger than that of the analyte. The process has little impact on the large biological and polymer samples often analysed, however, issues arise in the lower mass range <sup>[57]</sup>. Matrices have low masses, in the same range as most low mass analytes<sup>[57]</sup>, the matrix peaks can, therefore, interfere with the results. The matrices will often produce stronger peaks than the compounds of interest and may produce peaks of the same mass to charge ratio, leading to confusion and inaccuracy, associated with false positive results. As the samples investigated in this thesis are in the low mass range, the initial technique investigated is a matrix-free method, analysing directly from the plate. Compounds like ink are ionizable enough to be easily detected without any outside assistance <sup>[58]</sup>.

### *Surface Assisted Laser Desorption Ionization*

Limitations associated with the application of MALDI to lower mass samples, due to matrix interference, have led to the development of Surface Assisted Laser Desorption Ionization (SALDI). SALDI is an alternative to the traditional MALDI. This technique introduces a surface onto which the sample of interest is placed <sup>[57]</sup>, generally a pre-treatment has been undertaken to give these surfaces optimal physical properties, and leads to lower levels of contamination, negating the need for a conventional matrix. Some examples of surfaces used include Carbon black slurries <sup>[59]</sup> and Carbon tape<sup>[27]</sup> as well as Porous silica <sup>[60]</sup>.

The most popular surface alternative used is a type of porous silicon, with the associated technique often referred to as Desorption Ionization on Silicon (DIOS) <sup>[61]</sup>. DIOS, developed in the 1990s, uses no matrix and, therefore, results in no external background interference <sup>[61]</sup>. The surface is made of silicon, which has been chemically and structurally modified for ideal ionization properties, usually dependant on the analysis being performed <sup>[60, 61]</sup>. The pores on the surface of the silicon trap analyte molecules to be vaporized using the laser and then ionized for analysis, the system can be optimized for different samples in terms of thickness, porosity and resistance of the silicon wafer <sup>[60, 61]</sup>. DIOS is sensitive and compatible with silicon based technologies and results in little to no fragmentation of samples <sup>[61]</sup>. It has been proved to work in a variety of applications, including roadside drug test analysis <sup>[62]</sup>. DIOS was used successfully as the surface in the analysis of oral fluid samples containing amphetamines and marijuana derivatives, in this case minimal treatment was required, with only one species requiring extraction <sup>[62]</sup>. DIOS has also been combined with atmospheric pressure MALDI in

the analysis of drugs such as amphetamines and fentanyl sourced from drug seizures where the samples were in the form of tablets <sup>[63]</sup>.

In terms of carbon surface research, a study conducted at Flinders University, used activated carbon slurry surfaces to analyse steroids. This successful technique required little sample preparation and yielded results with little interference <sup>[59]</sup>. In a further simplification of carbon surfaces, Matthews *et al* 2011, used carbon tape as a surface to which solid samples were adhered<sup>[27]</sup>. This meant no derivatization or solvation and little sample preparation. It was utilized in cases of document analysis, where a single fibre of paper, laden with ink, was removed from the surface of the document of interest and stuck on the carbon tape to be analysed <sup>[27]</sup>. It proved useful in identifying different inks from single fibres with minimal document damage <sup>[27]</sup>. This technique was further investigated when the carbon tape was replaced with double-sided sticky tape and yielded the same results, showing that an assisting material is not necessary for all samples <sup>[58]</sup>. This is a quick, easy and cheap alternative to carbon tape.

The surface in this investigation needed to be multipurpose, as the proposed sample was in the form of a solid, as fibres. Not only do these types of samples require matrix-like assistance, but also some form of adhesion. Carbon tape was the first multipurpose option that was considered, as mentioned above; it has been used in previous research as an adhesive assisting surface. Regular double-sided tape was also used, as a control and cheaper alternative. A copper tape was also investigated due to increased conductivity of the surface mimicking that of the target plate.

### **Graphite**

The other major alteration that occurs in MALDI methods is in the use of an alternative matrix. Standard matrices, which are used in basic MALDI experiments, are compounds able to easily absorb and transfer energy <sup>[1]</sup>. Alternative matrices are compounds that behave similarly to matrices but are different types of molecules, or matrices that have been significantly altered. An examples of an alternative matrix is the use of inorganic powders, such as aluminium and titanium oxide, which were applied to the detection of polyethylene glycol and methyl stearate <sup>[64]</sup>. The performance of standard matrices can be optimised, in this case by adjusting pH levels (at pH 2, 5 and 10), to minimize the matrix interference in the analysis of a variety of small molecules including organic acids, chelating agents and the salts of oxyanions <sup>[11]</sup>. The addition of a surfactant, such as Cetriumonium Bromide, can also aide in the analysis of low molecular mass prescription drug samples, including beta blockers, antipsychotics and antihistamines <sup>[57]</sup>. In another study p-toluenensulfonic acid was used as a surfactant for the analysis of methylephidrine <sup>[65]</sup>.

Many common alternatives to matrices are carbon based, this includes graphite. A suspension consisting of graphite and glycerol has been utilised frequently<sup>[66]</sup> and was found to be most useful for the analysis of peptides and proteins<sup>[67]</sup>, but loses sensitivity for samples in the higher mass range<sup>[66]</sup>. Colloidal graphite, suspended in glycerol, has also been used in conjunction with Imaging Mass Spectrometry to analyse the components of fruits, including organic acids, flavonoids and oligosaccharides<sup>[68]</sup>. Both components in the suspension serve a different purpose, the graphite absorbs the laser energy and transfers it, leading to desorption of the sample analytes in the mixture<sup>[66]</sup>. The purpose of the liquid matrix, which in the example above is the glycerol, is to protonate the analytes of interest and assist desorption, as well as limiting decomposition and increasing the lifetime of the sample<sup>[66]</sup>. This mixture can be altered with additives such as sucrose and methanol to aid in the analysis of samples which are less sensitive<sup>[65]</sup>. Activated carbon particles have also been used to form a thin layer onto which samples are pipetted, with a small amount of glycerol<sup>[69]</sup>. This method is simple, has high sensitivity and can be used on a range of samples<sup>[69]</sup>. Another innovative use of graphite has been its use in conjunction with Ambient MALDI, with the surface being filter paper with a graphite coating provided by a “lead” pencil<sup>[45]</sup>. In this study samples of tea were analysed<sup>[45]</sup>. Graphite in the form of lead pencil was also used in the analysis of peptides, polymers and actinide metal, in this study the graphite was used as a surface, placed directly on the target plate prior to the samples<sup>[70]</sup>.

This use of pencil graphite will be further investigated here along with the idea of analysing solid samples adhered to an assisting tape. In this experiment the samples being investigated are drug-soaked fibres attached to the plate via the aforementioned adhesive tapes.

### ***Binary Matrices***

The issues associated with the use of traditional matrices in low mass samples have been discussed in detail within this thesis. These issues have led to the development of alternative matrices and systems, however some of these options are based on the troublesome traditional matrices themselves. Not all of these alternative matrices have the primary focus of minimizing matrix interference in low mass sample analysis. Binary matrices, also referred to as combination matrices or co-matrices, are involved in a system of combining multiple matrices or a separate additive to a base matrix, in order to improve analysis by MALDI-MS<sup>[16]</sup>. Some of the properties of proposed improvement are shot-to-shot reproducibility, crystal inhomogeneity, and signal degradation, as well as reduction of interference that can be caused by a single matrix<sup>[71]</sup>. Combination matrices have been used several times to analyse samples that have been unsuccessfully trialled with traditional MALDI experiments. Initially these additives were simple carbohydrates such as fucose which along with 5-methoxysalicylic acid (5-MSA) was added to DHB<sup>[72]</sup>, it was also used with DHB and ferulic acid in a study aiming to improve

quantitation <sup>[71]</sup>. The best results in terms of homogeneity and signal intensity from these experiments were yielded from a tri-matrix, which combined three compounds <sup>[71, 72]</sup>. Many of these analyses were focussed on high mass or biological samples, primarily proteins and peptides <sup>[73]</sup>. Additives were used in a quantitative analysis of oligosaccharides to help prevent the issues discussed above and provide an internal standard. <sup>[71]</sup>. In the analysis of oligosaccharides found in human milk, again being biological samples, an optimized matrix was developed using a layering technique with DHB. The additive used was 5-chloro-2-mercaptobenzothiazole (CMBT) the combination has become known as superior DHB <sup>[74]</sup>.

A true binary matrix was first seen as a combination of the two most commonly used matrices, DHB and CHCA, which was developed for use in protein identification <sup>[75]</sup> and peptide mass mapping <sup>[76]</sup>. This combination was also used to increase homogeneity, spot-to-spot reproducibility, signal to noise ratio and tolerance to impurity <sup>[76]</sup>. In 2007 a new binary system was introduced which consisted of a combination of CHCA and 9-aminoacridine (9AA). This binary matrix took advantage of the differing acidities of the matrices to increase ionization while maintaining low interference in the analysis of inositol phosphates in complex plant extracts <sup>[77]</sup>. The analytes of interest were compounds found in tobacco plants. The rationale for the combination of CHCA and 9AA was that the different pH values of each matrix led to more proton competition and, therefore, less matrix clusters and less noise <sup>[77]</sup>. The system is also highly pKa dependant, requiring the sample value to be significantly different from both matrices, which limits its applicability to a number of samples, requiring a specific pKa range <sup>[77]</sup>.

A combination of 6-aza-2-thiothymine (6-ATT) and 3-hydroxycoumarin (3-HC) was also investigated <sup>[48]</sup> for the analysis of low molecular weight drug samples, which is highly applicable to the samples of interest in this thesis; importantly the samples in this case were, pharmaceutical tissue samples <sup>[48]</sup>. This is applicable due to the similar nature of the inclusion of drug-based samples, however the differences in sample type may lead to complications. Amino acids were also analysed with the binary matrix, here it's primary purpose was to decrease background peaks and sustain analyte peaks. 6-ATT has a molecular mass of  $143.17\text{g}\cdot\text{mol}^{-1}$  and was chosen due to its homogeneity and high ionization efficiency, with a downside being a noisy background. Alternatively, 3-HC, which has a molar mass of  $162.144\text{g}\cdot\text{mol}^{-1}$ , does not have as high ionization efficiency but has low noise. The improvement of the spectra in this investigation warranted further investigation of this binary matrix.

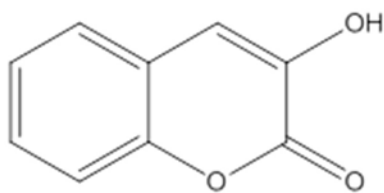


Figure 1.6: Structure of 3-hydroxycoumarin

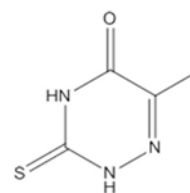


Figure 1.7: Structure of 6-aza-2-thiothymine

### *Nanoparticles*

Nanoparticles (NPs) are a subcategory of nanomaterials, materials which are of submicron size; more specifically nanoparticles are discrete particles with a defined size of 100-1000 nm.<sup>[78]</sup> or 1-100 nm<sup>[79]</sup>. This is a loose definition, as the term nanoparticle can generally be applied to all particles in the nanometre range. Nanotechnology is currently a very popular area of study across various disciplines. Nanoparticles are hugely diverse in properties and have many potential applications which has led to them being heavily investigated in recent years. Nanoparticles can be made from a range of different core materials; metals, metal oxides and organic compounds have all been used in a variety of different applications. Examples of the core materials that have been used for applications in nanoscience include silicon, gold, silver, iron, metal oxides<sup>[51, 79]</sup> and platinum<sup>[23]</sup>. Nanoparticles have been used throughout history, targeting them in synthesis, even before they were able to be recognised as nanoparticles. Originally found as naturally occurring substances<sup>[80]</sup> nanoparticles were found biologically in proteins, polysaccharides and viruses<sup>[80]</sup>. Inorganic examples include iron hydroxides, aluminosilicates and metal nanoparticles, these can be formed by weathering, volcanic activity, wildfires or microbial processes<sup>[80]</sup>. Historically, metal nanoparticles have been used for their pigmentation properties<sup>[80]</sup>, with ancient Egyptians dyeing their hair using PbS particles, created from galenite<sup>[81]</sup>. Celtic art used copper-based nanoparticles to create red enamels, and the ancient Romans used silver and gold nanoparticles in the production of colour-changing glass<sup>[80, 81]</sup>. Knights in ancient Europe were known to use ultra-strong Damascus steel, which made sharp and shatter-resistant blades, this steel was fortified with nanowires and Fe<sub>3</sub>C tubelike nanostructures<sup>[81]</sup>. An early step towards nanoscience and understanding colloidal chemistry was Michael Faraday's investigation of light interactions with metal nanoparticles in the mid-1800s<sup>[80]</sup>. Modern nanotechnology was sparked by Richard Feynman's concept of atomic-level manipulation of matter in 1959, he is now known as the father of modern nanotechnology<sup>[82]</sup>. Years later Norio Taniguchi, in Japan, was the first to apply the concepts initiated by Feynman<sup>[82]</sup>. Nanotechnology became a more popular subject of investigation during the 1980s<sup>[83]</sup>, a time that was known as the golden era of nanotechnology [82], developing a better understanding and proposing innovative techniques for their production<sup>[82]</sup>. Nanoparticles are used in many different applications, including medical and pharmaceutical, food, cosmetics and even in industry<sup>[82]</sup>. Not only do nanoparticles provide flexibility in terms of size and

core materials, they have a range of properties than can be optimized for different applications. Nanoparticles can be altered with many different functional groups, or can be used in the bare form<sup>[84]</sup>. Some nanoparticles are magnetic<sup>[51, 79]</sup>. Some functionalisation treatments allowing the NPs to be used in very specific analyses as probes, concentrating the analyte for analysis<sup>[23, 85]</sup>; other NPs are anchored to materials as a treatment of larger surfaces, an example uses silicon plates with gold nanoparticles attached, for the analysis of peptides<sup>[23]</sup>. Many of the magnetic NPs are used as the aforementioned probes, and can be biologically functionalised and can aid quantification<sup>[86]</sup>. Interestingly, many nanoparticles behave differently to their bulk material<sup>[79]</sup> and small molecules<sup>[83, 87]</sup>. For example, nanoparticles of copper, silver and gold, in solution are intensely coloured, a property that neither their bulk or molecular counterparts display<sup>[88]</sup>. The thermal, optical and electronic properties possessed by nanoparticles<sup>[89]</sup> are dictated by their size and shape<sup>[83, 87]</sup>. There are many properties that nanoparticles possess that makes them ideal alternative matrices in LDI systems. The use of nanoparticles in this context is labelled as a form of either SALDI<sup>[90]</sup> or matrix-free LDI, however, it has also been abbreviated to nanoPALDI (nanoparticle Assisted Laser Desorption Ionization)<sup>[48, 91]</sup>. Among the most useful properties of nanoparticles for application in LDI-MS as matrix alternative are the ease of preparation, and functionalisation<sup>[92]</sup> and their optical absorption abilities<sup>[56]</sup>. Nanoparticles are thought to generate more homogenous sample spots minimizing issues with shot to shot reproducibility<sup>[48]</sup>, and less interference in the low mass range<sup>[91, 93]</sup>, due to their larger size. As compared to matrices, nanoparticles produce many more analyte ions per particle and can regenerate their ionizing abilities between shots, consequently, a lower amount of nanoparticles are required for successful analysis<sup>[84]</sup>. The use of nanoparticles as such can be traced back to the first protein analysis performed by Tanaka<sup>[39]</sup> which used fine cobalt powders suspended in glycerol as a type of matrix. From there the nanoparticle applications used with LDI have evolved to include the huge range of options available today. Magnetic Iron oxide NPs have been used before in drug metabolite analysis with LDI, in the case of morphine and 7-aminoflunitrazepam in urine samples<sup>[51]</sup>. Iron oxide has also been used to analyse peptide fragments from degraded proteins<sup>[94]</sup>, low molecular weight lipids<sup>[95]</sup> and oligonucleotides<sup>[93]</sup>. LDI is also a common tool used to identify some nanoparticles, to analyse for the size and structure measured in the higher mass range<sup>[96]</sup>. In this thesis, nanoparticles are investigated and applied to the analysis of drugs via LDI, from the MALDI plate and adhered fibre samples. Two traditional cores are focussed on in this study, silicon and gold. Silicon is frequently used in other SALDI experiments and gold has also been broadly researched.

### ***Silicon Nanoparticles***

There are many different options and possibilities associated with nanoparticles and their use in science. The use of silicon nanoparticles is investigated, due primarily to their availability and the

history of silicon use in SALDI techniques. Silicon nanoparticles have been less common throughout history than many of the well-known metal nanoparticles. They are currently used in the food industry as anti-caking agents <sup>[80]</sup>, and are more prominent in scientific research than in household products. The use of silicon in nanomaterials for LDI analysis is broadly used in the form of DIOS. The technique, whilst very useful and applicable across a range of different sample types, is less so in these circumstances due to the need to adhere a fibre to the surface. The use of silicon was, however, investigated, being not only the basis of DIOS but several other LDI-based experiments. Silicon nitride nanoparticles have been used in the analysis of prescription drugs in urine, by laying down the nanoparticles as spots prior to loading the drugs, acting as a surface<sup>[43]</sup>. Silicon nanopowders have been used in similar analyses of urine and soil samples and gave very good results<sup>[97]</sup>. Silicon Nanoparticles (SiNPs) were already being produced at Flinders University, therefore, advantage was taken of the availability of precursors and expertise of nanotechnologists. The function group attachment of these nanoparticles was a phenyl group, which coincided with ideas regarding the interactions between such groups and the structures of a variety of drugs. The idea behind this kind of functionalisation creating an effective environment for laser desorption and ionization of drugs comes from the interactions, or cross-linking, between aromatic groups on the nanoparticle and in the drugs of interest, an idea that has been investigated in functionalisation before <sup>[98]</sup>. Phenyl groups contain the conjugated double bonds so frequently seen in matrices, which strongly absorb at the laser frequency used. These interactions were predicted to lead to enhanced desorption and ionization of the samples, due to pi-pi interactions <sup>[98]</sup>. Phenyl functionalised nanoparticles, in the form of iron oxide with functional silicate sheets and phenyl attachment, were used to analyse a range of drugs, by selective trapping <sup>[98]</sup>. The drugs analysed were colchicine and reserpine, and were investigated alongside peptides and a polymer <sup>[98]</sup>.

### ***Gold Nanoparticles***

There are many options available for the synthesis of various nanoparticles and many other possibilities that are yet to be explored. A major differentiating factor between nanoparticles is the core material used. Some have been more heavily researched and are more popular today due to an increased understanding, and one of the more common cores is gold. The popularity of and several the properties, discussed later in this chapter, associated with gold nanoparticles, lead to their investigation in this study. While the selection of silicon nanoparticles for use in LDI experiments was influenced by the heavy use of DIOS there are some examples of the use of gold in LDI outside of nanoparticles. For example, an experiment analysing for amphetamines and fentanyl used a gold coated LDI plate in conjunction with CHCHA <sup>[63]</sup>. Gold Nanoparticles (AuNPs) have been recognised for centuries, the ruby red colour of these solutions was highly appealing throughout history <sup>[99, 100]</sup>.



Although the first forms were labelled colloidal <sup>[99, 101]</sup> or soluble gold <sup>[87]</sup>, some of the most interesting properties of this material were identified by its earliest investigators. Soluble gold was used in the 4<sup>th</sup> and 5<sup>th</sup> century BC for colouring purposes, including the production of coloured glasses <sup>[102]</sup> and in early medicine by the Egyptians and Chinese <sup>[87]</sup>. A lot of scientific research began in the 1850s <sup>[101]</sup> into the theoretical side of gold nanoparticles with Faraday's reduction of gold salt <sup>[100]</sup>. Gold nanoparticles have a large number of modern applications, these include in electronics, catalysis, medical and biological fields <sup>[103]</sup>. There are many advantages associated with AuNPs, they are the most stable metal nanoparticles <sup>[87, 104]</sup>, are not easily oxidised <sup>[101]</sup>, and have various optical properties <sup>[104]</sup> including strong absorption of light <sup>[56, 101]</sup>, which can be exploited for use in LDI. AuNPs are popular due to a number of other qualities such as simple preparation <sup>[56, 105]</sup>, easy surface functionalisation<sup>[104, 105]</sup>, bioconjugation <sup>[104]</sup>, and the ability to control their size and shape <sup>[103]</sup>. AuNPs have, therefore, been used extensively to aid in LDI analyses, often for peptide <sup>[56, 105]</sup>, protein<sup>[56, 92]</sup> or polymer <sup>[105]</sup> analysis. The methods of production have included annealing <sup>[105]</sup>, etching<sup>[106]</sup>, and refluxing <sup>[56, 107]</sup>. Although, a disadvantage of AuNPs is that they are less homogenous than other NPs and thus have lower shot to shot reproducibility <sup>[23]</sup>, using them in the context of fibre loading minimizes this issue. The simplest particles with the most straight forward synthesis found are of bare nanoparticles, which have only hydrogen functionalisation <sup>[84]</sup>. Bare AuNPs have been used before in the analysis of low molecular mass samples, specifically neutral carbohydrates and steroids, which are difficult to ionize species <sup>[84, 108]</sup>. The prior successful use of bare gold nanoparticles in low mass sample analysis suggest they will be them ideal for the initial analysis in this thesis. Bare nanoparticles use the inclusion of a sodium borohydride (NaBH<sub>4</sub>) to supply protons as "capping agents" as opposed to the various other chemicals used to coat functionalised NPs. Bare nanoparticles were chosen as a lack of functionalisation will minimise the fragmentation of the attachments, and allow more interaction between the sample and the gold itself as there is no functionalised layer with which to interact <sup>[84]</sup>.

### ***Functionalised Gold Nanoparticles***

The advantages of functionalisation of gold nanoparticles are numerous; among them the different and beneficial properties such particles can possess once functionalised <sup>[103]</sup> and the simplicity of some methods of functionalisation <sup>[103]</sup>. One of the most popular, common and simple methods include citrate salts caps <sup>[109]</sup>. The ease of attachment of thiol species is also important <sup>[87]</sup>. The simplicity of functionalisation via thiol groups is due to the strong bond between gold and sulfur which occurs because of the soft nature these elements share<sup>[87, 110]</sup>. The definition of their soft nature is based on the hard-soft acid-base theory, which speculate that soft acids and bases are more likely to bond with each other <sup>[110]</sup>. Soft species are less electronegative, larger, less charged and more polarisable species than their hard counterparts <sup>[111]</sup>. There are a range of reasons for functionalized AuNPs to be used in

LDI. They have been used to help decrease noise and increase ionization or spot to spot reproducibility. In this investigation the purpose of functionalisation is to add matrix-like properties to the gold nanoparticles, such as strong absorption of laser energy and ionization ability. Many compounds that possess these properties have already been used extensively for this instrument, traditional matrices were the first natural option. As CHCA is one of the most commonly used and well reported matrices, it was investigated as a possible attachment. As previously stated, CHCA has been used in conjunction with a gold treated surface before <sup>[30]</sup>. A CHCA functionalised AuNP has been previously synthesized in a complex method undergoing a number of steps, using a reflux system and a cysteamine layer and has been used in the analysis of peptides <sup>[56]</sup>. A variety of different methods have been used to make adjustments to AuNPs, these include seed layers <sup>[56]</sup>, 2-phase systems <sup>[112]</sup>, microfluidic devices <sup>[113]</sup>, however, simpler methods performed at room temperature were favoured over the more complex. The simple attachment of thiolated species, in one-step methods was selected. The species selected for functionalisation were to be based on the structure of common matrices due to their ability to consistently assist the laser desorption and ionization of a variety of other analytes. Common matrices such as CHCA, DHB, and ferulic, cinnamic, sinapinic, sinapic, and caffeic acids all have similar structural properties. Properties that are common to these compounds are a benzene ring and carboxylic acid attachment, materials consisting of these functional groups and along with a sulfur link were sought out. There are many such compounds in existence however, the most viable in terms of availability and likelihood to work were mercaptobenzoic acids. The three different isomers of mercaptobenzoic acid, with sulfur groups at the para, ortho and meta positions can be seen in Figure 1.8, Figure 1.9 and Figure 1.10 respectively. Mercaptobenzoic acid functionalised gold nanoparticles have been synthesized previously using each of the isomers. 2-mercaptobenzoic acid produces  $2.1 \text{ nm} \pm 0.9$  nanoparticles, with a shelf-life of minutes and 3-mercaptobenzoic acid produces nanoparticles that are stable for days and which are  $1.6 \text{ nm} \pm 0.6$  <sup>[114]</sup>. 4-mercaptobenzoic acid (4-MBA) functionalised particles have been synthesized to be  $1.8 \text{ nm} \pm 0.4$  and to be stable for months <sup>[114]</sup>. 2-mercaptobenzoic acid, also known as thiosalicylic acid (TSA), and 3-mercaptobenzoic acid are much less stable nanoparticle options, due to the ortho and meta positions of the functional groups <sup>[114]</sup>. The thiosalicylic acid was chosen to be an option out of interest despite its short shelf life due to a much lower cost compared to the other two compounds. 4-mercaptobenzoic acid was chosen due to its stability, successful synthesis and para positional similarity to common matrices. Multiple methods were found for this synthesis, one was performed as a 2-phase reaction <sup>[115]</sup> and another using etching <sup>[116]</sup>. Pre-synthesized citrate-capped AuNPs were used for an analysis for peptide mixes, and selective analysis <sup>[109]</sup>, the previously mentioned methods were all much longer and more complex than the one selected <sup>[117]</sup>. The physical properties of the nanoparticles synthesized with

mercaptobenzoic acids were found to reflect the nature of the functional groups of their attachments [117].

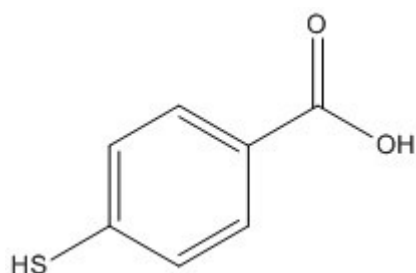


Figure 1.8: Molecular structure of 4-mercaptobenzoic acid

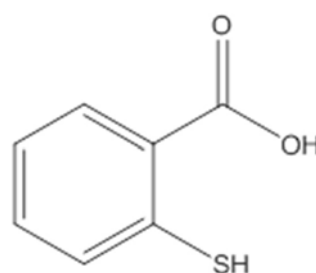


Figure 1.9: Molecular structure of thiosalicylic acid

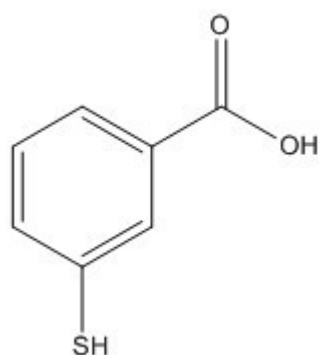


Figure 1.10: Molecular structure of 3-mercaptobenzoic acid

### **Nanoclusters**

Nanomaterials, as previously mentioned have countless configurations, differing in core, size and functionalisation. Studies have been found that investigated very small particles, defined as nanoclusters [99, 118], these particles are measured by number of atoms as opposed to measured size, as they are generally less than 2 nm in diameter [99, 101, 118]. They differ in behaviour to standard nanoparticles due to decreased size and there is much interest in these new ultra-small particles [99, 118]. Nanoclusters have discrete electronic energy levels as opposed to the bands of nanoparticles [99] and have multiple absorption peaks [99]. The use of these smaller particles was considered for this application as their decreased size may lead to fewer peaks caused by fragmentation of the nanoparticle. There is less literature on nanoclusters than nanoparticles, as they are defined, due to their more recent discovery, but there have been a number of different types synthesized. The purpose of many experiments was to understand their properties and reaction mechanism of the synthesis [101, 119-121], which included the use of MALDI. In these experiments the nanoclusters, with 25 and 145 Au atoms, were analytes, not as assisting mediums and MALDI was used to measure the size of the clusters [122-125]. An investigation that looked at 3 different sizes ruled out a gold nanoclusters

with a 21 atom core, as useful for this investigation because it generated a LDI peak at around 300  $m/z$  <sup>[99]</sup> which is in analyte range of interest. The method chosen created thiolated Au<sub>25</sub> clusters, with the addition of phenylethyl mercaptan via a facile one-phase method <sup>[118]</sup>. The structure of phenylethyl mercaptan can be seen in Figure 1.11, it has a molecular mass of 138.228  $gmol^{-1}$  and the phenyl groups, as mentioned in the introduction to silicon nanoparticles, may aid in desorption and ionization. This method was investigated for phenylethyl mercaptan attachment, as well as an altered version, to investigate any effects that might be seen from 4-mercaptobenzoic acid functionalisation.

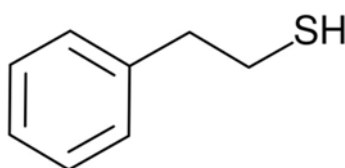


Figure 1.11: Molecular structure of phenylethyl mercaptan

## 1.5 Drug samples

Whether licit or illicit, drug analysis is of high interest in a range of areas of life. They can be analysed from pure samples or in human samples after consumption. The analysis of drugs in their pure form is useful in the confirmation of synthesized products and the confirmation or identification of seized controlled substances. Drugs can be used for medical and recreational purposes. The monitoring of both the licit and illicit use of drugs is vital in modern society and the mode and ease of analysis is important. Drug testing is necessary for maintaining sobriety in the workplace, or to assess those in rehab programs. They are also very important to prevent driving under the influence. While not all drugs tested for are illegal, some prescription and over the counter medicines are not suitable for the use of heavy machinery or in workplace environments.

### *Drug tests*

Increased usage of drugs, awareness of the consequences and the control of such substances has led to an increased need for sensitive drug tests. Initial drug tests are on the spot drug screens, which are able to identify the presence of different classes of drugs, based on reactivity, often with biological assays <sup>[126]</sup> and are typically followed up with other conformational methods. These immunoassays are screening processes based on the specificity of biological affinities. Certain enzymes only react with compounds of the appropriate size and structure <sup>[127]</sup> giving binary results which are either positive or negative and are susceptible to false positive results.

Drug detection can be carried out from various bodily sample types including blood, urine, oral fluid and hair, these are collected using various techniques. The collection of the most common types of

sample, blood or urine can be invasive uncomfortable and inconvenient. Not all circumstances which require urine tests can be as stringently observed or controlled as other methods and rely on having a full bladder <sup>[128-130]</sup>, they are also susceptible to tampering. There are three primary types of adulteration: in vivo, in vitro and substitution. In vivo involves taking a substance to alter the sample, this can be something as simple as water to dilute the urine sample, there are also a range of chemicals that can be taken. In vitro involves adding an adulterant to the sample and substitution is replacing the sample with a different sample <sup>[131]</sup>. Blood samples are the most reliable but cannot be taken without the appropriate qualifications <sup>[128-130]</sup>. Hair samples are ideal for long term drug monitoring as drugs are stored in the hair, each shaft providing a timeline for usage <sup>[132]</sup>. Drugs can be detected in hair for between 7 and 100 or more days, urine for 1-3 days and oral fluid 1-36 hours <sup>[132]</sup>. These difficulties with other sample types has increased interest in drug testing based on oral fluid (OF). Oral fluid is often casually referred to as saliva, however, the two are distinctly different. Oral fluid is a mixture of fluids from a variety of glands and crevices in the mouth, whereas saliva comes from a specific gland and is just one component of oral fluid <sup>[133, 134]</sup>. Oral fluid also contains other products from the mouth, such as cells, food debris and biological organisms found in the mouth <sup>[133, 134]</sup>. Oral fluid, as shown by the ROSITA (Roadside testing assessment) investigation, is the most popular alternative sampling method to blood <sup>[128]</sup>. The preference for oral fluid is due to the less invasive means of collection <sup>[128-130]</sup> which can be observed <sup>[129]</sup> and overseen by non-medical personnel <sup>[128]</sup>. Unlike urine oral fluid is consistently present in the body, oral fluid also has an appropriate correlation to the impairment being experienced by the drug user <sup>[128, 135]</sup> as well as to the relative plasma concentration <sup>[134, 136]</sup>. While this is not a requirement of drug testing, it is advantageous as it provides a better context to the result. Another advantage of oral fluid testing is that the major analyte detected for this sample type is the parent drug, rather than the metabolites <sup>[130, 137]</sup>. This may provide explain why oral fluids provide a better correlation with impairment than other samples <sup>[137]</sup>. The increased presence of the parent drug is associated with lipophilicity of the drugs providing a pathway into oral fluid via passive diffusion through the lipid membranes <sup>[133]</sup>. These drugs are also hydrophilic enough to stay in the oral fluid, the ionizability of most drugs makes them more soluble in the water-based oral fluid <sup>[133]</sup>.

The drug classes most often analysed for are benzodiazepines, cannabinoids, amphetamines, barbiturates, opiates and cocaine <sup>[128]</sup>. Some popular oral drug screen brands available include Oraline, Orascreen and Toxsure, which look at a range of illicit substances <sup>[138]</sup>. In South Australia, drug tests initially only screened for  $\Delta$ -9-tetrahydrocannabinol (THC) which is the active ingredient in cannabis <sup>[139]</sup>, methamphetamines and methylenedioxymethamphetamine (MDMA), commonly known as ecstasy <sup>[139, 140]</sup>. More recently the range has been expanded to include other drug classes like

barbiturates, cocaine and diazepam <sup>[141]</sup>, however the drugs mentioned above are still the types most commonly screened for. Oral fluid drug screens provide an initial indication whether a drug is present but require confirmation. When oral drug tests are found to be positive, like the proceedings followed with alcohol testing, a urine or blood sample is taken to confirm these findings. Confirmatory techniques are often performed with Gas Chromatography (GC) <sup>[142]</sup>, Gas Chromatography Mass Spectrometry (GCMS) <sup>[142, 143]</sup> or High Performance Liquid Chromatography (HPLC)<sup>[142]</sup>. An LDI method of analysis, may, however, be used to analyse the oral sample quickly to confirm the presence of drug or false positive and to differentiate between drugs of the same class. As mentioned in the previous chapter there are a number of drugs that have been analysed by LDI for different purposes. An antipsychotic drug, olanzapine, has even been used as an alternative matrix in the analysis of peptides<sup>[144]</sup>. It was shown to be as effective as a matrix as CHCA and investigated to precisely test its thermochemical properties<sup>[144]</sup>. This showed it to be similar to standard matrices <sup>[144]</sup>. Having properties similar to those of a matrix is an encouraging feature for drugs as analytes of LDI. As previously mentioned, DIOS-MALDI was used in the analysis of amphetamines from roadside drug tests of oral fluid, these samples were, however, liquid saliva samples. The drug collection method in this investigation focused on fibres taken from oral drug tests. If the fibres used for on the spot tests are proven to be storable and able to be used again in the lab to identify or confirm the specific drug, rather than just for the determination of class, further testing can be less invasive and quick. These samples, under the correct conditions might also be able to be stored for future reference or later testing. LDI as a high throughput, sensitive and specific instrument would be useful for the analysis of these samples. As it can target different mass ranges, low mass analysis would not be impacted by interference of any biologicals found in the mouth as they are typically of be higher mass.. The parent drug being the primary product of drug testing in oral fluid is also advantageous for analysis as it means that the parent drug is the only sample to look for in the analysis.

### *Other drug samples*

An alternative use for this fibre-based method is in analysing samples associated with attempted smuggling. As seen in Pablo Escobar's biography<sup>[145]</sup>, where a pair of jeans were soaked in an illicit solution and worn, or transported as needed, fabrics have been used previously as a vehicle for transporting illegal drugs with minimal suspicion. Similarly, a woman entering the Republic of Ireland from South America was found to be smuggling cocaine impregnated into the fibres of her clothing <sup>[146]</sup>. DESI has been used in the past to investigate a range of different fabrics embedded with drugs and high explosives <sup>[42]</sup>, in a simulation of airport security-based screening of passengers and luggage. The fabrics involved could be as inconspicuous as paper in a book, other items of clothing or luggage.

A method of analysis that would do minimal damage to potential evidence would be ideal for such situations.

### *Drugs to be analysed*

In this thesis a few drugs are initially investigated, with a narrowing focus on codeine to optimise the technique. The drugs used are discussed below. The opioid drug class is based on the natural drug opium, which comes from the poppy flower, and can include a range of different drugs <sup>[147]</sup>. The opioid drug class includes opiates which are direct opium derivatives, such as codeine and morphine, semi-synthetic derivatives; such as heroin and oxycodone, and entirely lab synthesized drugs like methadone <sup>[147]</sup>. The most prominent action of opioids is analgesia, or pain relief, other effects include support for anaesthetics and cough suppressing, and they can also cause drowsiness <sup>[147]</sup>. The effects of the different opioid drugs are similar but differ in terms of intensity of effects, oral absorption rates, lipid solubility, analgesic potency, duration of action and rate of metabolism <sup>[147]</sup>. The pain relief provided by opioids is the strongest of analgesic drugs and is capable, in large doses, of euphoric effects, as well as decreased anxiety <sup>[142, 147]</sup>. These side effects, and the emotional numbness often felt as a side effect, contribute as causes for the recreational use and consequent addiction to opioids <sup>[142]</sup>. A physical side effect associated with overuse is related to respiratory issues, specifically the over-relaxation of respiratory muscles, which can lead to death <sup>[142]</sup>. The three most popular drugs in the opioid class are morphine, codeine and heroin, which are discussed further in the following paragraphs. Fentanyl is a synthetic opioid increasing in popularity but was not explored in detail here but warrants investigation in future applications of this research. An important problem associated with all drug testing is the continued increase in new and synthetic drugs being manufactured at a rate faster than they can be researched and prohibited.

Morphine was the first drug to be derived from opium, the discovery of morphine incited further research into purifying other natural drugs, as well as developing other opioids <sup>[142]</sup>. All opioids are metabolized back to morphine in the body, which can be further metabolized <sup>[142]</sup>, therefore the effects of all opioids mimic those of morphine <sup>[147]</sup>. Morphine will be analysed in the form morphine hydrochloride, a drug used in the medical industry, but is illicit for unlicensed use.

Codeine is a less potent version of morphine and is, therefore, less addictive and is found in a variety of over the counter drugs <sup>[142]</sup>, such as antitussives and painkillers, often blended with paracetamol and ibuprofen. As a more easily accessible drug codeine will be analysed in these experiments in the form codeine phosphate. The frequent use of this drug may be mistaken in a positive drug test for an illicit opioid, like heroin, but it is a drug that is frequently abused.

Heroin is an illegal substance originally derived from morphine to synthesise a drug with similar painkiller power but less addictive. The resultant drug, however, was a stronger, more addictive painkiller [142]. Heroin is used medically in cases of severe pain often associated with terminal illness [142]. The potency of heroin can be attributed to the active nature of not only the parent drug but also the first metabolite, 6-monoacetyl morphine (6-MAM) [148]. Heroin is quickly converted to 6-MAM [148] and it is this species that can be detected in drug tests. 6-MAM may still be detected in oral fluid when it may not be present in urine due to a short half-life [149]. 6-MAM is specific to heroin metabolism, it is not a metabolite of codeine or morphine in the body [142] it is therefore a specific indicator for the use of heroin.

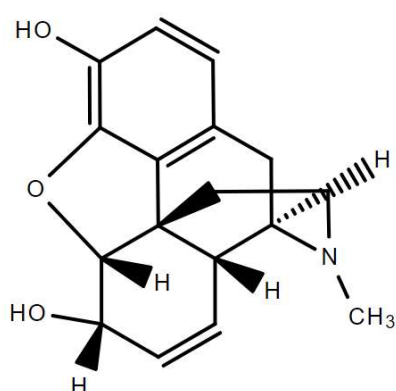


Figure 1.12: Molecular Structure of Morphine [142]

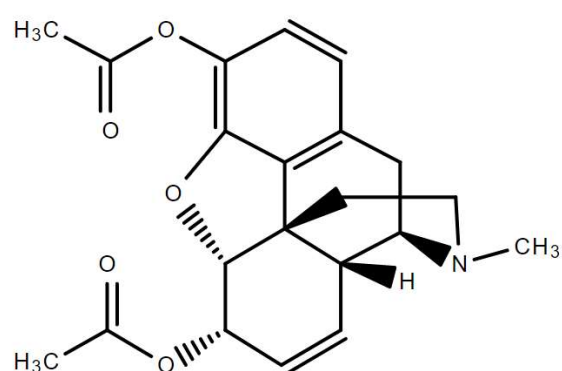


Figure 1.14: Molecular Structure of Heroin [142]

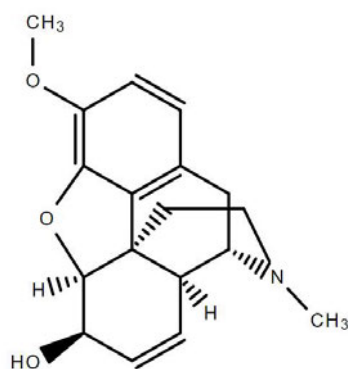


Figure 1.13: Molecular Structure of Codeine [142]

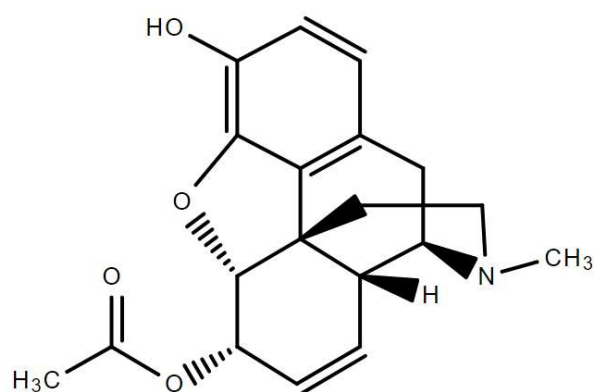


Figure 1.15: Molecular structure of 6-monoacetyl morphine [142]

The opioid drug class is a good example of why this research is important. Within this class of drugs three of the primary forms range from over the counter, to prescription to an illegal substance. Being able to differentiate these three forms of opioid from the fibres of an oral drug test would be greatly advantageous. The structures of these drugs are very similar as can be seen in Figure 1.12, to Figure 1.15. They differ in side groups where morphine contains a hydroxide, codeine has an ether group,



and heroin and 6-MAM contain esters. This makes each drug a different molecular mass, codeine is  $299.36 \text{ g}\cdot\text{mol}^{-1}$ , morphine is  $285.34 \text{ g}\cdot\text{mol}^{-1}$ , heroin is  $369.41 \text{ g}\cdot\text{mol}^{-1}$  and 6-MAM is  $327 \text{ g}\cdot\text{mol}^{-1}$ . The differences in mass means they can be differentiated via mass spectrometry, especially using a soft ionization technique that minimizes fragmentation. These drugs also contain benzene rings, which may efficiently absorb UV light found in the LDI laser.

Amphetamine is defined as a class of drugs consisting of synthetic stimulants, which are derived from the base amphetamine structure <sup>[150]</sup>. The use of drugs in this class started innocently enough; there are a number of medical applications for which various amphetamines were used including narcolepsy, nasal congestion, obesity and treatment for attention deficit hyperactivity disorder (ADHD) <sup>[139, 150]</sup>. Amphetamines were used heavily throughout World War II to treat a variety of ailments, including shock, barbiturate overdose and encephalitis <sup>[150]</sup>. They were also used along with caffeine and other stimulants to increase soldier's stamina and keep them awake for longer <sup>[151]</sup>. Simple chemical substitutions alter the structures to produce different drugs with a range of clinical effects. As stimulants there are a number of effects that are common in amphetamine use associated with a general increase in processes in the body, including raised heart rate, blood pressure, breathing rate, sweating and body temperature, and twitching <sup>[150, 152]</sup>. Other side effects, which have led to the abuse and subsequent illicit status of these drugs, include euphoria, increased stamina and decreased appetite <sup>[150, 152]</sup>.

Amphetamine and Methamphetamine are discussed below, analysis in this class is important as these drugs, though similar in their structure have very different applications, amphetamines can still be used to treat behavioural disorders and narcolepsy <sup>[139, 150]</sup>, while methamphetamine is much more commonly used as an illicit party drug or hard drug <sup>[152]</sup>.

Amphetamine, the drug was initially synthesized as a replacement for the plant derived ephedrine <sup>[150, 152]</sup>. As a chiral molecule, there are two enantiomers of amphetamine, both with similar clinical properties but different potency than the other <sup>[152]</sup>. Amphetamine based medicines consist of both enantiomers in different ratios adapted into different salts.

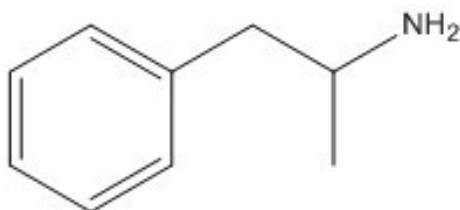
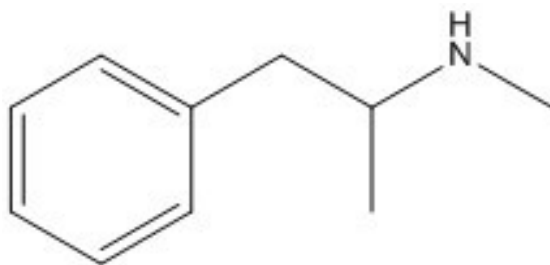


Figure 1.16: Molecular structure of amphetamine

Amphetamine sulfate is the sample used throughout these experiments <sup>[152]</sup>. The structure of Amphetamines can be seen in Figure 1.16. Once again, the benzene ring is present, this structure has a molar mass of  $135.21 \text{ g}\cdot\text{mol}^{-1}$ . Amphetamines come in powder and tablet forms with a variety of delivery methods, these include ingestion, injection, smoking and snorting <sup>[150]</sup>.

Methamphetamine was developed not long after amphetamine; its structure only differs in the addition of a methyl group to the Nitrogen of the amino group, as can be seen in Figure 1.17. While it is similar to amphetamine, it is considered to have stronger and more rapid effects <sup>[150]</sup>. It is available in liquid and crystal form, the crystal form is a high purity product known as ice, which exists as a hydrochloride salt <sup>[150]</sup>. Methamphetamine also gives its user increased energy and concentration, as compared with amphetamine <sup>[150]</sup>.



**Figure 1.17: Molecular structure of methamphetamine**

The methamphetamine used in these experiments was in liquid form as a hydrochloride. The structure seen in Figure 1.17 differs from amphetamine in the methyl attachment on the amine group. This drug has a molar mass of  $149.23 \text{ g}\cdot\text{mol}^{-1}$ .

## 2 Experimental

### 2.1 Instrument settings

The instrument used throughout this research was the Bruker Autoflex III MALDI MS/MS, which is housed in the laboratories of Flinders Analytical. The following settings were used consistently throughout. Each experiment discussed in the following chapters was carried out under these conditions, unless otherwise indicated. It was used in positive reflectron mode, in the low mass range the instrument, classified as less than 2000 m/z although most of the low mass values are below 800 m/z, with no matrix suppression. A 337 nm pulsed Nitrogen laser was used in this instrument and laser strength varied throughout analyses. The laser fluence is controlled on a percentage scale ranging from to 100% using a lower laser fluence is preferable, this should result in less background peaks in the spectra as particles that are not of interest are excited. Lower laser usage also means less power output from the instrument. Most spectra consisted of the combination of 10 pulses at 100 shots per pulse, and the analysis software was FlexAnalysis.

Table 2.1: MALDI spectrometer settings

Spectrometer	
Ion Source 1	19.00-19.08 kV
Ion Source 2	16.80-16.87 kV
Lens	8.25-8.29 kV
Reflector 1	21.00-21.33 kV
Reflector 2	9.40-9.48 kV
Pulsed Extractor	0 ns
Matrix Suppression	OFF

Table 2.2: MALDI detection settings

Detection	20.20-20 Low mass range
Detector Gain	Reflector 3.3X
Sample Rate	2.00
Resolution	2.00 GS/S
Electronic gain	Enhances 100 mV
Realtime smooth	OFF
Spectrum size	93368 pts

Delay	10608 pts
-------	-----------

Table 2.3: MALDI setup settings

Setup	
Low Range Mass	
Frequency	200 Hz
Digitizer	1000 mV
Detector gain voltage offset	Linear 1300 V
	Reflector 1400 V
Laser Attenuator	Offset 66%, Range 30% Set – 5-Ultra
Laser Focus	Offset 0% Range 100% Value 120%
Shots added	100
Frequency	200

### Calibration

Calibration is a vital step in the use of LDI-MS. It must be completed prior to each set of analyses and is required to ensure accuracy in the mass spectrum. This is done via the analysis of a reference material in the correct mass range that is known to have a consistent repeating unit. These known masses can be used to ensure the instrument is in ideal order before use. The original calibrant used was Caesium Iodide (CsI); it is a relatively low mass calibrant, with cluster peaks ranging from 133 to 1172 m/z. This was made up in a solution of 100 mg/mL in deionized water. The peaks in positive analysis, consisting of a variety of ions formed by combinations of Caesium (Cs) and Iodide (I), are shown in Table 2.4 and Figure 2.1

Table 2.4: CsI calibrant positive peaks

Positive Ion	Peak position (m/z)	Actual peak position (m/z)	Difference (%)
Cs <sup>+</sup>	132.905	132.731	-0.131
Cs <sub>2</sub> <sup>+</sup>	265.810		
Cs <sub>2</sub> I <sup>+</sup>	392.715	392.397	-0.081
Cs <sub>3</sub> I <sub>2</sub> <sup>+</sup>	652.525	652.066	-0.070
Cs <sub>4</sub> I <sub>3</sub> <sup>+</sup>	912.335	911.958	-0.041
Cs <sub>5</sub> I <sub>4</sub> <sup>+</sup>	1172.145		

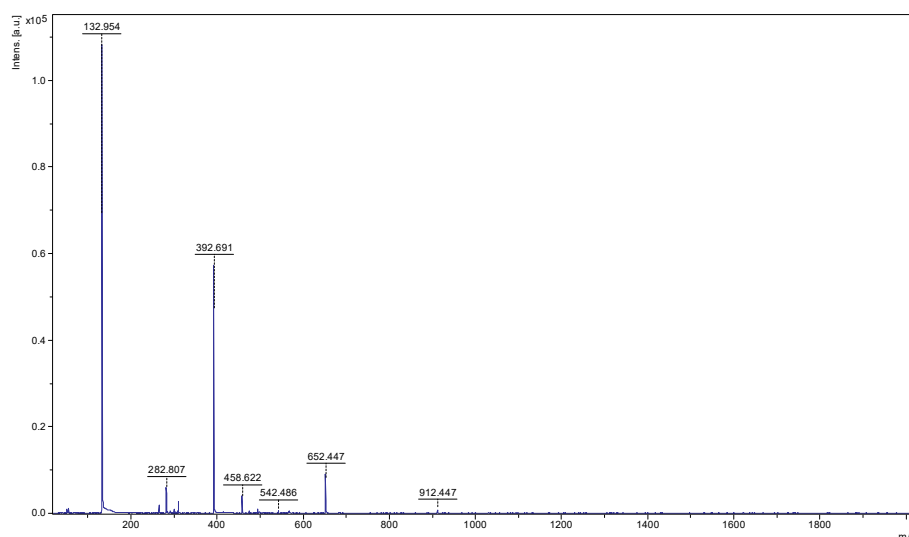


Figure 2.1: Spectrum of CsI calibrant from the MALDI plate

## 2.2 Sample Preparation

### Solutions

Drug	Source
Codeine phosphate	FSSA provided standard
Morphine hydrochloride	FSSA provided standard
Methamphetamine (liquid form)	Synthesized by another student at Flinders University
Amphetamine sulfate	FSSA sourced, labelled suspected amphetamine

When the FSSA standard source of codeine phosphate ran out, it was sourced from a basic separation from over the counter analgesics, the procedure of which is detailed below. When this sample was analysed via LDI in the same way as the FSSA standard the spectra gave spectra with the same peaks with similar strengths indicating no impurities.

Codeine was accessed from over the counter tablets, specifically panadeine forte, each tablet of which is reported to contain 500 mg of paracetamol and 30 mg of codeine. In order to extract the codeine from the other contents of the tablets the simple procedure outlined below was followed<sup>[153]</sup>.

It was calculated that 6 tablets would yield 0.18 g of codeine phosphate. These were crushed and mixed with 300 mL of water then filtered using a Buchner funnel – this removes the binding agents, diluents and other non-aqueous soluble additives. The filtrate was then placed in a separating funnel, to which solid sodium hydroxide (NaOH) was added slowly to increase the pH to 11; this was tested with universal indicator. The basic codeine was extracted with around 5 mL of chloroform for three washes. The chloroform was evaporated using gentle heat. The remaining codeine was made up to concentration using water. The aqueous layer contained the paracetamol.

All other drug samples were made to solutions in the concentrations detailed in Table 2.5, with deionized water.

**Table 2.5: Concentrations and molar masses of drug solutions**

<b>Drug</b>	<b>Concentration</b>	<b>Molar Mass</b>
<b>Codeine phosphate</b>	0.1 mg/mL	299.364 g.mol <sup>-1</sup>
<b>Morphine hydrochloride</b>	0.54 mg/mL	285.34 g.mol <sup>-1</sup>
<b>Methamphetamine (liquid form)</b>	10-fold dilution	149.2337 g.mol <sup>-1</sup>
<b>Amphetamine sulfate</b>	0.74 mg/mL	135.2062 gmol <sup>-1</sup>

All drug samples were analysed in the above concentrations throughout the experiments detailed in this chapter. The primary drug of interest was codeine, due to its availability, its over the counter nature, the fact that it is used frequently and its direct relation to more illicit drugs. All samples were analysed via LDI either directly from the MALDI plate or from the fibres, whose preparation is described below. Those analysed from the plate were always pipetted in triplicate in the pre-set wells. Each time 1 µL was used per well and these spots were allowed to dry before analysis could be conducted, not only to prevent disturbance of the sample but also because moisture slows down the vacuum process in the MALDI. In situations where multiple layers were required for sample preparation, each layer was allowed to dry prior to adding the next.

### *Fibre analysis*

To analyse drugs from paper, the liquid samples were first soaked into paper sources, before single fibres could be removed. The samples were analysed from two types, stock printer paper and filter paper. To remove single fibres from the paper a sharpened tungsten wire and super fine point tweezers were used under the magnification of an Olympus S260 Microscope at 400 times magnification. Small samples were obtained by digging in the wire and pushing up the top layer of fibres. They were then removed using the tweezers and placed directly onto tape. The tungsten wire was sharpened electrolytically using a carbon electrode and a 10% NaOH solution<sup>[154]</sup>. All fibre-based analyses undertaken throughout this thesis used this method of fibre preparation.

## **2.3 Alternative Matrices**

### *Matrix Free*

The initial experiments discussed were performed using a matrix free method, a term that often refers to alternative matrices or Surface Assisted Laser Desorption Ionization (SALDI)<sup>[16]</sup>, which will be discussed later. In this section the analysis was done without any means of assistance at all, to determine if drugs had any ability to be analysed without assistance. Codeine was analysed matrix free at 0.1 mg/mL from the MALDI plate. 1  $\mu$ L of the solution was pipetted in triplicate onto wells of the plate, giving three 1  $\mu$ L sample spots. These spots were then allowed to dry and analysed using the settings indicated above in the instrument settings. The laser energy required for this analysis was between 90-100%.

### *Surface Assisted Laser Desorption Ionization*

Several double-sided tapes, with varying conductivities were used to attach solid samples to the plate. To confirm their conductivities their individual voltages were measured using a multimeter. The crocodile clips were clamped onto different segments of an intact piece of each tape and the resistance in ohms was read from the screen display. These tapes were of varying thickness and composition and it was thought that changes in elevation and thus starting point may alter the starting points of the ions and thus the accuracy of the spectra. Due to the high sensitivity of the instrument and the large drift distance it was deemed unnecessary to make any adaptations. These tapes were stuck to the plate in small enough sections that the sample well positions could be easily predicted. The solutions were pipetted onto each of the tapes for baseline analysis. Single fibres of the samples were then removed using the procedure described in the sample preparation above and placed on each of the different tapes.

### *Graphite*

An EXP HB pencil was used in a rubbing motion to transfer graphite onto the surface of a piece of paper; 3 drops of each sample were then spotted onto separate pieces of graphite coated paper. These were allowed to dry before sampling. Sampling involved removal of fibres being adhered to the plate on copper, carbon and double-sided tape. Further to this analysis a piece of paper was removed using a hole-punch and adhered with double-sided tape to maximize sample surface area. Samples were taken at maximum laser intensity.

### *Binary Matrix*

Preparation of the binary matrix began with the dilution solution consisting of 50% acetonitrile and 0.2% trifluoroacetic acid in milliQ water. Separate 10 mg/mL samples of 3-HC and 6-ATT were made using the dilution solution. These were mixed in equal parts and vortexed to combine.

To analyse using this matrix a ratio of 1:2 analyte: matrix was initially used for all four drug samples. The analyte and matrix were mixed together thoroughly before spotting onto the sample plate and loading onto the paper, before removing fibres and adhering to the plate using the same procedure and tape options mentioned in above. Further to this, the codeine was mixed with the binary matrix in ratios of 2:3, 1:3, 1:5, 8:1, 10:1 and 15:1 which were also investigated in the same manner to optimise the process. Samples of the individual matrices as well as the combination of both were also analysed from the plate and from fibres samples to understand any background spectra.

## **2.4 Nanoparticles**

### *Silicon Nanoparticles*

The silicon nanoparticles used and method described below were provided by Dr Daniel Mangos from processes developed during his PhD at Flinders University <sup>[155]</sup>.

To a container of 46.4 mL of water 3.6 mL 28% ammonium ( $\text{NH}_4$ ) was added. This mixture was stirred using a magnetic stirrer at a high enough rate for a vortex to be seen until the mixture was completely homogenous, which took around 10 min. 1 mL of phenyl functionalised mercapto-silane was then added dropwise to form layer. This mixture was then stirred until this layer dropped to the bottom; this was then stirred again on high for 30 minutes. These particles were provided both as a solution and in dried form.

A scanning electron microscope (SEM) was employed to confirm the presence and conditions of the silicon nanoparticles after the initial analysis. The provided solution of the sample was sprayed onto



paper using a pump-action dispenser and the paper was then stuck to the mount using carbon tape and viewed on the screen by a trained instrument operator.

The dried particles were solvated using four different solvents: Ethyl Acetate, Ethanol, Acetone and water. 200  $\mu\text{L}$  of each solvent was added to small amounts of dried nanoparticles, sampled using a capillary tube and mixed.

10  $\mu\text{L}$  of codeine solution and 10  $\mu\text{L}$  SiNPs suspended in the solvents were mixed in a 1:1 ratio and agitated to combine, then 4.5  $\mu\text{L}$  of each was pipetted onto the MALDI plate 1.5  $\mu\text{L}$  at a time. Codeine and SiNPs in solvents were also layered on the plate. 1.5  $\mu\text{L}$  of solvated SiNPs was pipetted onto the plate and allowed to dry before being coated with 1.5  $\mu\text{L}$  of codeine solution, and vice versa with SiNPs as the top layer.

Silicon nanoparticles were prepared using ethanol at three different concentrations, <1 mg/mL, 1.5 mg/mL and 4.75 mg/mL. 1  $\mu\text{L}$  of codeine was allowed to dry on the plate before being topped with 1  $\mu\text{L}$  of the nanoparticles in various concentrations. Fibre samples were also prepared in a similar fashion, with equal parts of codeine and SiNPs, and SiNPs as the top layer.

Spectra were taken using 40-60% laser power, consisting of 100 shots, and were accumulated to make up 1000 shots per spectrum, to make it easier to compare spectra.

### *Bare Gold Nanoparticles*

To 48 mL of deionized water on a stirring plate, 2 mL of 0.005 M  $\text{HAuCl}_4$  (49 mg in 25 mL  $\text{H}_2\text{O}$ ) and 600  $\mu\text{L}$  of fresh 0.05 M  $\text{NaBH}_4$  (10 mg in 5mL  $\text{H}_2\text{O}$ ) were added with stirring. The solution turned from pale yellow to a deep red with this addition. The solution was then stirred at room temperature for 2 hours<sup>[84]</sup>. This method produces nanoparticles at about 3.5 nm, which last for a couple of weeks.

The bare gold nanoparticles were pipetted directly onto the MALDI plate for analysis as a blank. They were also diluted for analysis with codeine in factors of 1:2 and 1:4 and undiluted. A sample of 1  $\mu\text{L}$  of codeine was topped with 1  $\mu\text{L}$  of bare nanoparticles. Samples of each drug were also analysed, 1.5  $\mu\text{L}$  of each drug was pipetted onto the plate with 0.75  $\mu\text{L}$  of the pure bare nanoparticles pipetted on top. Further to that, a piece of filter paper was loaded with 1 drop of codeine and topped with 1 drop of the bare nanoparticles, fibres were removed as described previously and adhered to each of the three tapes. Samples were analysed via the LDI settings used in earlier chapters with laser strength of between 30-70%.

### *Thiolated Gold Nanoparticles*

2 mL of thiol solution (3-mercaptobenzoic acid, 4-mercaptobenzoic acid or thiosalicylic acid) of choice (0.95 M, 29.8 mg) was added to a solution of 2 mL of  $\text{HAuCl}_4$  (0.053 M, 40.4 mg) in methanol at 20°C. With vigorous stirring, 1.25 mL of cold  $\text{NaBH}_4$  (0.891 M, 42 mg) was quickly added. Upon this addition the mixture turned immediately black from a pale yellow and was then left to stir for 3 hours at room temperature <sup>[117]</sup>.

Each of the thiolated gold nanoparticles options were applied to the plate and fibres using methods mentioned earlier, using 1  $\mu\text{L}$  of each, over 1  $\mu\text{L}$  of codeine on the plate, and one drop of each on the fibres. These fibres were then applied to the tapes as above and analysed as such. Analysis was done at 50-70% laser strength.

### *Gold Nanoclusters*

To a 3-neck flask, 6.2 mg of  $\text{AuCl}_4$  in 4.4 mL of THF was added and cooled to 0°C in an ice bath. At low stirring speed (~60 rpm) 112  $\mu\text{L}$  of phenylethyl mercaptan was slowly added, this was left stirring for 8 hours or so, once it turned colourless stirring speed was increased (~12000 rpm). After this time aqueous  $\text{NaBH}_4$  (60 mg in 1.5 mL ice cold  $\text{H}_2\text{O}$ ) was rapidly added and this mixture was stirred for another 3 hours. After this time the ice bath was removed and the mixture was allowed to increase to room temperature, this reaction was then allowed to proceed, stirring, for over 60 hours <sup>[118]</sup>.

This technique was also adapted for the attachment of 4-mercaptobenzoic acid. Initially the chloroauric acid was dissolved in water and the 4-mercaptobenzoic acid in methanol. However, the 4-mercaptobenzoic acid seemed to be insoluble and did not dissolve, nor blend well with the gold solution. It was re-attempted, using 15.4 mg of  $\text{HAuCl}_4$  in 5 mL methanol and 121.5 mg of 4-mer again dissolved in 4 mL of methanol, this time, however, more aggressive agitation of the sample was used to dissolve it. The second attempt was also done in a glass vial, as opposed to a 3-neck flask, which was deemed inconvenient and not necessary. Upon addition of the thiol, the gold solution went white and creamy. After the overnight stirring the  $\text{NaBH}_4$  was added, at this point the solution went immediately dark, and was left to stir for another 3 hours before the removal of the ice-bath and a further 60 hours of stirring.

The samples were pipetted onto the plate on top of codeine using 1  $\mu\text{L}$  of each, as well as on the paper samples using one drop of each, like in the previous. sample preparation methods This procedure was repeated using the same samples 4 weeks later.



# 3 Results and Discussion

## 3.1 Alternative Matrices

### *Matrix-free/ Surface Assisted Laser Desorption Ionization*

The process of matrix-free analysis of codeine was performed on a solvated sample from the MALDI plate with no assisting matrix or surface. This resulted in the spectrum seen in Figure 3.1. The peaks of interest occur at 299, 322 and 338 m/z. These peaks represent the molecular ion of codeine, and the sodiated and potassiated adducts respectively. Sodium and Potassium adducts are quite common as major peaks due to their abundant presence in the atmosphere <sup>[67]</sup>. These peaks will be used throughout to identify the presence of the codeine and, therefore, the effectiveness of any matrices, or alternatives used.

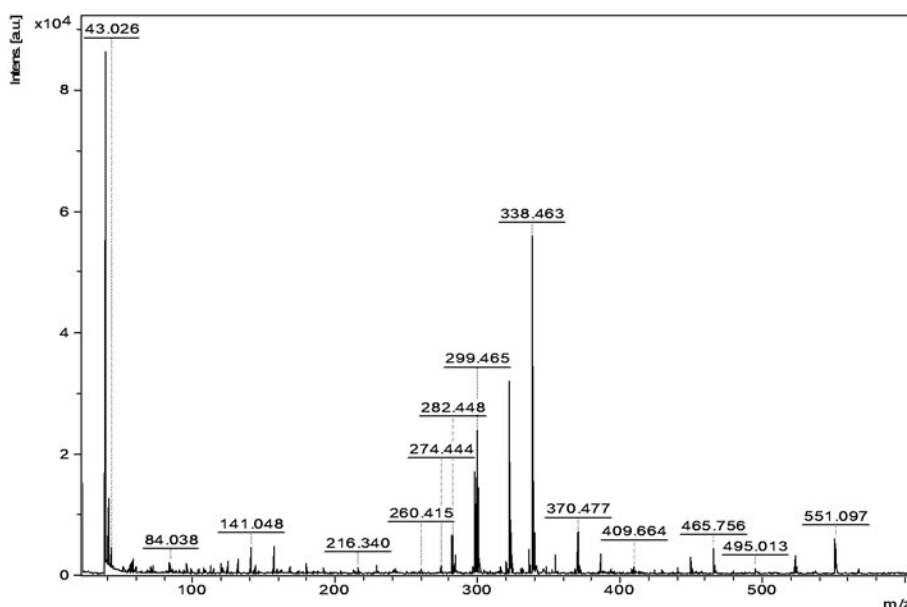


Figure 3.1: Spectrum of codeine from MALDI plate

The codeine was unaccompanied on the plate, i.e. no substances were added to assist, so the presence of these peaks confirmed that it can be analysed alone. However, the laser energy required was very high meaning that this would not be a viable method going forward. Higher laser strength is not a desired setting, as it uses high energy and can damage the sample and lead to more fragmentation. Importantly, despite not being recognised as having matrix-like properties, the peaks of interest for codeine were still found. From these results the concept that the plate was providing the required energy transfer, i.e. to acting as an assisting surface, was concluded. It is proposed that the conductive nature of the steel target plate supported the absorbance of energy from the laser and it to the

analyte. This was an interesting development and was investigated further in the selection of tapes used for adhering the solid fibre samples to the plate.

The conductivities of the copper, carbon and double-sided tapes are shown in the table below in Table 3.1 and confirm that the three tapes investigated cover a range of different conductivities. Copper tape is the most conductive, the least conductive is double-sided tape and carbon tape is medium range.

**Table 3.1: Conductivities of a variety of double-sided tapes**

Surface	Resistance	Conductivity
Copper Tape	0.5 $\Omega$	highly conductive
Carbon Tape	200-350k $\Omega$	moderately conductive
Double-sided tape	$\infty$	not conductive

The carbon tape was selected due its mid-range conductivity and the use of carbon in a variety of forms in LDI, including as carbon tape. The properties that carbon tape possesses which make it an option as an alternative matrix, such as its ability to absorb laser light mean it is also easily analysed in the process. It can be seen in Figure 3.2, in the analysis of a codeine solution from carbon tape, that any peaks associated with codeine cannot be seen amongst those of the strongly analysed carbon tape. It can be seen in Figure 3.3 that there are several evenly spaced peaks separated consistently by 12 m/z. The peaks seen in Figure 3.3 coincide with the peak masses of 8 carbons to 19 carbons. Any other peaks that may be attributed to the codeine analyte are minimized by the very dominant carbon spectrum. This appears to be a case of matrix interference, these carbon cluster peaks have been observed before and occur with the use of higher laser fluence on a carbon rich material <sup>[90]</sup>. As these peaks often appear under 300 m/z <sup>[90]</sup> the use of carbon tape is not ideal for low molecular mass drug based analysis. It can also be seen in Figure 3.2 that there are a numerous tailing peaks in the higher mass region of the spectrum. It is suspected that these peaks are representative of polymers found in the glue of the tape. This is another contaminant associated with carbon tape. In terms of analysis from fibres, the fibres being investigated are very small and there is difficulty associated with aiming the laser at the fibres alone, the combination of this and carbon tapes strong peaks, results in many of the spectra taken being primarily representative of the carbon tape itself. Combined with the difficulty associated with removing the tape from the sample plate this information makes carbon tape a less than ideal adhesive option, however, it was investigated throughout the experiments for consistency, it did not, however, prove to be a useful option in any other experiments.

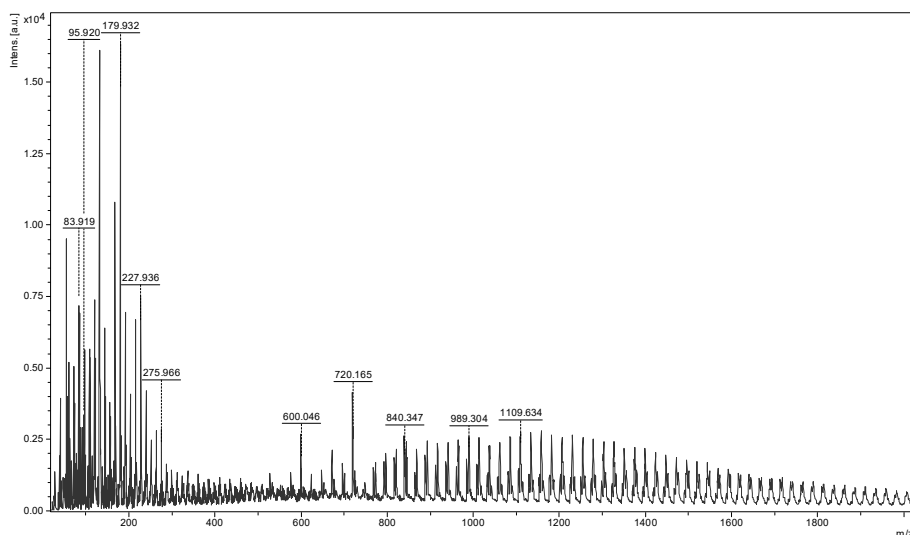


Figure 3.2: Spectrum of carbon tape

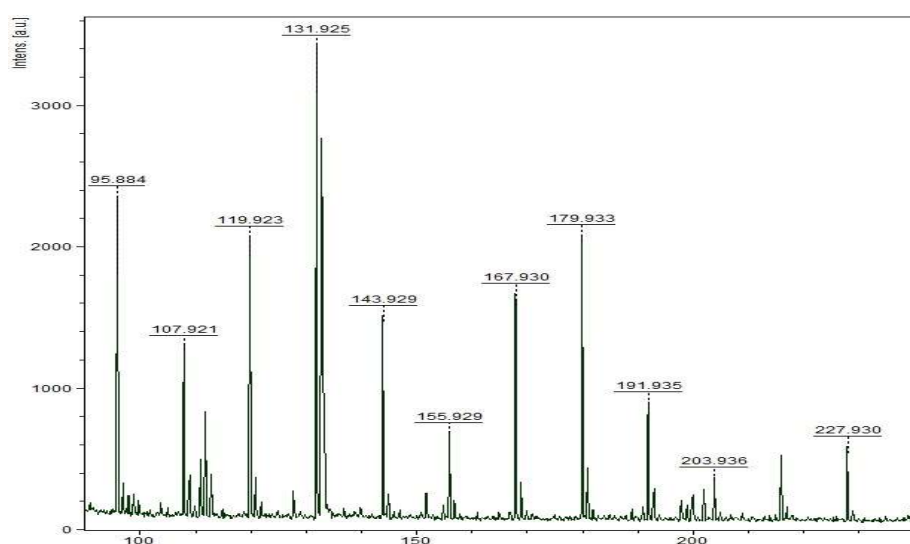


Figure 3.3: Spectrum of carbon tape

The analysis of codeine from copper tape was much more successful than from carbon tape. It should be noted that there is a variation in peak positions for the samples taken from fibres, this is due to the change in height of the sample due to the addition of the fibres and the tapes. The inconsistencies in the surface of these samples is also why these peaks have more side peaks, instead of the single signal. These peaks are therefore described by an approximate value. As can be seen in Figure 3.4 the potassiumated peak ( $\sim 340$  m/z) can be seen strongly, with little background noise present, when a sample was spotted directly onto the tape. The fibre-based sample in Figure 3.5 provided this peak, along with that of the sodiated adduct ( $\sim 320$  m/z), though this spectrum has significantly more background noise and lower signal to noise ratio than the sample directly on the tape. This may be due to interference from the paper itself or a less sample being present on the fibres than on the plate. Again, the laser

power required to see these very small peaks was very high, which is not ideal. This result proved that codeine was able to be analysed from fibres and showed that although a matrix-free method was not optimal, it was possible.

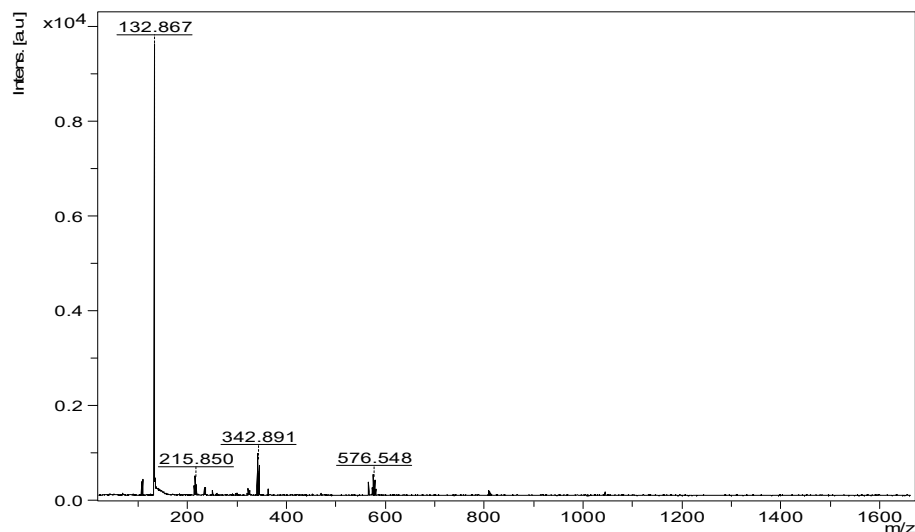


Figure 3.4: Spectrum of codeine on copper tape

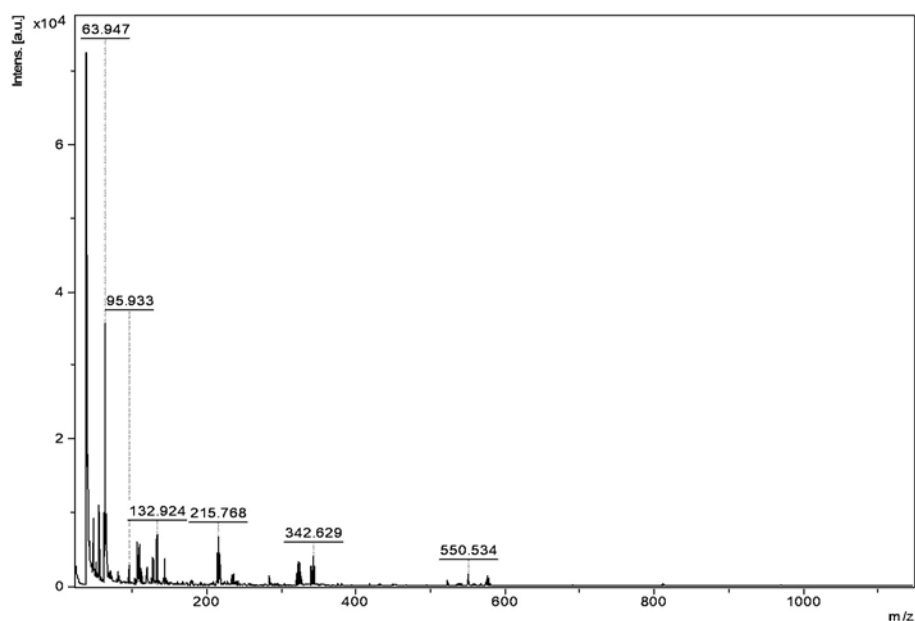
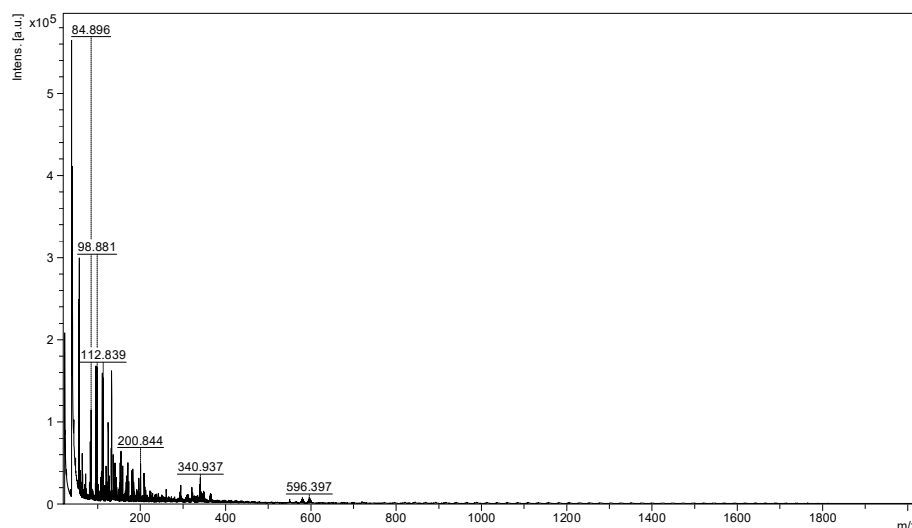


Figure 3.5: Spectrum of codeine fibres from copper tape

The spectrum in Figure 3.6 is that of the codeine fibres on non-conductive double-sided tape. The potassium peak at around 340 m/z was once again seen, though not as strong a peak as in Figure 3.5, there are more and larger background peaks. This result indicates that analysis is still successful on a non-conductive tape as one of the peaks of interest is still present. Although, repetition of the experiment gave the same results for the copper tape more often than for the double-sided tape. This

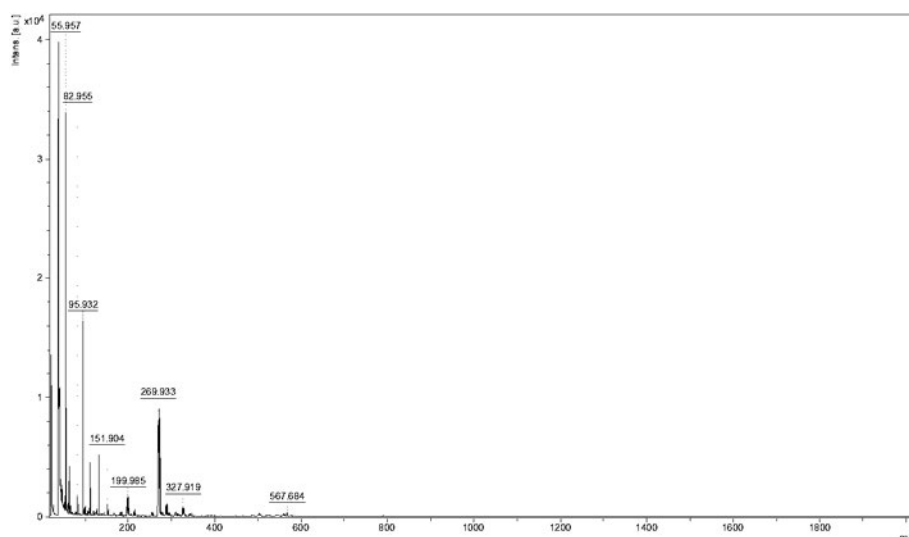
shows that the copper tape method is more reproducible. Copper tape seems to provide conductivity-based assistance for samples soaked into paper, but this assistance may not be strong enough to necessitate its use over a cheaper alternative, like double sided tape. These codeine peaks are present in both methods but not consistently, nor strongly enough for this to be considered an adequate method, once again the laser fluence required was also quite high. Other matrix-like mediums were investigated and introduced to the system.



**Figure 3.6: Spectrum of codeine fibres from double-sided tape**

In the analysis of morphine, it can be seen from the Figure 3.7 below, from a fibre sample on copper tape that there is a larger peak at 269 m/z. This peak may be representative of a morphine ion having lost one of the hydroxide groups. While no spectra of use were encountered for any other combinations of morphine, from either tape it encourages further investigation. It also supports that increased desorption and ionization is provided by the copper tape, as neither of the other tapes yielded any positive results.





**Figure 3.7: Spectrum of morphine fibres from copper tape**

No results of interest were yielded for either of the amphetamine class drugs; their spectra were noisy with small peaks being produced. The focus of this investigation was on optimizing the process for codeine before testing its application on the others, so the other drugs were only investigated for a few of the other techniques used.

### **Graphite**

The application of the graphite to the paper was a simple and very quick process, using an inexpensive and readily available material in a pencil; however, no spectra of interest were yielded for the individual fibres using this method. No peaks were seen across the spectra indicating no sample or graphite was being desorbed or ionized. However, the hole-punched sample did contain some peaks of interest, primarily those around 300 and 320 m/z representing the codeine molecular ion and its sodium adduct, see Figure 3.8. These peaks, while present, were also of low intensity and at 320 m/z the sodiated adduct peak is lower than it is normally found. The hole-punch is not an ideal sampling method due to increased destruction of the sample. Little could be done to optimize this method to improve the spectrum, although application of the graphite could have occurred after sample deposition, it would have been a less viable option, due to the increased chance of tearing the paper during application.

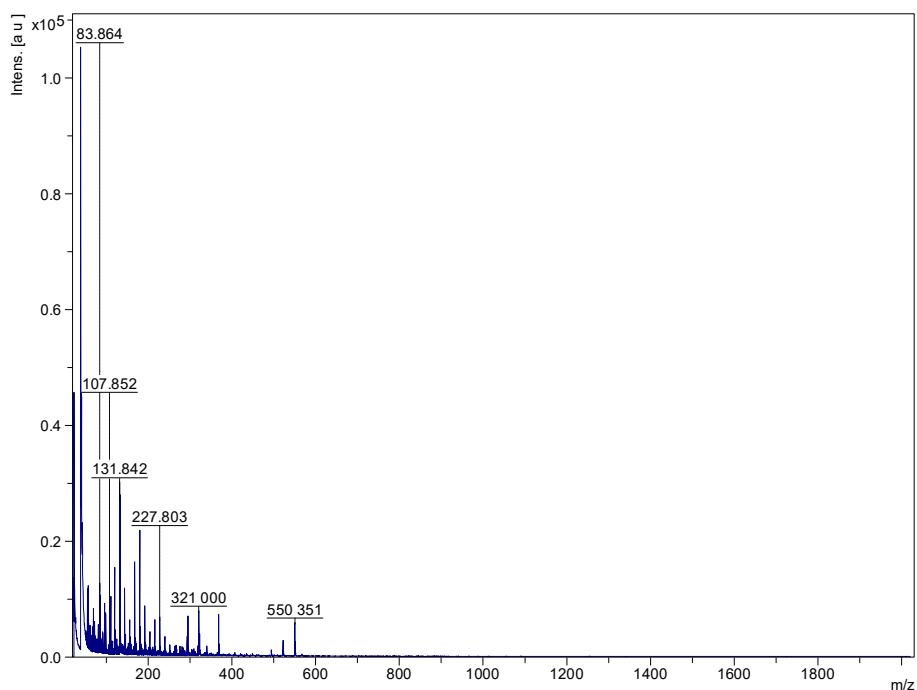


Figure 3.8: Spectrum of codeine with graphite from hole punch

### **Binary Matrix**

The resulting spectra from the investigation of the use of a binary matrix were able to be taken using 30-40% laser strength, this laser fluence is a lot lower than the 90-100% that was required in earlier experiments. This information was not unexpected due to the nature of the compounds, and their favourable use as matrices in MALDI. The spectrum of the combination matrix used, and its individual components can be seen below in Figure 3.9, Figure 3.10, and Figure 3.11. The spectrum of 3-HC in Figure 3.9 shows a number of peaks, at good intensities below 400 m/z.

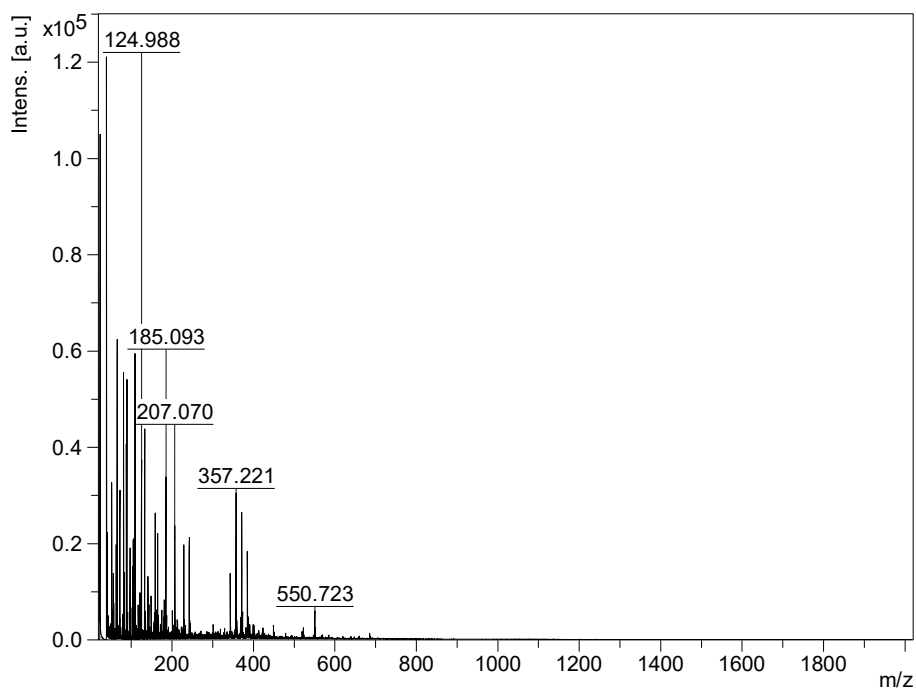


Figure 3.9: Spectrum of 3-HC from MALDI plate

Figure 3.10 shows the spectrum of 6-ATT, which has far fewer peaks than the 3-HC, but has a very strong peak around 285 m/z representing a dimer of 6-ATT. While the low mass peaks in the spectra of both matrices is not ideal for drug analysis, these peaks were predicted to be minimized when combined with a second matrix. The combination spectrum in Figure 3.11 still exhibited a strong 6-ATT peak at 285 m/z and the smaller peaks represented in the spectrum of 3-HC, if a little less intense, than in the individual spectra.

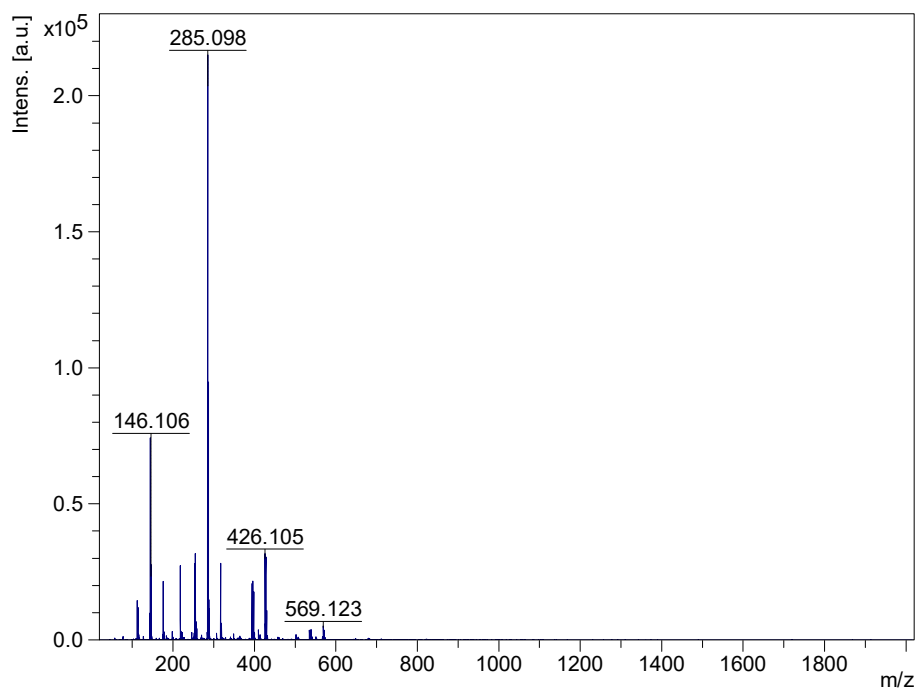


Figure 3.10: Spectrum of 6-ATT from MALDI plate

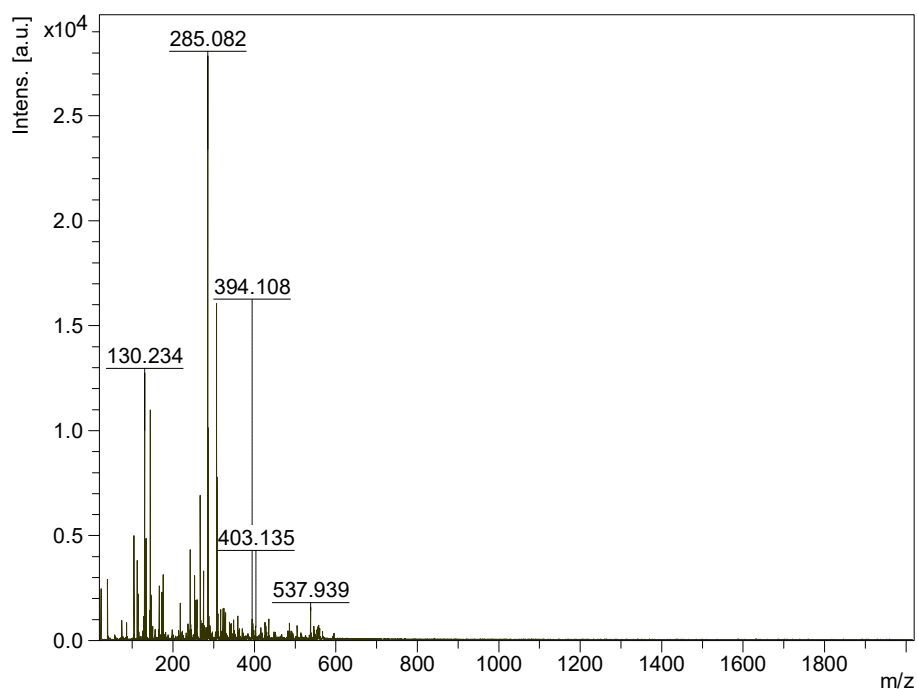


Figure 3.11: Spectrum of binary matrix from MALDI plate

Figure 3.12 to Figure 3.18, shown below are the spectra from codeine solutions assisted by the binary matrix at a range of concentrations. The only peak present is proposed to be that of the codeine molecular ion. The sodium and potassium adducts are not present due to the matrix providing adequate protons to ionize the sample, and not having to use environmental protonation sources. The

peak at 298 m/z is representative of codeine, it is, however, lower than expected. This may be attributed to the calibration having been done as a combination of CSI and the matrix, or due to an interaction occurring between the codeine and matrix molecules. Across the different ratios, those with more analyte than matrix have the strongest codeine peaks as compared to the background peaks. The best combination has the highest peak intensity for the codeine, and the lowest intensity background peaks. There is very little difference between the samples with ratios of 8:1, 10:1 and 15:1, from this 8:1 has been deemed optimal, since it minimized sample consumption and maximized signal peaks. However the 1:5 ratio has a very similar spectrum to the 8:1 and uses significantly less sample than the other options, making it the most advantageous.

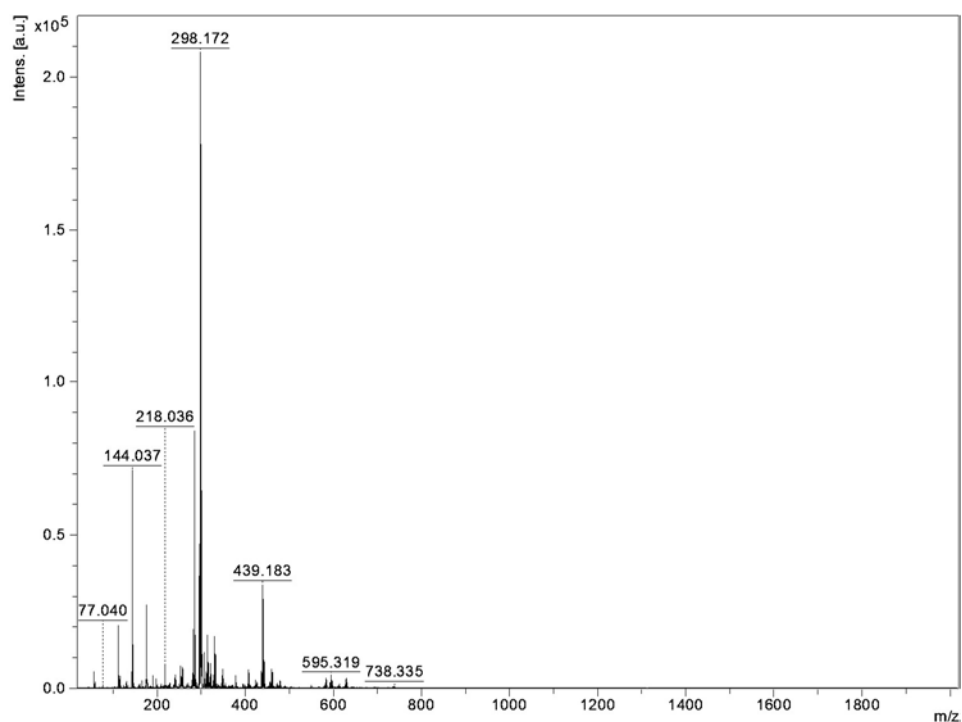


Figure 3.12: Spectrum of 2:3 codeine: binary matrix from MALDI plate

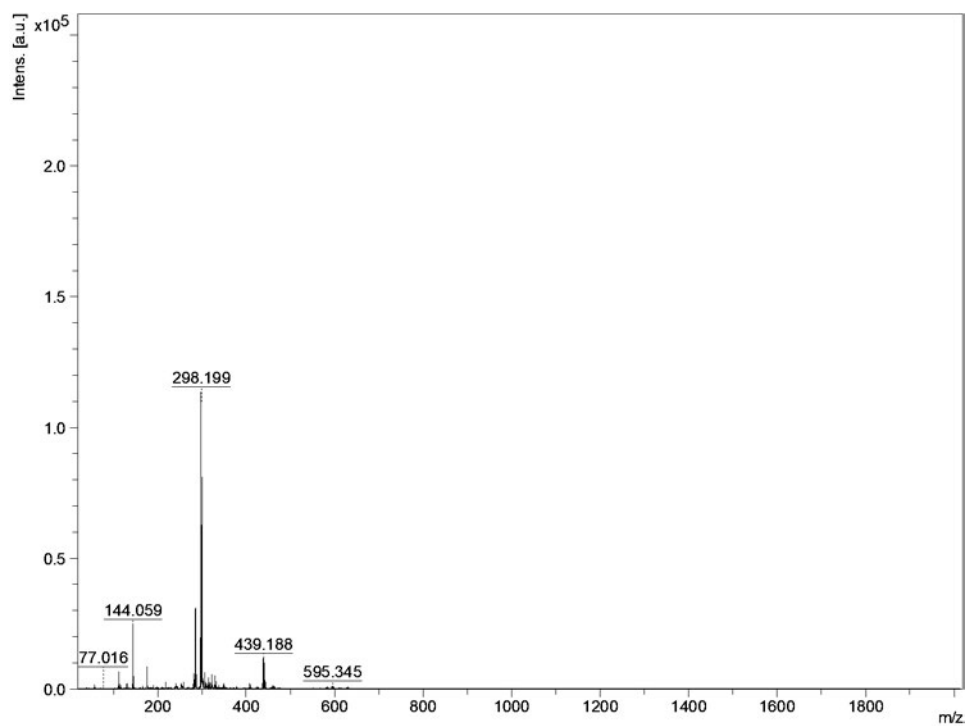


Figure 3.13: Spectrum of 1:2 codeine: binary matrix from MALDI plate

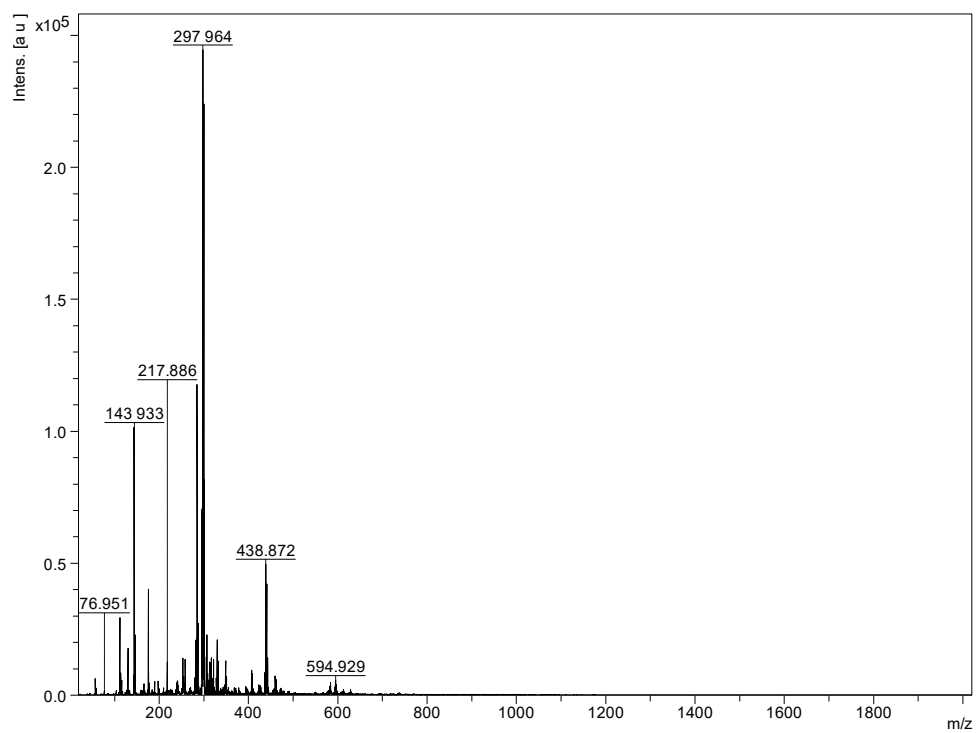


Figure 3.14: Spectrum of 1:3 codeine: binary matrix from MALDI plate

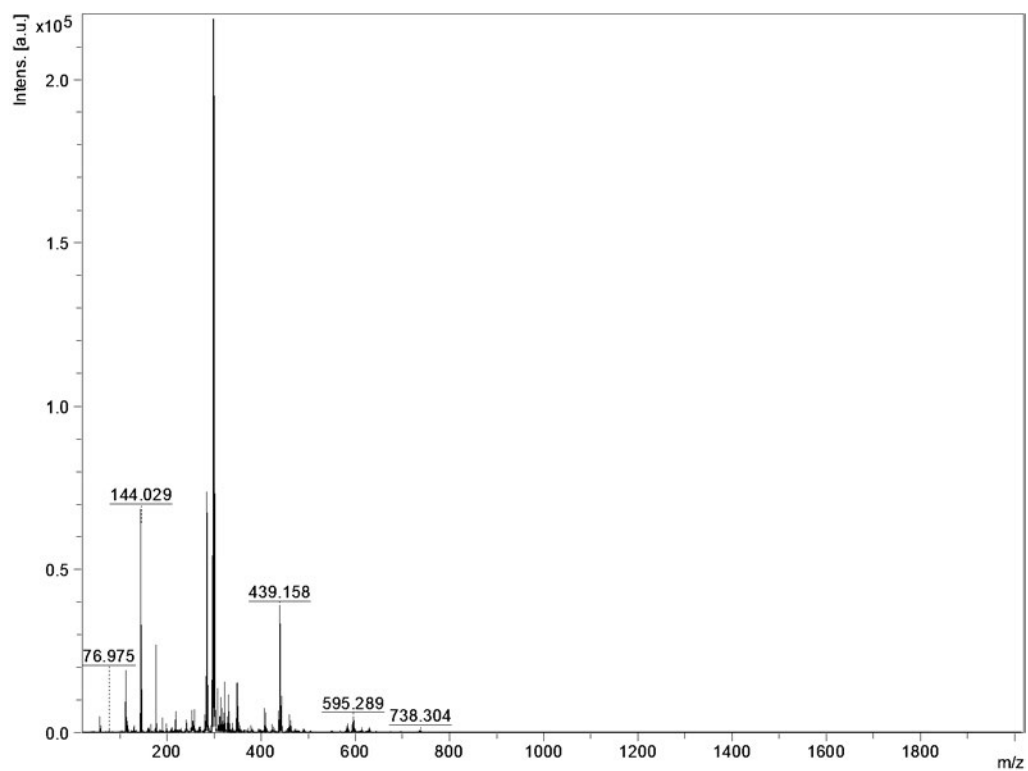


Figure 3.15: Spectrum of 1:5 codeine: binary matrix from MALDI plate

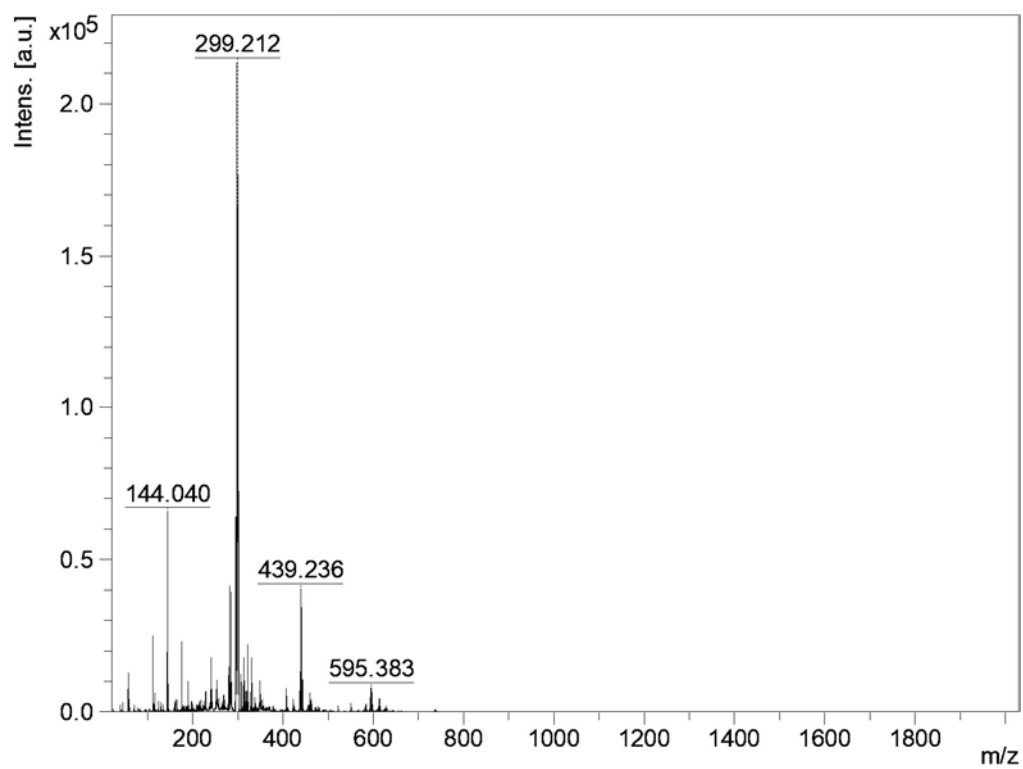


Figure 3.16: Spectrum of 8:1 codeine: binary matrix from MALDI plate

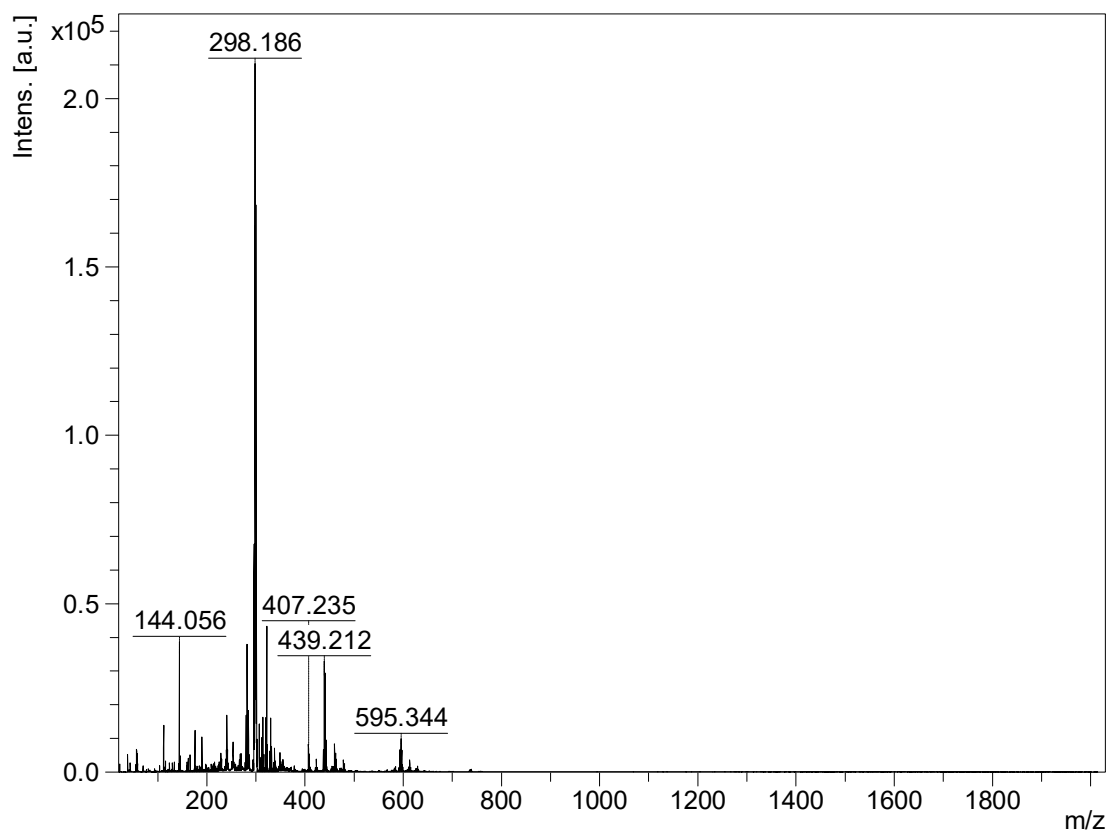


Figure 3.17: Spectrum of 10:1 codeine: binary matrix from MALDI plate

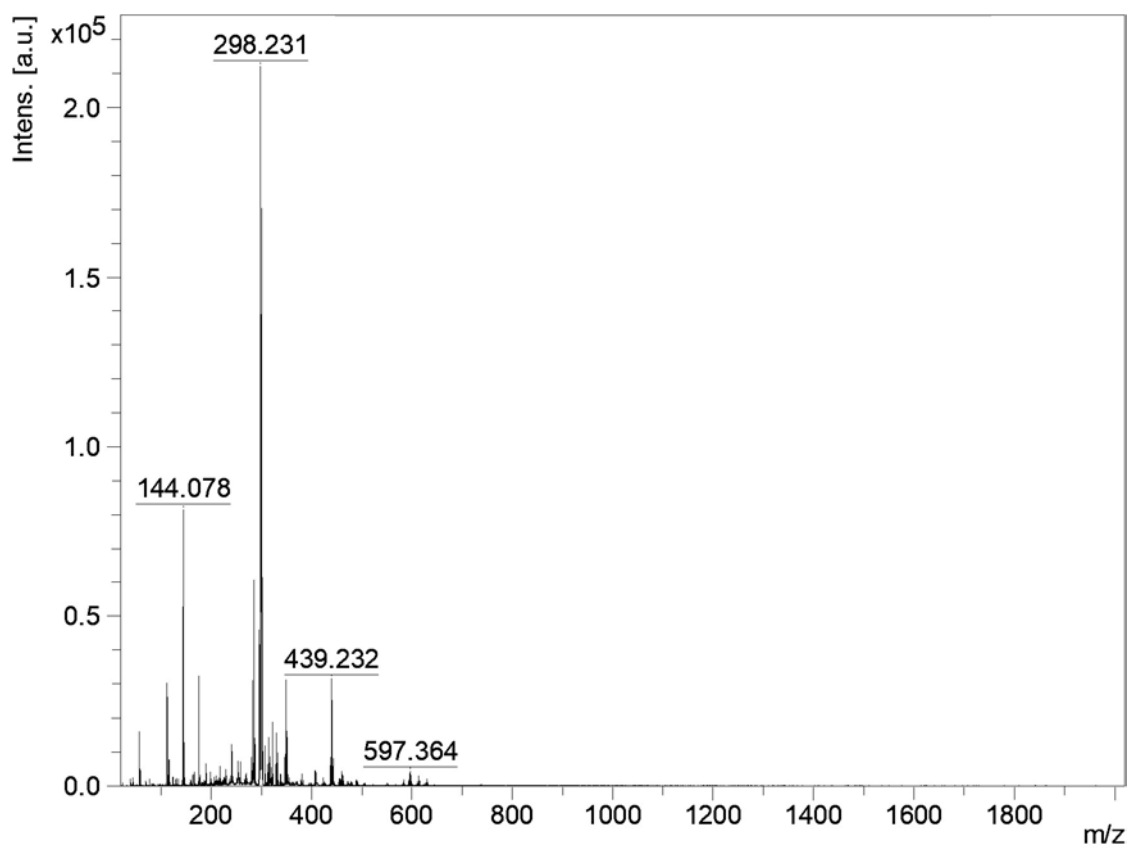
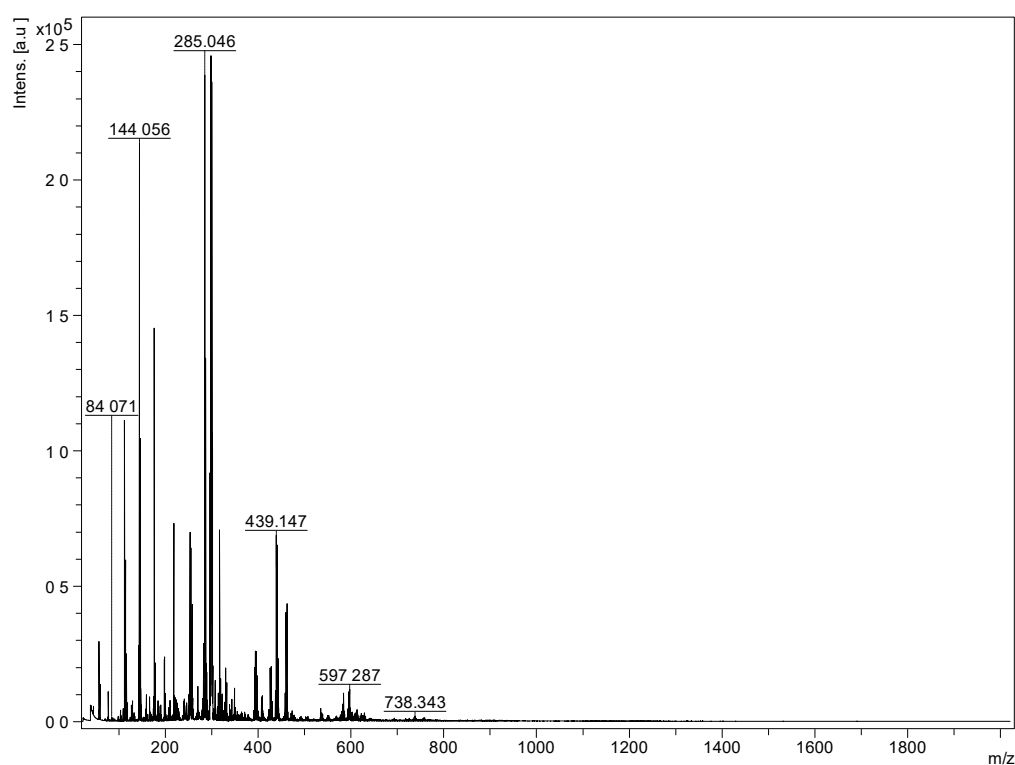


Figure 3.18: Spectrum of 15:1 codeine: binary matrix from MALDI plate



The analysis of morphine gave a positive result with a strong peak at 285 m/z, indicative of the morphine molecular ion, seen in Figure 3.19. This ion was strong, with peaks close to those of the binary matrix; the initial assessment was re-evaluated upon further inspection of Figure 3.11, the binary matrix spectrum. The peak at 285 m/z was also representative of the 6-ATT dimer, previously mentioned, and provided a false positive based interference problem for the morphine spectrum. A deuterated sample of the matrix could be an option to differentiate the two, but the proximity to the morphine and other peaks is not ideal due to these matrix peaks dwarfing any possible molecule peaks. The next peak, the most intense in the spectrum, was seen at 307 m/z a peak which could indicate the presence of the sodiated morphine ion; however, it could also represent a sodiated 6-ATT dimer. This low molar mass peak presents a problem for analysis of drugs with this matrix, as it is detected in the same mass range as many of the drugs, even sharing a peak with a sample of interest.



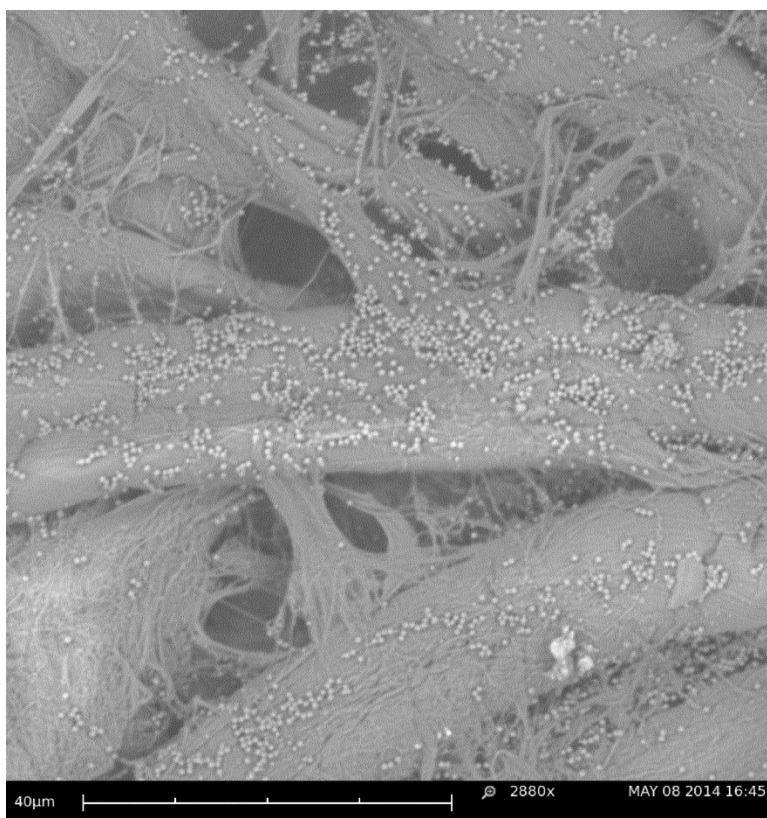
**Figure 3.19: Spectrum of 1:2 morphine: binary matrix from MALDI plate**

The amphetamine class drugs had few peaks in their spectra and did not have any that were clearly molecular or simple adducted ions. There were also, importantly, no spectra with any peaks of interest yielded for any of the laden fibre samples. This indicates that the matrix did not provide enough assistance to be able to analyse from the paper samples.

## 3.2 Nanoparticles

### *Silicon Nanoparticles*

The nanoparticles were synthesized and suspended in solution when the question arose of whether the particles applied to the paper surface would adsorb and remain in place prior to analysis. The S.E.M was, therefore, employed to confirm this prior to any analysis.



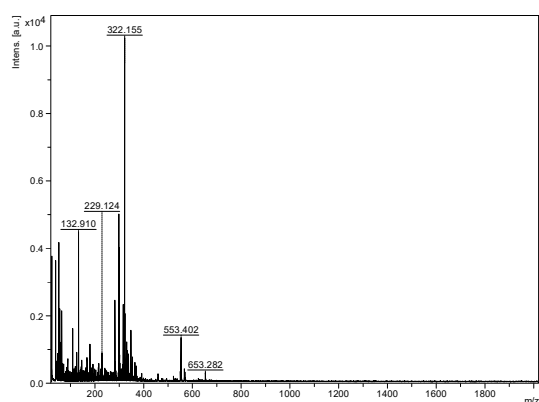
**Figure 3.20: SEM image of silicon nanoparticles distributed on filter paper fibres**

The image in Figure 3.20 shows that application of nanoparticles to the paper surface was successful, as can be seen by the relatively even spread of particles across the paper fibres. The nanoparticles were applied and were not lost or easily removed by the vacuum conditions applied by both SEM and MALDI instrumentation set ups. Another less expected result that was found from this analysis was in paper choice. The paper being used prior to this analysis was regular A4 printer paper; however, the analysis via S.E.M was unable to be done using this base. The nature of printer paper, via some form of additive, like a filler or whitening agent, did not allow for an image to be viewed via the S.E.M camera, instead showing only a clear bright white screen. Another sample was prepared on standard filter paper and re-analysed more successfully, and, therefore, became the paper used in all fibre-based analyses from this point on.

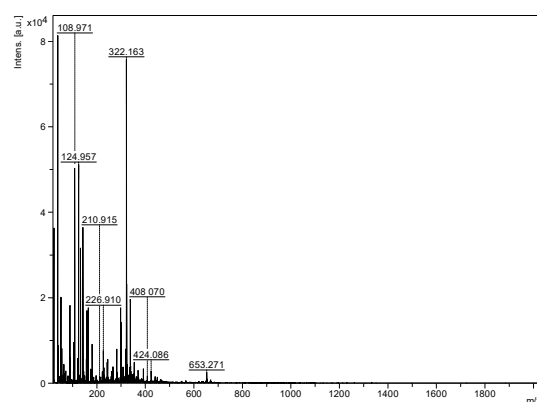
The relative solubilities of the dried nanoparticles in different solvents are presented below, ranging from acetone, where the nanoparticles were fully dissolved to water where they were merely dissipated.

*Acetone > Ethyl Acetate > Ethanol > Water*

The solvation of SiNPs using ethanol, ethyl acetate and water looked to be more of a suspension than a solution. Despite its lack of ability to completely solvate the nanoparticles, ethanol proved to be the most versatile solvent. Ethanol was the only solvent that provided spectra for all three methods for applying the nanoparticles, either before, after or with the analyte. The codeine peaks are visible in Figure 3.21, Figure 3.24 and Figure 3.26 for the ethanol spectra. It is suspected that the ethanol may have been the only solvent capable of protonating the samples during the ionization process. This is due to the hydroxyl group that ethanol possesses, unlike acetone, water and ethyl acetate, the hydrogen from the hydroxyl group can be transferred. There were no spectra generated for the any other solvents mixed with codeine, or for those which the codeine was the top layer. Strong spectra were taken for all solvents when the nanoparticles were the top layer, as can be seen in Figure 3.22, Figure 3.23, Figure 3.24 and Figure 3.25. This indicates that the LDI system is most effective when the silicon nanoparticles are hit by the laser first, and, therefore, able to pass the energy on to the analytes. This is ideal for future samples, as it means that the nanoparticles can be used as a post treatment option. The pre-mixing option is not something that is practical, as samples are required to be in liquid form before being applied to fibres. Codeine as the top layer is also not as practical as it is only useful for fibres that are able to be pre-treated, not for those samples being investigated for use in smuggling.



**Figure 3.21: Spectrum of mixed codeine SiNPs in ethanol**



**Figure 3.22: Spectrum of SiNPs in acetone on codeine**

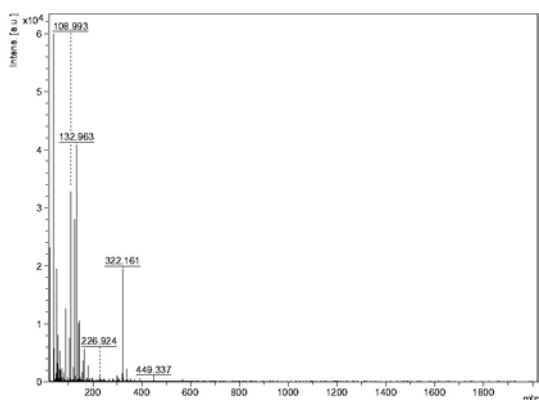


Figure 3.23: Spectrum of SiNPs in ethyl acetate on codeine

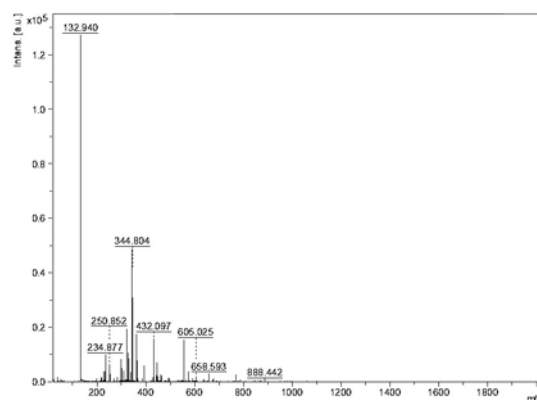


Figure 3.25: Spectrum of SiNPs in water on codeine

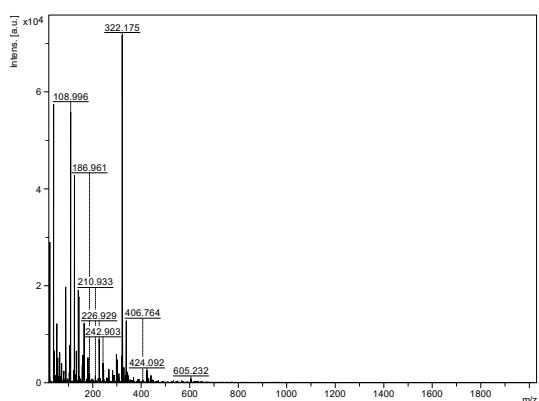


Figure 3.24: Spectrum of SiNPs in ethanol on codeine

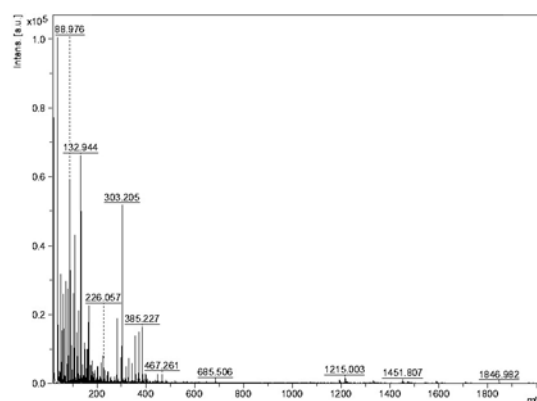


Figure 3.26: Spectrum of codeine on SiNPs in ethanol

The different concentrations of silicon nanoparticles were all successful in providing spectra for codeine, with the sodiated peak at 322 m/z, as seen in Figure 3.27, Figure 3.28 and Figure 3.29. The proton and sodium adducted peaks are frequently seen in SiNP investigations [43]. The best spectrum was yielded from the lowest concentration of silicon nanoparticles at less than 1 mg/mL. All three figures have peaks of similar intensities; however, the peak in Figure 3.27 had the strongest peak as compared to the background

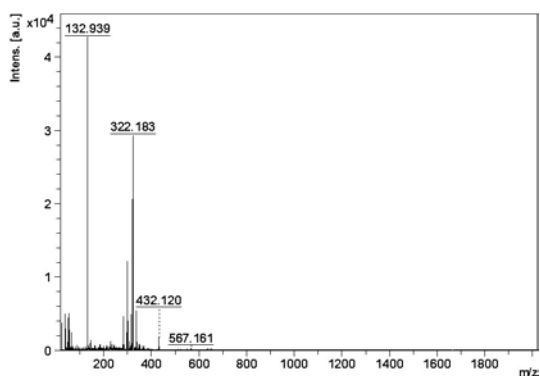


Figure 3.27: Spectrum of codeine with < 1 mg/mL SiNPs from plate

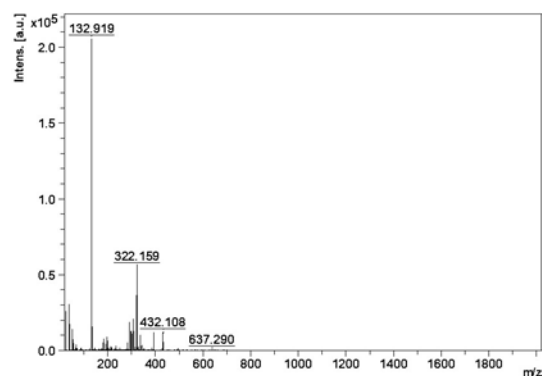


Figure 3.28: Spectrum of codeine and 1.5 mg/mL of SiNPs from plate

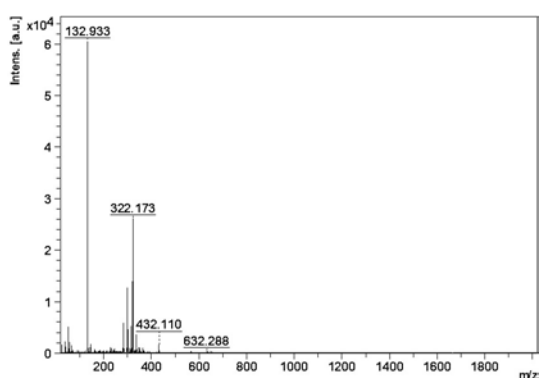
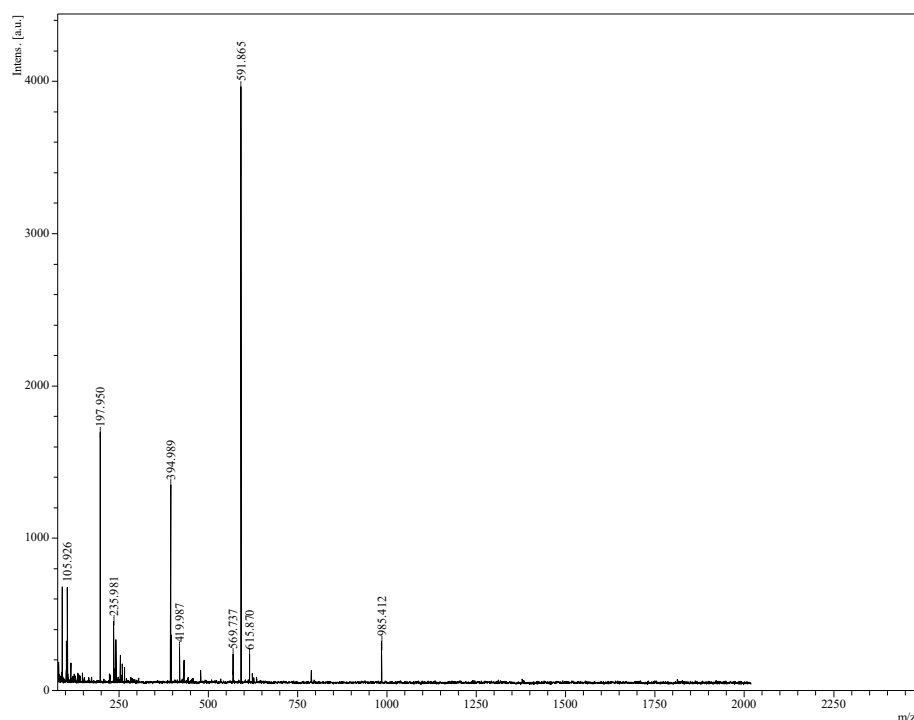


Figure 3.29: Spectrum of codeine and 4.75 mg/mL SiNPs from plate

Silicon nanoparticles did not prove to be useful for the analysis of codeine from fibres. No spectra with peaks indicative of codeine were taken with any of the solvents or concentrations of nanoparticles.

### *Bare Gold Nanoparticles*

The bare gold nanoparticles were analysed individually and found to give strong peaks for gold, as seen in Figure 3.30. The peaks at 197.9 m/z, 394.9 m/z and 591.8 m/z represent a single protonated gold atom, two gold atoms, which have been protonated and three gold atoms which have been protonated.



**Figure 3.30: Spectrum of Bare AuNPs**

Throughout these experiments the potential of the bare gold nanoparticle samples was identified, with strong evenly spaced sample peaks, as a potential calibrant. Table 3.2, below, shows the peaks which could be used for a gold nanoparticle based internal calibrant. An idea that is very appealing for not only qualitative, but quantitative analysis, AuNPs have been used for such purposes before [51]. The appeal of quantitative analysis is due to the ability to not only quickly identify which samples are present, but also how much of these samples. A rapid analysis being able to both quantify and qualify an illicit substance would be greatly useful especially in forensic situations where the quantity could indicate whether the amount found is significant or not.

**Table 3.2: Calibration peaks for gold**

Ion	Peak Position (m/z)
AuH <sup>+</sup>	197.967
[2Au+H <sup>+</sup> ]	394.934
[3Au+H <sup>+</sup> ]	591.901
[4Au+H <sup>+</sup> ]	788.800
[5Au+H <sup>+</sup> ]	985.750

It can be seen in Figure 3.31 to Figure 3.34 that all of the AuNPs aided with the analysis of codeine, with all spectra demonstrating the codeine indicative peaks around 299 m/z and 322 m/z. The strong alkali peaks have been found to be a common occurrence for samples analysed using AuNPs [56, 84, 156]. The quality of the results from this investigation varied across the different dilution factors. The spectrum in Figure 3.32, the 1:5 dilutions has the strongest gold peaks in the background indicating that not enough of the sample was able to be analysed compared to the gold. The 1:10 dilution seen in Figure 3.31 has stronger analyte peaks, these are paired with a much lower signal intensity which might be due to slight assistance being provided by the small amount of nanoparticles, but not enough of them to be strongly analysed. The comparison of background peaks to analyte peaks is good, but the weak signal intensity is not ideal. Upon viewing the spectra in Figure 3.33 and Figure 3.34 it is clear that the 1:2 dilution is the best option. The signal intensity is much stronger with smaller background peaks, which are minimized again using 30% laser fluence, the improved signal to noise and reduced laser strength is the best option for the analysis.

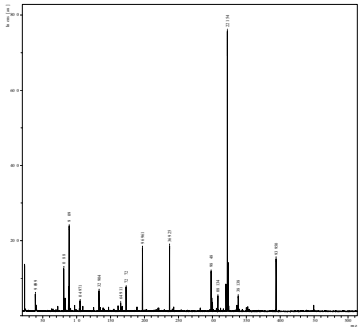


Figure 3.31: Spectrum of codeine with AuNPs diluted 1:4

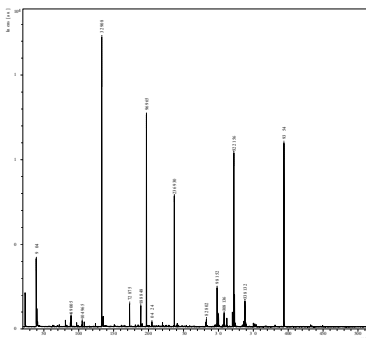


Figure 3.32: Spectrum of codeine with AuNPs diluted 1:2

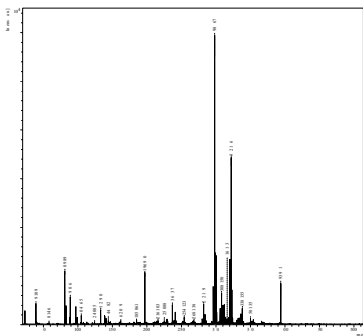


Figure 3.33: Spectrum of codeine with undiluted

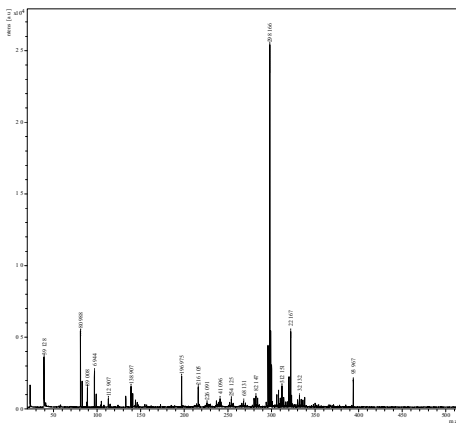
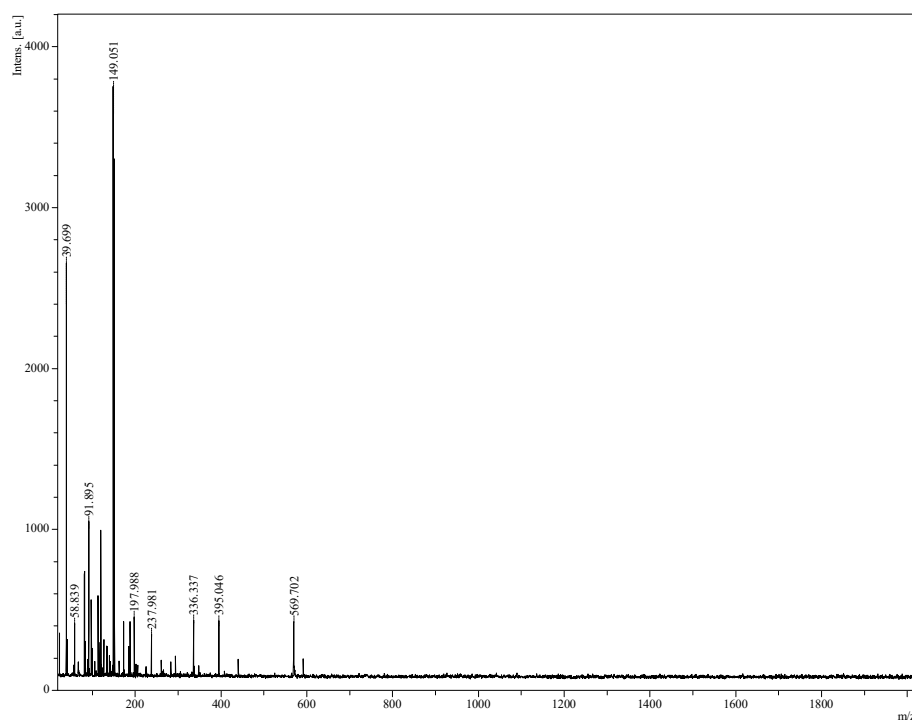


Figure 3.34: Spectrum of codeine with undiluted AuNPs at 30% laser



Analysis of the fibre-based samples proved unsuccessful, indicating that the bare gold nanoparticles did not provide adequate assistance to the desorption/ionization to enable analysis from a non-transferring substance like cellulose. These results indicated that functionalisation of the nanoparticles was required to increase their ability to absorb and transfer the laser energy.



**Figure 3.35: Spectrum of sample indicating presence of methamphetamine with bare AuNPs from plate**

Bare gold nanoparticles were also found to be useful for the analysis of amphetamines, generating a spectrum with a peak stronger than those representing the gold ions. Figure 3.35 was a spectrum taken for what was labelled suspected amphetamine, the very large peak at 150 m/z, however, is indicative of the molecular ion of methamphetamine. As this sample has been labelled as such there is the chance that this sample actually contains methamphetamine.

### ***Thiolated Gold Nanoparticles***

Gold nanoparticles thiolated with two attachments, thiosalicylic acid and 4-mercaptobenzoic acid. Figure 3.36 and Figure 3.37 show the spectra for the thiosalicylic acid functionalised gold nanoparticles from the MALDI plate, alone and combined with codeine respectively. There are very few peaks in the nanoparticle sample giving a clean spectrum for both the nanoparticle sample and the codeine sample, providing strong representative peaks for the codeine.

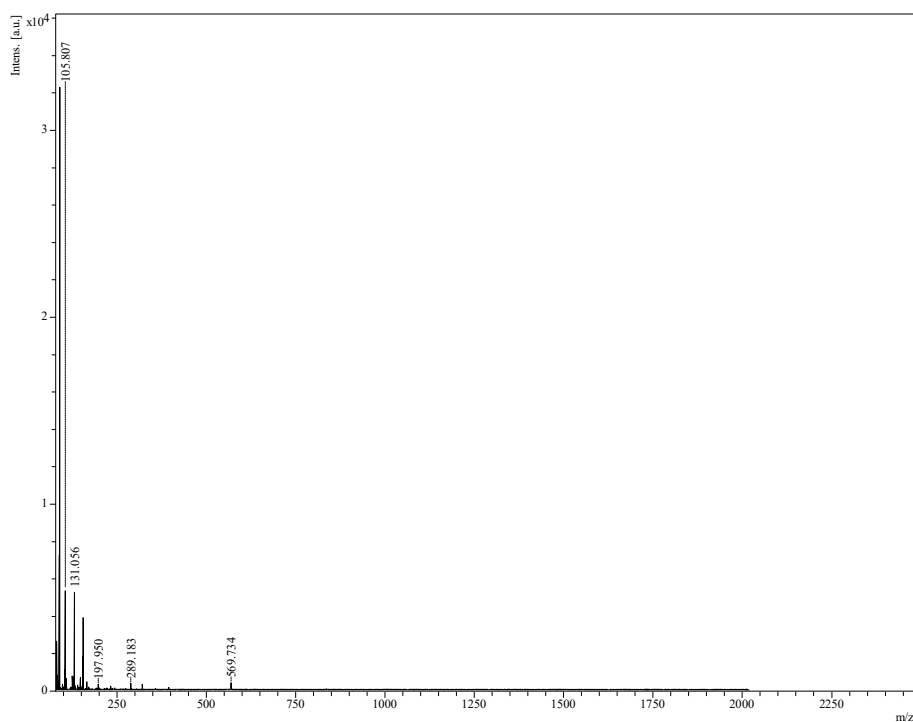


Figure 3.36: Spectrum of TSA AuNPs from plate

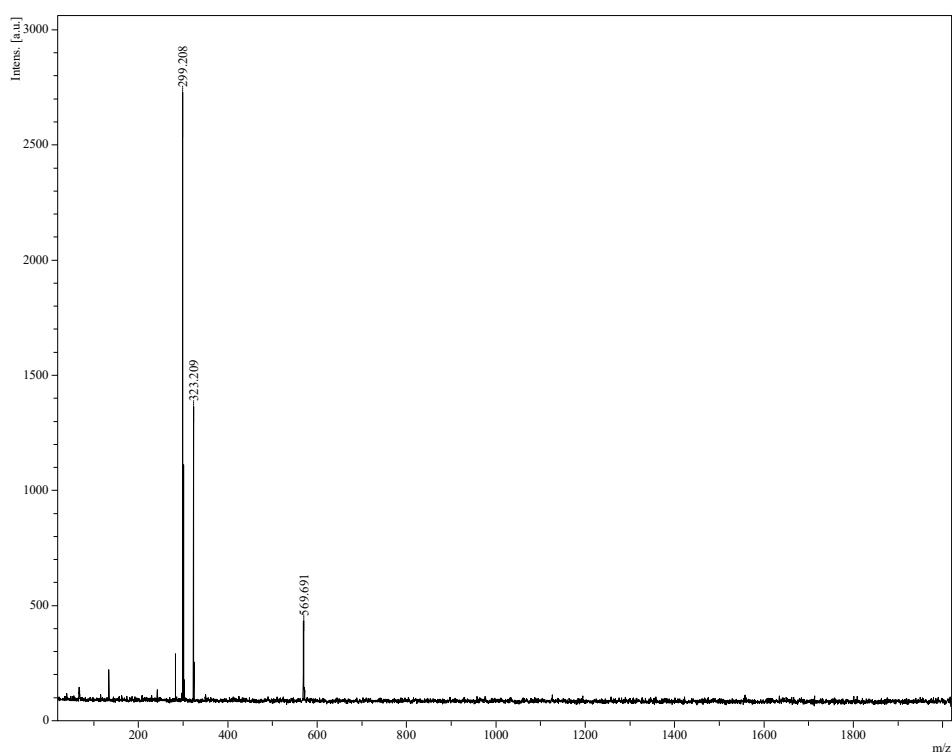


Figure 3.37: Spectrum of codeine with TSA AuNPs from plate

The 4-mercaptobenzoic acid gold nanoparticles provided similar spectra in Figure 3.38 and Figure 3.39 to those of thiosalicylic acid, with few background peaks, but strong peaks for codeine. While thiosalicylic acid is a more affordable option, it has also been found to have a shorter shelf life <sup>[114]</sup>,

resulting in a need for more frequent synthesis. Both these functionalised gold nanoparticles have been proved to be successful for the analysis of codeine using LDI, from the plate.

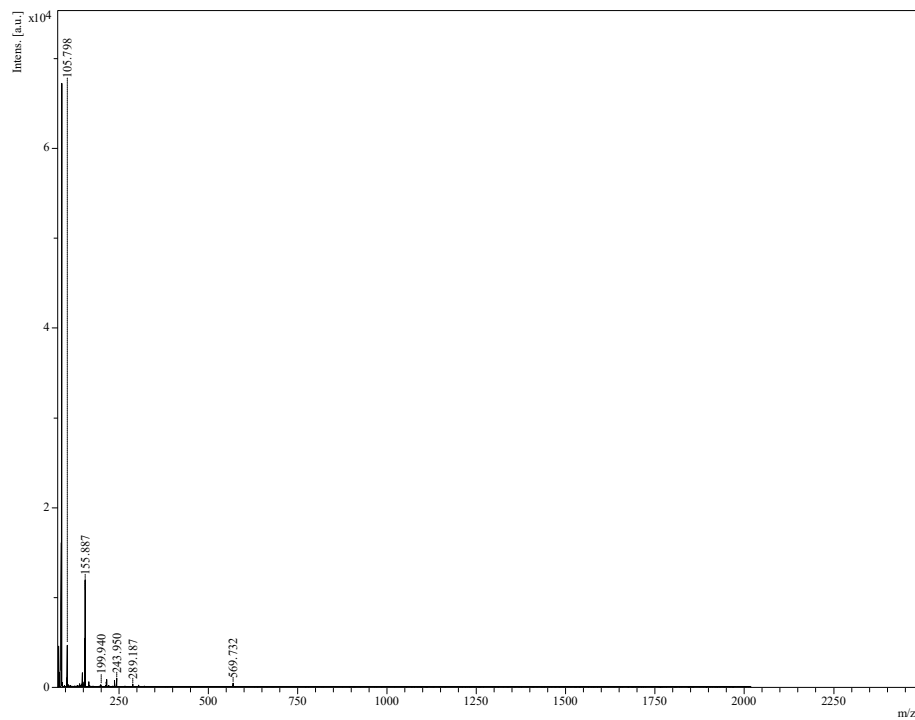


Figure 3.38: Spectrum of 4-MBA AuNPs from plate

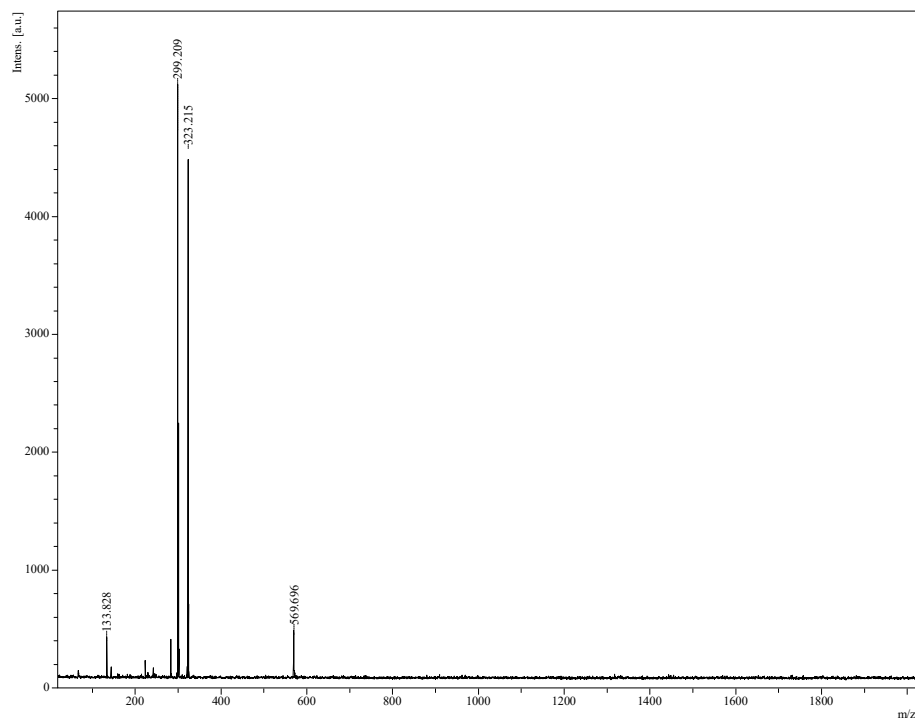


Figure 3.39: Spectrum of codeine with 4-MBA from plate

Figure 3.40 and Figure 3.41 below show the analysis of codeine from fibres using thiosalicylic acid functionalised gold nanoparticles, these were performed from copper tape. Unlike the plate sample there are more peaks associated with the nanoparticles and it can be seen in Figure 3.41 that there are no peaks for codeine or either of its common adducts. Instead there are peaks at 298 m/z and 328 m/z. The use of these nanoparticles has not been successfully translated to the fibre analysis.

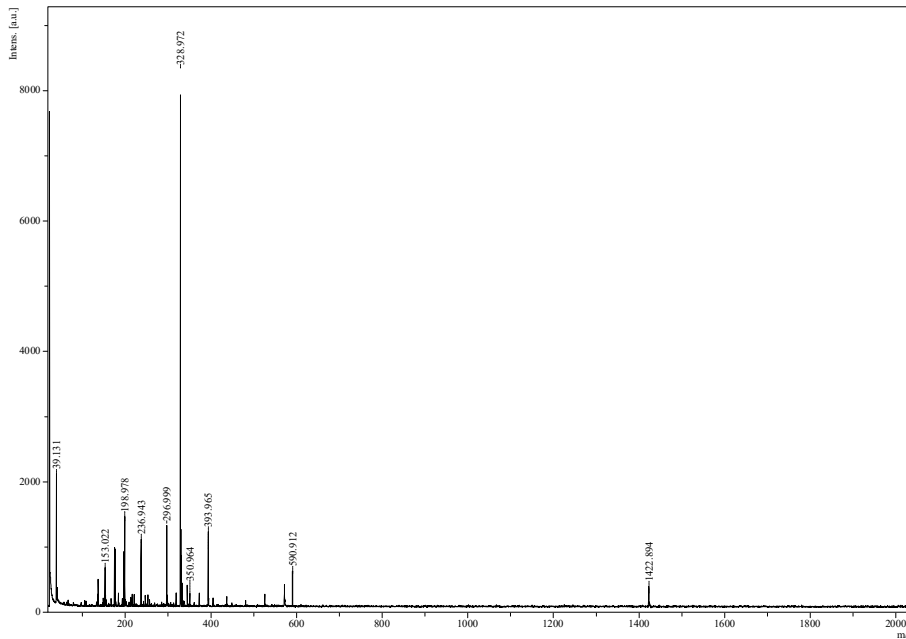


Figure 3.40: Spectrum of TSA AuNPs from fibre on copper tape

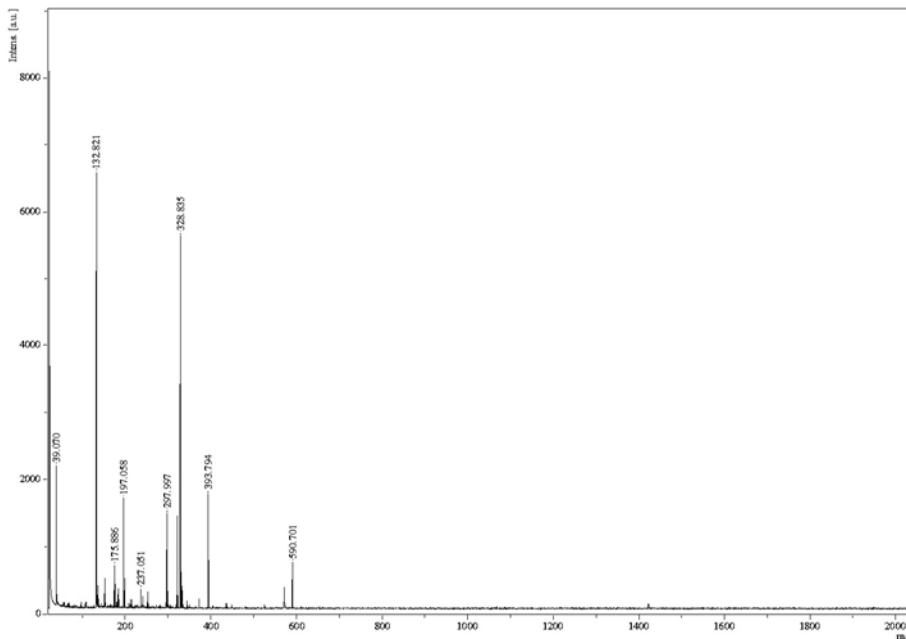


Figure 3.41: Spectrum of codeine with TSA AuNPs from fibres on copper tape

Similar to the thiosalicylic acid samples the 4-mercaptobenzoic acid gold nanoparticles had more peaks in the background of the spectrum, including the peak at 328 m/z which can be seen in Figure 3.42. Figure 3.43 still contains the background peaks shown in the nanoparticle sample, however, these have lower signal intensity compared to the codeine peaks at 300 m/z and 323 m/z. Importantly, the signal intensity for the peaks in this spectrum is ten times higher than the thiosalicylic acid gold nanoparticle assisted sample and contains analyte peaks of interest. 4-mercaptobenzoic acid functionalized gold nanoparticles are useful for the analysis of codeine from fibre samples, from copper tape.

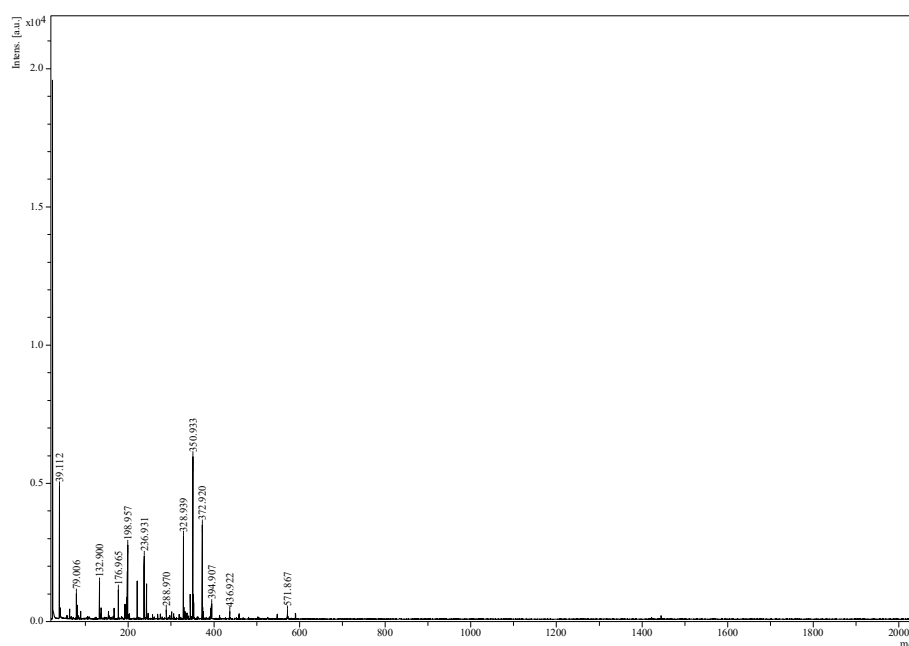


Figure 3.42: Spectrum of 4-MBA AuNPs on fibre from copper tape

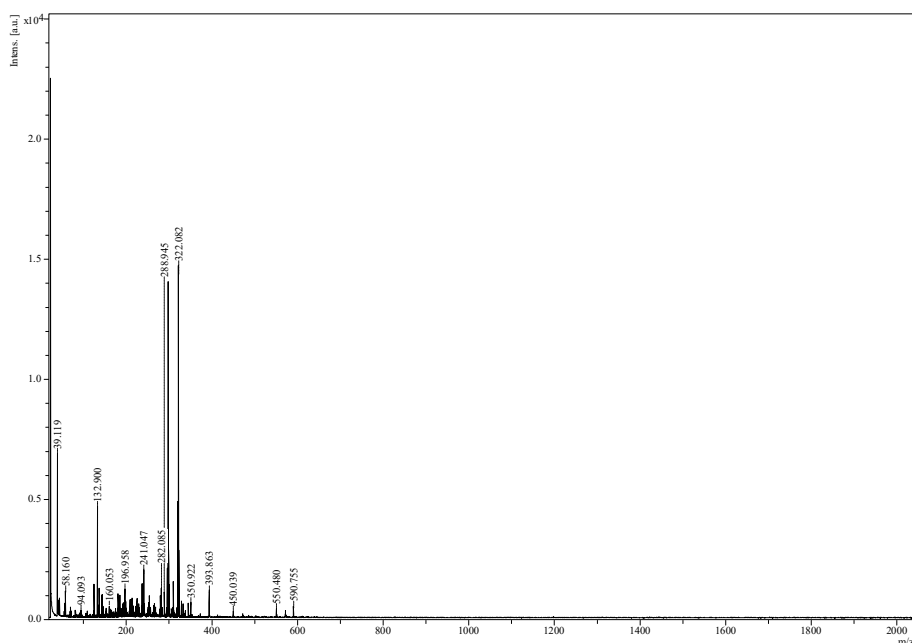


Figure 3.43: Spectrum of codeine with 4-MBA AuNPs on fibre from copper tape

### Gold Nanoclusters

Gold nanoclusters were used fresh after synthesis but were also used 4 weeks later for the same analysis. Interestingly the appearance of the 4-mercaptobenzoic acid gold nanoclusters changed greatly. They became much more difficult to analyse and showed less of a crystallized structure, providing something of a barrier against the laser, preventing analysis. Figure 3.44 and Figure 3.45 show the spot images displayed on the MALDI control screen in the analysis process. Images like these are taken by the instrument's internal camera at 100 x magnification and are visible for all samples analysed.

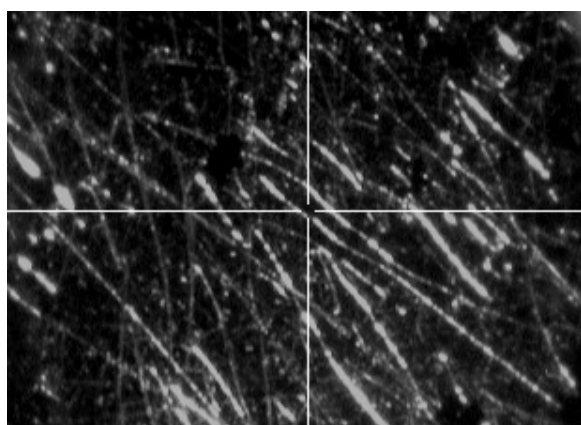


Figure 3.44: Older sample of 4-mercaptobenzoic acid gold nanoclusters on plate

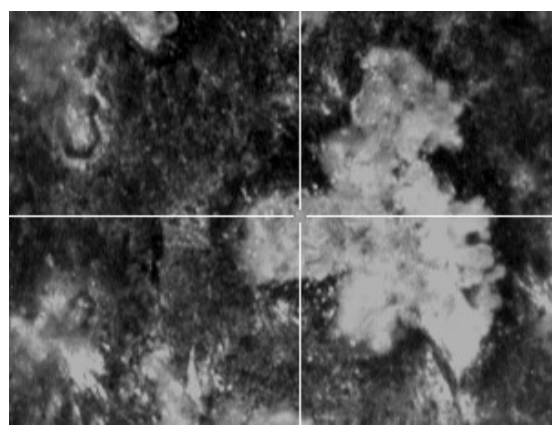


Figure 3.45: Fresh sample of 4-mercaptobenzoic acid gold nanoclusters on plate

These samples were analysed on the same day, but loaded weeks apart, clearly the sample that was loaded while fresh has been kept in a much better state. The plate has preserved much better than the sample allowed to sit. The phenylethyl mercaptan gold nanoclusters showed no difference over this time and clearly have a much longer shelf life.

The synthesis process of nanoclusters was much more time consuming than those of the other nanoparticles produced in the other experiments. Overnight stirring at less than zero degrees Celsius was required as well as consistent monitoring over 8 hours. However, the process was just as simple. These samples turned very dark upon addition of the  $\text{NaBH}_4$  and the phenylethyl mercaptan functionalised particles had an oily texture that made them more difficult to handle, not being an aqueous based system.

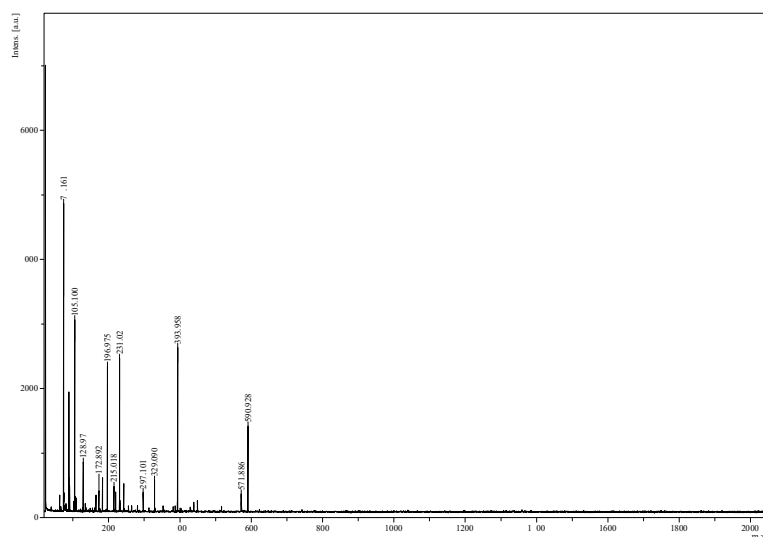


Figure 3.46: Spectrum of phenylethyl mercaptan gold nanoclusters from the plate

The spectra produced using phenylethyl mercaptan gold nanoclusters were analysed at 30-50% laser fluence. It can be seen in Figure 3.46, the spectrum of the nanoclusters, that there are once again strong peaks representative of protonated gold, as well as its protonated dimer and trimer. Other noise peaks are present, but with lower intensity than in previous spectra. Figure 3.47 shows the spectrum of codeine with the phenylethyl mercaptan attached nanoclusters, this shows very strong peaks around 299 m/z and 322 m/z representing codeine and its sodium adduct. This spectrum also contains very little noise, specifically in the region below 200 m/z where there were several peaks even in the relatively clean blank spectrum of the nanoclusters. This was one of the few occasions when the strongest peak in the entire spectrum was representative of the codeine and not a noise peak below 200 m/z, which were representative of a common environmental ion, frequently potassium, or a contaminant.

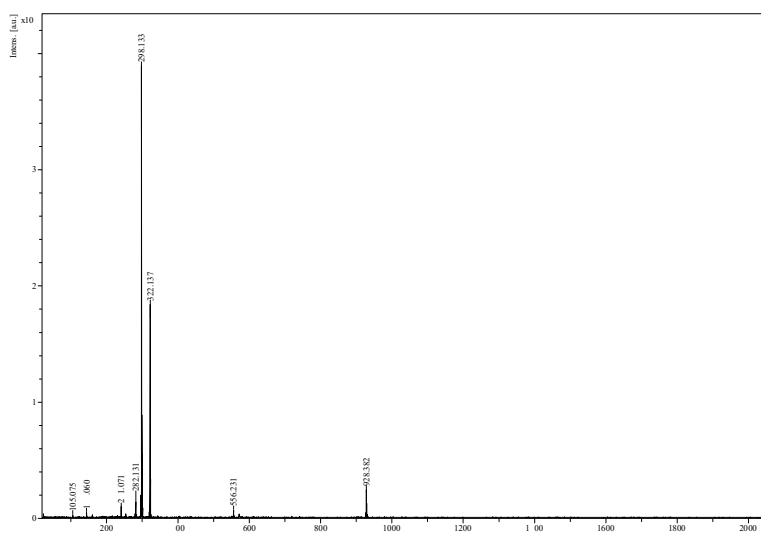


Figure 3.47: Spectrum of codeine with phenylethyl mercaptan gold nanoclusters from plate

Unfortunately, no spectra were yielded from the loaded paper samples, even at higher laser fluence. This was disappointing due to the distinct lack of peaks in the lower part of the spectrum in Figure 3.47.

The 4-mercaptobenzoic acid attached nanoclusters were then considered, it was proposed that the decreased size of the nanoclusters were the source of the lower noise in the spectrum in Figure 3.47. The attachment of the 4-mercaptobenzoic acid would deliver energy transfer and aid in desorption and ionization, found to have been provided in the functionalised gold nanoparticle experiments.

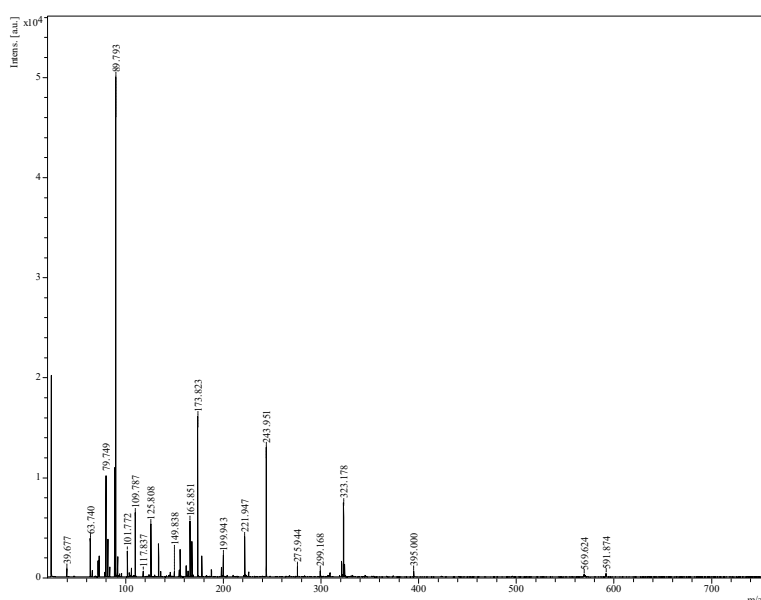


Figure 3.48: Spectrum of codeine with 4-mercaptobenzoic acid attached gold nanoclusters from plate



Figure 6, however, indicates that the strongest peaks by far are those of the gold ions, as well as a strong peak at 243 m/z, which is representative of mercaptobenzoic acid itself. The codeine peaks were also very weak indicating that this was not a successful matrix alternative. Alternatively, it might also have been an indication of a poor synthesis from an altered method. The idea that these nanoclusters were not performing well as a matrix was strengthened by a lack of spectra yielded from the fibre samples using these nanoclusters.

## 4 Conclusions

Matrix-free analysis of codeine phosphate was investigated by analysing the sample directly from the target plate, without any surface treatments or additions made to solution. A positive result from this analysis showed peaks of interest to be at 299, 322 and 338 m/z. These peaks required high laser energy for low peak intensity, but the idea of assistance via the conductive steel sample plate generated ideas for optimization options.

The investigation of conductive materials aiding in the desorption and ionization process of LDI was investigated after the matrix-free results. Analyses using carbon tape were hindered by the frequency with which the tape itself was competitively analysed over the sample of interest. Copper and double-sided tapes proved much more useful, yielding spectra indicative of codeine's common adducts. Copper gave better results, but the spectra were not good enough to warrant this as a stand-alone technique. The other issue associated with these spectra is the high laser power that was required to yield these results. Alternative assisting materials, therefore, needed to be investigated to be used in combination with these tapes, for solid based analysis. The successful results yielded later in the experiments were all combined with fibres adhered to copper tape, this indicates that it is the best adhesive for fibre application.

The use of graphite as an alternative assisting medium for analyses undertaken from fibres was investigated due to the well-established use of a carbon in its many forms, including graphite itself, in MALDI. Throughout the experiments, analysis proved difficult, due to the lack of usable spectra and the reasons mentioned above, the use of graphite in this context was deemed unsuccessful and further investigation unnecessary. Graphite was abandoned as a possible solution and different assisting alternatives were investigated.

Binary matrices were applied to the codeine sample to increase the signal peaks, whilst minimizing the matrix interference. The ratio of analyte to matrix which gave the best results was found to be 8:1 analyte: matrix. The spectra generated by ratios with more analyte than this showed little difference and those with more matrix gave analyte peaks with lower intensity compared to the background. While the assistance from the matrices gave strong spectra with using lower laser power, the decrease in interference was not obvious, and in fact gave a false positive result for the morphine sample. In this sample the peak at 285 m/z was mistaken for a morphine molecular ion peak, but in fact was a dimer of 6-ATT. The low peaks from the binary matrix which may be useful for very specific sample masses, were not appropriate for the range of masses from different drugs that could be analysed and were deemed to be too strong to continue with this type of analysis. The binary matrix also did not

prove to be useful for fibre-based samples at any of the tested ratios. From this experiment, it was found that an assisting medium of higher mass, with less potential for interference was therefore, required.

Many standards for the procedures required for LDI analysis were realised in the experiments using codeine and silicon nanoparticles. From the SEM analysis the paper used for the fibre analysis was required to be filter paper rather than printer paper to avoid a bleaching effect. It was also confirmed that the nanoparticles were retained by the fibres and were not lost in the vacuum process of the MALDI instrumentation. From the LDI analysis, the nanoparticles led to a lower laser fluence requirement for results than unassisted samples, at 40-60%. The most effective solvent for the silicon nanoparticles was deemed to be ethanol, providing spectra for all combinations of nanoparticles with codeine, beneath, on top of and mixed. The best combination procedure required the nanoparticles to be the top layer, coating the analyte, which is ideal for post-sampling treatment. Finally, lower concentrations of the silicon nanoparticles resulted in spectra with lower intensity background peaks as compared the peaks of interest. While there was no improvement in results for the fibre samples, plate samples showed enhancement compared to the binary matrix. The silicon nanoparticles in a similar manner to a matrix, aided in analysis, but with less interference, they are, therefore, an option for further investigation.

The use of gold nanoparticles has been common over the years, for a variety of different applications. Bare gold nanoparticles have once again been shown to be useful in the application of drug analysis via LDI. Their presence has been shown to aid in the desorption and ionization process, with stronger molecule peaks and lower laser energy required than for the matrix free option. Samples of gold nanoparticles analysed with undiluted gold nanoparticles gave the best results, indicating that small amounts of the nanoparticles do not provide enough energy transfer for this type of analysis. The samples were not able to be analysed from fibres of paper and, therefore, further investigation into gold nanoparticles and their functionalisation was required

It can be seen throughout this chapter that the functionalisation of nanoparticles can greatly decrease the amount of background peaks in the analysis of codeine from the MALDI plate. Most importantly 4-mercaptobenzoic acid has been shown to be successful in analysis of codeine, not just from the plate but from fibres. Results included a spectrum done at lower laser strength, with better signal to noise ratio, than any previous fibre sample. While 4-mercaptobenzoic acid may be more expensive than thiosalicylic acid the nanoparticles it produces have a longer shelf life and produced better spectra, making them a more viable option. These samples could still be improved upon, specifically in

decreasing the intensity and number of background peaks, which was an aim in the synthesis of gold nanoclusters.

The use of phenylethyl mercaptan attached nanoclusters proved to be a useful matrix alternative for on-plate analysis of codeine. The analysis was undertaken at low laser strength and yielded strong peaks with minimal background peaks. The adaptation of these nanoclusters with mercaptobenzoic acid, did not aid in the analysis from fibres, nor provide better spectra for the plate analysis. From information in the previous nanoparticle experiments it can be established that 4-mercaptobenzoic acid functionalised gold nanoparticles are the best option for the analysis of codeine from fibres. This chapter established phenylethyl mercaptan functionalised nanoclusters to provide the least background for plate analysis.

# Part Two – Propellant based Samples

Part two of this thesis focuses on the analysis of propellants, the primary method of analysis is LDI. Again, the introduction to LDI still applies in these chapters, as well as the instrument settings mentioned in the experimental, but no alternative matrices are explored, only matrix free analysis. Different techniques are also explored in the following chapter for the analysis of these samples.

## 5 Introduction

### **5.1 Propellants**

Propellants are low intensity energetic materials that produce hot gases, which, when contained generate sufficient force to result in the propulsion of a projectile. They are not technically explosives, as they do not explode <sup>[157]</sup>. There are two major classes of propellants; those used in guns and those used in rockets <sup>[157]</sup>, this project investigates firearm propellants. In firearms, propellants are found in the bullet casing. When the pin of the gun hits the base of the cartridge upon firing, it provides enough force to initiate the burning <sup>[158]</sup>. The propellant then burns, providing enough gas to propel the bullet forward, out of its casing, out of the barrel of the gun and towards the target <sup>[158]</sup>. The original gun powder, known as black powder consisted of potassium nitrate (as the explosive component), charcoal as the fuel and sulfur <sup>[159]</sup>. However, this propellant produced a lot of smoke, which led to the development of smokeless powders <sup>[159]</sup>. Smokeless powders contain many different components including the explosives, plasticisers, stabilisers and lubricants. Propellants come in a range of shapes and sizes, some examples of shapes include balls, discs and tubes <sup>[160]</sup>. The three energetic materials commonly used in smokeless powders are Nitrocellulose (NC), a compound derived from cotton, Nitroglycerin (NG) and Nitroguanidine <sup>[160]</sup>. Figure 5.1, Figure 5.2 and Figure 5.3 show the structure of these three explosives respectively. Propellants are often classified either as single, double or triple base <sup>[160]</sup>. This classification is based on the number of explosive components <sup>[160]</sup> single base propellants contain only nitrocellulose, double base propellants also include Nitroglycerin and triple base propellants include all three and are generally only used in large calibre weapons, such as cannons. Nitroglycerin has a molecular mass of  $227.0865 \text{ g}\cdot\text{mol}^{-1}$ , Nitroguanidine has a molecular mass of  $104.07 \text{ g}\cdot\text{mol}^{-1}$ , nitrocellulose, being a polymeric compound, has a single repeating unit mass of  $605.252 \text{ g}\cdot\text{mol}^{-1}$ .

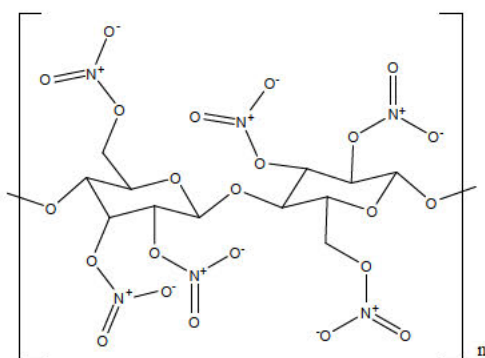


Figure 5.1: Structure of Nitrocellulose

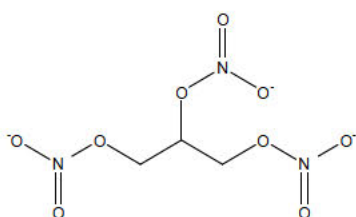


Figure 5.2: Structure of Nitroglycerin

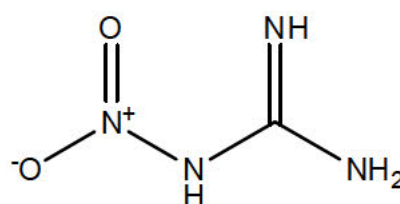
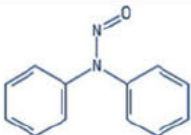
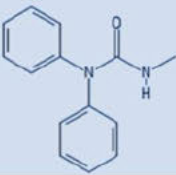
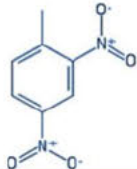
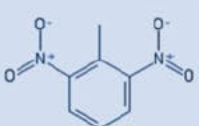
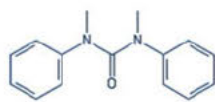
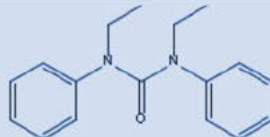
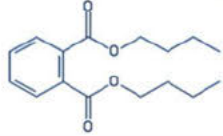


Figure 5.3: Structure of Nitroguanidine

Stabilizers are added to propellant mixtures due to the unpredictable nature of the explosive component. Stabilizers are included to be consumed in reaction with degradation products of the energetic materials. They react in preference to the explosive compound, which would otherwise degrade and become unstable <sup>[161]</sup>. The analysis of propellants is often performed to track the levels of stabilizers and therefore the overall stability of the propellant. A study performed at Flinders University measured the concentrations of various stabilizers and derivatives and developed an HPLC method <sup>[162]</sup>. Common stabilizers found in propellants are diphenylamine and its various derivatives, as well as ethyl and methyl centralite, dibutyl phthalate and akardite II <sup>[163]</sup>. Dinitrotoluenes are used as plasticizers or coatings in propellants <sup>[164]</sup> and can also be used as flash suppressant stabilizers <sup>[165]</sup>. The structures and molar masses of these additives are summarized below in Table 5.1.

Table 5.1: Common propellant additives and their properties

Name	Structure	Molecular Mass
Diphenylamine (DPA)		169.227 g.mol <sup>-1</sup>
2-Nitrodiphenylamine (2n-DPA)		214.224 g.mol <sup>-1</sup>
4-Nitrodiphenylamine (4n-DPA)		214.224 g.mol <sup>-1</sup>

N-nitroso-diphenylamine (Nn-DPA)		198.225 g.mol <sup>-1</sup>
Akardite II (AK II)		226.27 g.mol <sup>-1</sup>
2,4-Dinitrotoluene (2,4-DNT)		182.134 g.mol <sup>-1</sup>
2,6-Dinitrotoluene (2,6-DNT)		182.134 g.mol <sup>-1</sup>
Methyl Centralite (MC)		241.65 g.mol <sup>-1</sup>
Ethyl Centralite (EC)		268.36 g.mol <sup>-1</sup>
Dibutyl Phthalate (DBP)		278.34 g.mol <sup>-1</sup>

Propellants have been analysed in many different ways, often using techniques that require solvation and longer time analyses <sup>[163]</sup>. It is predicted that due to the ionic nature of some of the components of propellants that they will be easily analysed via LDI. Furthermore, if these components can be analysed with little sample preparation using SALDI, it may be a proposed advantageous technique for analysis in forensic investigations, due to the speed of analysis and minimal sample damage. Other advantages include the high throughput and simple preparation, a lot of samples can be analysed and rather rapid results can be obtained, qualities that are always advantageous in forensic applications. The disadvantages associated with the use of this technique in the forensic field relate generally to the bulk and cost of the instrument, as well as the expertise required for its operation. These shortcomings may be solved in time as technology progresses, the instrument can become more compact, cheaper and more user friendly, as many instruments do.

Gunshot residue (GSR) or cartridge discharge residue (CDR) is the product of discharging a firearm <sup>[166]</sup>. This material is made up of particles formed by the burning of energetic materials in the bullet as well as by-products of the cartridge, jacket and barrel of the weapon <sup>[167]</sup>. Importantly not all GSR samples are completely burnt, some remain intact. GSR particles still contain similar chemical makeup to their propellants.

GSRs can be separated into two major categories; organic and inorganic <sup>[166]</sup>. Organic components tend to be associated with the propellants and firearm lubricants; and can be burnt or unburnt particles <sup>[168]</sup>. Whereas inorganic components may originate from the propellant, primer, and weapon components, these particles tend to be nitrogen or metal based <sup>[168]</sup>. The particles come in various shapes, sizes and compositions depending on a range of environmental factors <sup>[169]</sup>. Importantly, discrepancies between morphologies and chemical compositions of different particles from the same source have been found <sup>[170, 171]</sup>. Some particles are also homogenous throughout, whereas others are not <sup>[169]</sup>. This means that several particles of GSR are required for analysis and comparison purposes.

## 5.2 Analysis

The analysis of propellants and will always be a difficult task due to the complexity of the samples involved. The first step in analysis of any sample is collection. GSR is the primary propellant-based form of forensic sample. Through the formation of the GSR plume after firing a weapon, GSR becomes airborne, spreading to various surfaces on the shooter and in their vicinity <sup>[172]</sup>. This means there are various areas that GSR can settle and, therefore, be collected from, leading to a range of collection techniques. The range of collection techniques associated with GSR includes tape lifts, vacuum lifts, swabbing, glue lifts, nasal swabbing and collection from hair <sup>[166]</sup>. Most commonly inorganic GSR is collected from the hands via a tape lift <sup>[173]</sup>. Tape lifts are popular due to ease of use and their ability to be used in conjunction with the most widely used method of analysis, Scanning Electron Microscopy with Energy Dispersive X-ray spectroscopy (SEM-EDX)<sup>[173]</sup>. Tape lifts allow particles to be observed prior to solvation and also allow for analysis of the solid samples. Organic GSR is more often sampled via a swabbing technique <sup>[173]</sup>.

The primary method of analysis for propellant and GSR analysis used is simple observation of the sample. Some samples can be physically differentiated, but this must be supplemented and confirmed via other techniques <sup>[171, 174]</sup>. The next most simple method of analysis is a spot test, these tests are performed on site, and are presumptive techniques used to indicate quickly whether a sample could be GSR, prior to further, more intense, laboratory analysis. Spot tests include the paraffin test, the Griess test and the use of sodium rhodizonate. The reagents associated with these techniques react with different components of GSR are often based on a colour change <sup>[173]</sup>. They are techniques that



include results with a large number of false positives; the reactions are dependent on compounds within GSR but are not specific to GSR <sup>[166]</sup>.

There is a large range of laboratory techniques which have been used to analyse propellants and GSR. There is yet to be a single process that can efficiently analyse both the organic and inorganic residues simultaneously. The standard combination of techniques used is SEM-EDX for inorganic components and GCMS for organic <sup>[166, 175]</sup>. Capillary Electrophoresis (CE) is a technique that can be used for the analysis of both components <sup>[167, 176, 177]</sup>, however, the instrument set-up is different for each sample type and, therefore, two separate analyses must be run, neither of which is as effective as the techniques currently used <sup>[167]</sup>. ToF-SIMS has also been used for the analysis of both organic and inorganic GSR but has been deemed not as effective as the currently used analyses <sup>[178, 179]</sup>.

Alternative inorganic techniques include Inductively Coupled Plasma (ICP) techniques <sup>[180-184]</sup>, Atomic Absorption Spectroscopy (AAS) <sup>[184-186]</sup> and Neutron Activation Analysis (NAA) <sup>[187-189]</sup>. These techniques focus on the metal particles often associated with GSR, antimony, barium and lead. Unfortunately, the development of non-toxic, lead free propellants has made these techniques less effective, as antimony and barium are quite abundant in nature <sup>[163]</sup>. Other techniques used for organic GSR analysis include HPLC <sup>[162, 175]</sup>, Liquid Chromatography Mass Spectrometry (LCMS) <sup>[163, 190]</sup> and GC <sup>[191, 192]</sup>. Liquid Chromatography in the form of LC and Thin Layer Chromatography (TLC) were used early in understanding the nitration mechanisms of DPA and identifying each of its derivatives <sup>[193]</sup>. Although these analyses are losing their applicability over time as samples become more similar.

Both original propellant samples and GSR particles are important for analysis purposes to link scenes and original sources <sup>[194]</sup>. The analysis of these samples in an efficient manner is, therefore, important to strive for. LDI is a technique that may be used for this in the future. These experiments investigate the possibility of analysing propellants as a starting point, to confirm whether the technique has the potential for further analyses. The analysis of propellants using LDI is encouraging due to the nature of many of their components. Table 5.1, Figure 5.1, Figure 5.2 and Figure 5.3 show the structures of common components, many of which include conjugated double bonds, a property shared by most laser absorbing compounds. LDI was investigated for several propellant samples, after short investigations into their contents using common chromatography techniques. Several the propellant components investigated throughout have been used before in LDI analysis. DPA has been used before as a stabilizing additive for the analysis of aldehydes, but was not observed in the analysis <sup>[195]</sup>. Nitrocellulose has also been used in a number of LDI analyses, once again, as an additive <sup>[196-199]</sup>, in the analyses of triglycerols <sup>[199]</sup>, DNA <sup>[197]</sup>, proteins <sup>[198]</sup> and polycyclic aromatic hydrocarbons <sup>[196]</sup>.

Nitrocellulose has been found to decrease fragmentation, minimize matrix interference and improve shot to shot reproducibility [197, 199].

Laser-based instruments have been used previously to analyse a few different energetic samples including some propellant analysis. Earlier work in this in the tape-based part of this study found LDI capable of analysing a plastic energetic material [58]. DESI, a similar technique to MALDI has been used for the detection of RDX, HMX, TNT and PETN in a study mentioned in part one, investigating fabrics and airport security [146]. Smokeless powders have also been analysed by other laser based and soft ionization techniques. Direct Analysis in Real Time (DART) MS was used in the analysis of partially burnt smokeless powders and the discrimination powers were compared to that of GCMS [200]. TOF-SIMS was used in the differentiation of three smokeless and six black powders [178]. Laser Electrospray Mass Spectrometry (LEMS) has also been used in smokeless powder analysis of five ammunition samples, EC, MC DBP and dimethyl phthalate were detected and the information was able to be referenced back to the manufacturers information [201]. Each of these studies were able to make characterisations and identifications by using statistical analysis software.

### *Mid to Far IR at the Australian Synchrotron*

Infrared (IR) spectroscopy is a light based, non-destructive analytical technique, based on the vibrations of atoms and molecules when they are treated with light in the infrared part of the spectrum [202]. There are three distinct areas of IR analysis, near IR which uses light between visible light and  $4000\text{ cm}^{-1}$ , mid IR between  $4000\text{-}400\text{ cm}^{-1}$  and far IR between  $400\text{-}4\text{ cm}^{-1}$  [203, 204]. Mid IR is the most frequently used of the IR ranges, it is separated into 4 distinct areas, there are three bands between  $4000\text{-}1500\text{ cm}^{-1}$  for which there are clear peak assignments and bond types at particular wave numbers. In this range molecular construction can be assigned, as different peaks represent different bond types [204]. The wave range between  $1500\text{-}600\text{ cm}^{-1}$  is known as the fingerprint region [204]. There are more variations for peaks in this range, as single molecule can yield hundreds of peaks and there are peak variations within the same molecule type. Instead of assigning all peaks, it is looked at as an overall picture, like in fingerprint analysis [204]. Far IR has a more limited scope than mid IR, it is usable for a lower number of samples and is similar to the fingerprint region in that it is less structurally defining [204]. Far IR is most applicable to molecules that contain heavy atoms and those capable of molecular skeleton vibrations, molecular torsions and crystal lattice vibrations [204]. Far IR can be used in the characterisation of halogen-based molecules, organometallics and inorganic molecules [203].

IR has many different variations, Fourier Transform IR (FTIR) is the most commonly used, it is a mathematical application to transform wave signals into a usable spectrum made of peaks and valleys [203]. Attenuated Total Reflectance (ATR) is an accessory and type of IR spectroscopy which is extremely useful and makes it a more accessible technique to a greater range of samples. It is based on reflection of the light beam, as opposed to the transmission of standard IR which requires a transparent sample for the light to pass through, which is not the case with ATR [205]. ATR is an internal reflection technique [206] which requires a small internal reflection element (IRE) that the sample needs to be in contact with, common IREs include ZnSe germanium and diamond [207]. The light is reflected from the IRE at an angle that allows repeated reflection [207]. The repeated reflection of light results in evanescent waves which produce radiation which is absorbed by the sample [206, 207]. The penetration depth of the sample is  $1\ \mu\text{m}$  [207] therefore the thickness of the sample is not important, this is also due to the light not passing through the sample [203]. As the sample does not need to be transparent or manipulated to have specific properties ATR samples can be liquid, solid or gas [202] with the right accessories, and does not require a sample matrix such as dichloromethane or nujol [207].

The opportunity arose to use the Far IR instrumentation at the Australian Synchrotron, a particle accelerator which produces light which is almost the speed of light [208]. This light has high brightness, it is intense and highly collimated which a wide energy spectrum and it has high polarization. These combine to make a very powerful and specific beam of light for analysis [208]. Far IR analysis at the Synchrotron has been recommended for the use with explosives [208] and but this analysis has not been limited to the synchrotron.

Terahertz studies have been performed multiple times, particularly in conjunction with an instrument called Time Domain Spectroscopy (TDS). This set up has been used for the analysis of a number of energetic materials, 3,5-DNA, 2,4-DNT and TNT have been investigated for characterisation purposes [209], as well as another investigation of TNT, RDX and PETN, and two plastic explosives; SEMTEX and SX2 [210]. An experiment with a similar set up observed changes in an  $80\text{-}10\ \text{cm}^{-1}$  spectrum of HMX, RDX and PETN with increasing temperature [211]. Another complex study was performed to simulate onsite analysis of concealed explosives. This article found “spectral fingerprints” in the far IR range for RDX, PETN, HMX, TNT, SEMTEX H, SX2 and Metabel, as well as for a number of “confusion materials” in which explosive may be concealed. The spectra were extremely different and the energetic material spectra were able to be detected even when obscured by the other materials [212]. Mid IR in conjunction with ATR has even been used for analysis of smokeless powders, although this involved crushing the smokeless powder to apply it to the IRE which is not an ideal preparation method [213].

The abilities of ATR based IR and the previously performed studies indicate that Far IR analysis of propellants has the potential of producing usable spectra for their differentiation.

# 6 Experimental




## 6.1 Samples







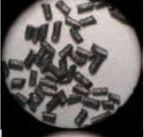

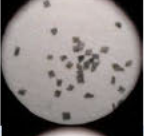

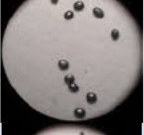


A variety of propellants were used throughout the experiments, from a range of sources. Two lists have been compiled in Table 6.1 and

The samples provided by the DST Group came with a lot more information, including the base type and some known ingredients such as the stabilizers. This information is summarized in Table 6.2.

Table 6.2, which provide information sourced from Forensic Science South Australia (FSSA) and the DST (Defence Science and Technology) Group respectively. The samples provided by the DST Group came with a lot more information, including the base type and some known ingredients such as the stabilizers. As can be seen in Table 6.1 the samples from FSSA were varying in terms of origin and information of the contents. Some were very old, others were minimally described and very little was known about the chemical composition of any of the samples. There were also a few samples of lower quality than the others, as can be seen in the description of Sample 5. Sample 5 is described as black powder from the turn of the century, and is thus, obsolete, containing none of the important modern propellant additives, nor the explosive compounds used in current firearm propellants. This sample was, therefore, not used throughout the experiments due to its irrelevant nature. Sample 12 was also of questionable content; upon visual inspection of the compound it appeared compromised, looking mouldy and decomposed. Less useful information was yielded from this sample, than many of the others. Sample 11 was interesting; its appearance differed greatly to the others, made from small orange cords. Research identified it to be cordite<sup>[214]</sup>, a smokeless powder developed in the late 1800s by the British to mimic ballistite, it combined nitroglycerin, gun cotton and mineral jelly, with the aid of an organic solvent<sup>[159, 215]</sup>

Table 6.1: Propellants sourced from FSSA

Number	Brand	Calibre	Description on vial	Photo
1	Strike	12 GA	Shotgun (cheap)	
2	Winchester	0.22	Super speed (Australia)	
3	Stirung	0.22	Super high speed (Philippines)	

4	Marlin	0.444	Remington Peters(rifle)	
5	Martini Nonry		450/577Obsolete turn of the century (black powder)	
6	Winchester		357 Magnum Revolver	
7	Vostor	0.22	Long rifle rim	
8	Unknown		8 mm Military German	
9	Winchester		243 W.W super (rifle)	
10	Unknown		7.7mm Japanese World War 2	
11	Webley		455 calibre revolver (WW1/WW2)	
12	Browning		FN 7, 65 calibre 32 calibre Belgium (pistol)	
13	Winchester		Super Speed	
14	Unknown		50 Calibre heavy machine gun	
15	RWS	0.22	High velocity (German)	
16	Fiocchi	0.22	Long rifle	

17	Federal		38 special (revolver)	
18	I. M. I	0.22	Long rifle	
19	Winchester		32AP-32Auto, 71GRF.M.C Winchester Western Division	

The samples provided by the DST Group came with a lot more information, including the base type and some known ingredients such as the stabilizers. This information is summarized in Table 6.2.

Table 6.2: Propellants provided by the DST group

Sample name	Base-type	Contents
A	Single	Nitrocellulose, DPA, possibly EC
B	Single	Nitrocellulose, DPA, graphite, CaCO <sub>3</sub> , K <sub>2</sub> SO <sub>4</sub> , KNO <sub>3</sub>
C	Double	Nitrocellulose, Nitroglycerin, DPA
D	Double	Nitrocellulose, Nitroglycerin, DPA, Potassium salts, graphite

The Victoria Police department provided a range of propellants sampled over many years, three sample groups were selected for specific comparison purposes. The samples were provided with sampling dates as well as approximations of their year of production. The three groups are different but interesting studies into the differentiation of propellant samples. These are summarized in Table 6.3, Table 6.4 and Table 6.5, there are images of each propellant post solvation in Figure 6.1 Figure 6.2 and Figure 6.3.

The first group of samples were World War II era propellants, labelled with the proposed area of origin seen in Table 6.3. The comparison of these samples is interesting as they were all produced around the same time and in a time when resources were limited. It was thought that these might contain similar components. Interestingly these samples can be quite easily differentiated by appearance alone, especially after solvation, as is clear in Figure 6.1. Little information could be found on their

chemical makeup, the information provided was central to brands and the grade of ammunition, as these samples are so old these companies do not have SDS information for these propellants available.

Table 6.3: World War II era propellants provided by Victoria Police

Number	Country	Brand	Calibre	Date	Type	Photo
91	USSR	Baikal	70 mm		Game cartridges	
100	France	Fulma	16 Ga	Jul-51		
103	Italian	Fiocchi		30/05/1951	22S Noxycentro/ 22LR	
119	Finnish	Oy SAKO	0.22	Oct-51	Hornet 32-20	
126	Italian	BDP	12 G	4/06/1951	"S4" Ballistite, low NG powder from BDP "Titan"	
146	Belgian		12 G	29/10/1951	CL "Stella"	
147	Austrian	OJP	12 G	13/12/1951	Kramsach	



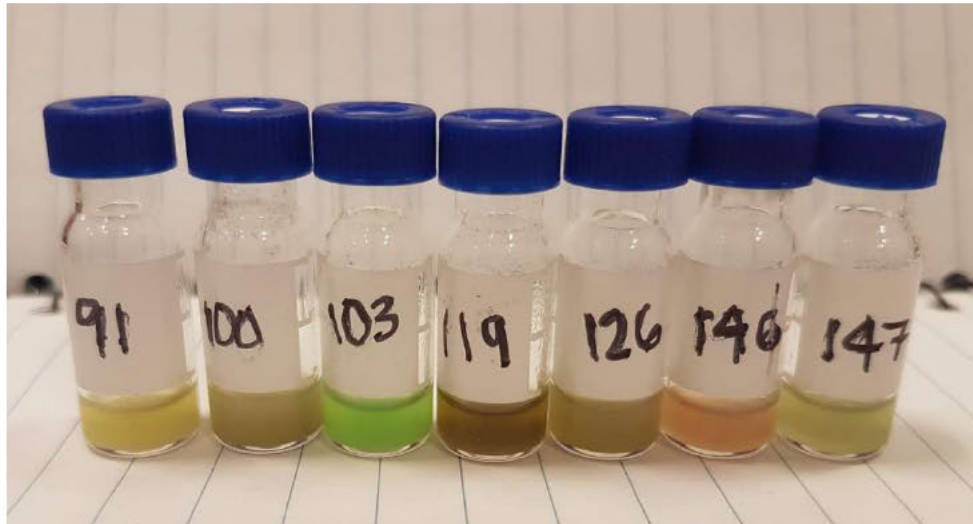







Figure 6.1: World war II era propellants provided by Victoria police

The next group contains propellants that are all the same brand and type of propellant the details of which are in Table 6.4: Winchester 760 ball powder propellants provided by Victoria Police. They are all Winchester 760 ball powders of different lot numbers. The comparison of these samples will reveal if the chemical make-up is the same or whether there are variations between batches and years. Winchester have few chemical details available online, however a basic safety data sheet was available, covering eleven of their powders. The list was very broad indicating that the nitrocellulose composition was anywhere from 50-100% and nitroglycerin 0-42%. It can be assumed that some of the propellants this SDS applied to are double base. The other ingredients that include DBP, EC, AKII, DPA, Nn-DPA and graphite may or may not be in each propellant <sup>[216]</sup>.

Table 6.4: Winchester 760 ball powder propellants provided by Victoria Police

Number	Lot Number	Labelled	Sampled	Purchased	Photo
253		76027138 AD01MD03	26/07/2007		
256	760288TE22A	W7601BP	26/07/2007		
274	760318VK1A		30/11/2017		
279	10623112430		30/11/2017	Sep-12	

285	2Y2Y5319	30/11/2017	
-----	----------	------------	---

It can be seen in Figure 6.2 that four of the five samples look very similar post solvation, with only sample 253 looking particularly different.

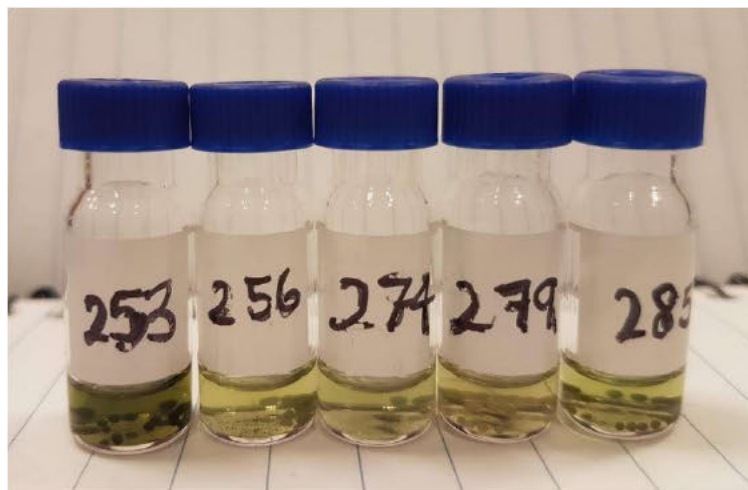



Figure 6.2: Winchester 760 ball powder propellants provided by Victoria Police

The propellants the third group, summarized in Table 6.5, are again the same brand, but are different types of smokeless powder, selected to see if there are any distinct similarities within a brand, across the different varieties. The Hercules samples include a green dot and blue dot variety that have visible, coloured taggants. The available SDS covered several different powders and had minimal information. It indicates that they are all very similar in their makeup. Nitrocellulose, nitroglycerin, DPA and MC are all included in the SDS <sup>[217]</sup>. The coloured taggants add a large note of difference. The green dot clearly had 3 green pieces in it., where as any blue dots appear to have faded. On closer inspection there was one piece that appeared bluer than the others. This grain did not fully dissolve as much as the other grains and appeared to have blue specks still in it. The dyes used for these taggants may strongly absorb light and be easily analysable.

Table 6.5: Hercules propellants provided by Victoria Police

Number	Sampled	Description	Vintage	Barcode	Photo
303	31/05/2018	Green Dot	1993	830710501	

304	31/05/2018	2400 Smokeless Rifle	1993	
305	31/05/2018	Blue Dot Premium	1993	

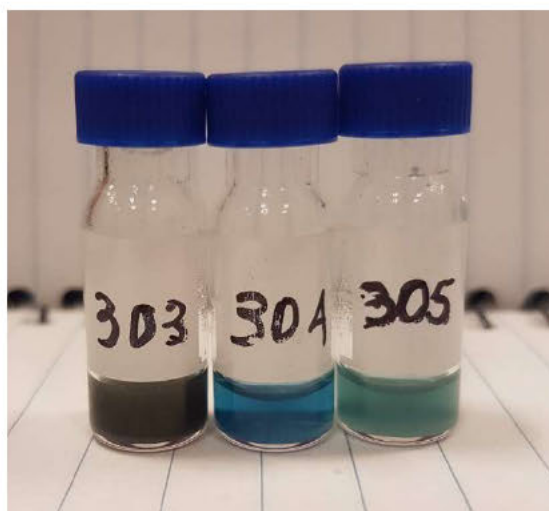


Figure 6.3: Hercules propellants provided by Victoria Police

## 6.2 Solutions

As can be seen from Table 6.6, while all the samples were solvated in methanol, only a small number were solvated for GCMS analysis. The GCMS sample preparation and analysis were time consuming, therefore, the number of samples was narrowed. Those selected were denser, were present in higher quantity, and appeared to be well preserved; they ranged in shape, size and colour. All alcohol solvated samples throughout all experiments were ultra-sonicated for 10 minutes and allowed to sit overnight before analysis.

Table 6.6: Solvation of FSSA propellant samples

#	LDI Preparation (methanol 1.5 mL)	GCMS Preparation	FTIR Preparation (methanol 300 µL)
	Mass (mg)	Mass(mg)	Mass (mg)
1	16.6		5.0
2	17.2	4.7	8.0
3	4.70		5.0
4	20.6	5.7	5.0
6	2.20	4.7	3.0
7	1.50		8.0

8	10.7		5.0
9	20.3	4.9	9.0
10	18.2		5.0
11	18.1		6.0
12	11.9		3.0
13	19.1	4.8	4.0
14	19.9		9.0
15	1.80		3.0
16	20.4	4.6	9.0
17	17.5		7.0
18	18.5		7.0
19	2.90		6.0

Table 6.7: Solvation of DST group propellant samples

Sample	Mass in 2 mL Methanol	Mass in 2mL Ethanol
A	6.1 mg	3.0 mg
B	5.0 mg	2.5 mg
C	5.3 mg	5.0 mg
D	5.3 mg	3.9 mg

The solutions made from the propellants provided by the Victoria Police used the masses provided below in Table 6.8 in 300 µL of methanol and prepared with 45 minutes of sonication. These preparation methods were optimised for the Synchrotron analysis by investigating a Winchester sample that was in excess, the concentration and number of drops applied were outlined with this sample.

Table 6.8: Solvation of Victoria Police propellant samples

Number	Mass	Number	Mass	Number	Mass
91	5 mg	253	5 mg	303	6 mg
100	5 mg	256	5 mg	304	5 mg
103	6 mg	274	6 mg	305	5 mg
119	5 mg	279	6 mg		
126	3 mg	285	6 mg		
146	5 mg				
147	4 mg				

Table 6.9: Standard preparation for LDI analysis

Standard	Amount in Methanol	Amount in Ethanol
DPA	10.1 mg in 5 mL	25.6 mg in 3 mL

<b>Nn-DPA</b>	5.8 mg in 5 mL	8mg in 2 mL
<b>2n-DPA</b>	2.5 mg in 5 mL	11.2 mg in 2 mL
<b>4n-DPA</b>	3.4 mg in 5 mL	7.5 mg in 2 mL
<b>EC</b>	14.0 mg in 5 mL	8.4 mg in 2 mL
<b>AK II</b>	16.4 mg in 5 mL	0.8 mg in 200 µL
<b>MC</b>	15.3 mg in 5 mL	11.4 mg in 2 mL
<b>DBP</b>	18 µL in 5 mL	Undiluted
<b>2,4-DNT</b>	7.0 mg in 5 mL	10.7 mg in 2 mL
<b>2,6-DNT</b>	8.7 mg in 5 mL	10.7 mg in 2 mL
<b>NC</b>	50 µL in 2 mL	0.5 µL in 0.5 µL
<b>NG</b>	2%	0.5 µL in 0.5 µL

### 6.3 High Pressure Liquid Chromatography

HPLC analysis was used to provide initial information for all the propellants provided by FSSA. The method used was that developed by Leigh Thredgold in his Honours thesis 2010 with the specifications described below <sup>[162]</sup>. Samples were prepared with methanol as in Table 6.6

Propellant standards were also made up as per Table 6.10 combined together in a 25 mL volumetric flask, solvated with HPLC grade methanol. All samples and standards were filtered using 0.45 µL nylon filters prior to analysis.

Table 6.10: Standard preparation for HPLC

Standard	Amount
<b>DPA</b>	1.6 mg
<b>Nn-DPA</b>	1.1 mg
<b>2n-DPA</b>	0.6 mg
<b>4n-DPA</b>	0.8 mg
<b>EC</b>	7.9 mg
<b>MC</b>	4.1 mg
<b>AK II</b>	5.1 mg
<b>DBP</b>	9 µL

The propellants and samples were analysed at the HPLC conditions stated in Table 6.11 with the solvent composition in

Table 6.12.

Table 6.11: HPLC conditions

Condition	Specification
-----------	---------------

Analysis Time	10 minutes
Temperature	Maintained at 30°C
UV-Vis absorption	282 nm
Injection volume	10 µL
Rate	1.0 mL.min <sup>-1</sup>
Column type	Eclipse XBD-C18
Particle Size	3.5 µm
Dimensions	150 x 4.6 mm

Table 6.12: Solvent composition

Time (mins)	% methanol	%H <sub>2</sub> O
0	72	28
7.5	72	28
8	90	10
9	90	10
10	72	28

## 6.4 Gas Chromatography Mass Spectrometry

GCMS analysis was introduced as a method for peak identification using a pre-established library, to confirm any of the components present in the FSSA propellants. Samples prepared for GCMS were prepared to the weights shown in Table 5.1, then solvated in 5 mL of ethyl acetate, a 0.3 mL aliquot was taken and dried with nitrogen gas, This sample was then reconstituted with dichloromethane in a GCMS vial with a polyspring insert to maximise analysis of small aliquots <sup>[218, 219]</sup>.

The instrument used was the Agilent GCMS Pyrolyzer with a 30 m length, 25 µm thickness, 0.25 mm internal diameter column, with a stationary phase consisting of 5% phenyl-arylene, 95% dimethylpolysiloxane. The method used was a based on a number of experimental procedures and was performed using Helium gas with an injection temperature of 220°C and a column temperature was initially 50°C, ramping at 10°C/minute to 280°C. 1 µL was used, with a 20:1 split with a needle depth reduced to 50%, due to the vial insert <sup>[218-220]</sup>.

## 6.5 Mid-Far IR at the Australian Synchrotron

The Far IR instrument coupled to the beamLine at the Australian Synchrotron is a Brüker IFS 125/HR Fourier Transform (FT) spectrometer. The internal light source was a Hg-Arc lamp. It was used with ATR using a diamond IRE. Dissolved samples were dropped onto the sample window, one drop at a time, waiting for the methanol to evaporate between each application. Each spectrum is a combination of 4 drops. A blank was taken prior to each sample and all blanks and samples were taken

with resolution of  $1\text{ cm}^{-1}$  and was an average of 10 spectra of 50 scans. The data was processed using OPUS 7.2 software, the blank averages were taken from the sample spectra and then transformed into absorption spectra. These were then compared at different peak positions.

## 6.6 LDI Analysis

Each different preparation of the samples mentioned above was pipetted onto the MALDI plate and analysed in turn, using the settings described in Part one. After initial failed attempts at analysing pure solid samples during honours<sup>[58]</sup>, sample preparation was deemed a necessary step for the analysis of propellant samples. And thus, no tape or fibre analyses were undertaken.

Negative LDI-MS was also undertaken for the propellant samples and stabilizers, using the same settings as mentioned in Part one but in negative mode. CsI remained the calibrant giving the calibration information in Table 6.13. The differences increase significantly as the ions get larger, but these analyses are still being used to establish usefulness and differentiation and thus are still useful.

Table 6.13: CsI calibrant negative peaks

Negative Ion	Peak Position (m/z)	Actual Peak (m/z)	Difference (%)
I <sup>-</sup>	126.906	126.319	-0.463
CsI <sup>-</sup>	259.810	258.756	-0.406
CsI <sub>2</sub> <sup>-</sup>	386.715	385.138	-0.408
Cs <sub>2</sub> I <sub>3</sub> <sup>-</sup>	646.525	643.745	-0.430

### *FSSA samples*

Upon inspection of methanol treated samples from Table 6.6 it could be seen that they were not fully solvated, residual materials ranged from sludge to relatively solid samples. These were transferred to the MALDI plate along with 1  $\mu\text{L}$  of each of the solutions. These samples were analysed between 50-90% laser strength.

The solutions from this extraction were done using the same samples as above; these were detected with a lower, 50-60%, laser strength.

### *Stabilizer standards*

The stabilizer ingredients were also investigated, the mixture created for the HPLC analysis was initially pipetted at 1  $\mu\text{L}$ , but this produced no spectra, 10  $\mu\text{L}$  was later loaded onto the plate, 1  $\mu\text{L}$  at a time which produced a spectrum with many peaks. Therefore, individual more concentrated samples were made as per Table 6.9, 1  $\mu\text{L}$  of each of these was pipetted onto the target plate and allowed to dry.

The nitrocellulose sample was water wet and the nitroglycerin was a 2% sample in alcohol, samples of pure dinitrotoluene and dibutyl phthalate were also added.

#### *DST Group samples*

1  $\mu$ L of each sample was pipetted onto the target plate in triplicate and analysed at with 70-90% laser fluence.

#### *Victoria Police samples*

1  $\mu$ L of each of the solvated samples was pipetted in triplicate onto the sample plate and allowed to dry, these samples required 80-90% laser fluence for analysis. The number of shots required for these spectra was between 1000 and 2000. One grain of the green taggant in sample 303 was also adhered to the plate using double sided tape. This was analysed using 45-65% laser fluence and required over 2000 shots.



# 7 Results and Discussion

## 7.1 HPLC of FSSA propellant samples

The standards used for the HPLC analysis showed retention times very close to those expected, indicating that the peaks referenced in the analysis should be quite accurate. The times can be seen in Table 7.1.

Table 7.1: Retention times (RT) of standards

Compound	Expected retention time (min)	Actual retention time (min)	Difference
DPA	4.83	4.94	+0.11
Nn-DPA	3.87	3.98	+0.11
2n-DPA	7.32	7.44	+0.12
4n-DPA	4.16	4.24	+0.08
EC	6.93	7.002	+0.072
MC	3.68	3.71	+0.03
AK II	2.31	2.46	+0.13
DBP	8.49	N/A	N/A

The results of the HPLC analysis of the FSSA samples can be seen, summarized in Table 7.2 on the next page. The HPLC analysis confirmed several contents of the FSSA propellants, giving peaks for each of the propellants except for sample 8, which upon inspection proved too deteriorated to give enough peak differentiation. There seemed to be inconsistencies in the spectra, increasing with each sample, some peaks were assigned based on their position relative to other peaks in the spectrum. The peaks around 2.90 were assigned to be DNT. These assumptions confirm that this method of analysis is not ideal for these samples, although some information can be used.

It can be seen in that there were many peaks for each of the samples analysed, most of them contain DPA and/or one of its derivatives. Samples 17, 18 and 19 are the only samples not to contain DPA or any derivatives. As so many of the peaks are shared and the profiles of the samples are so similar, they cannot be differentiated based on these contents.

Table 7.2: HPLC analysis of FSSA propellants, and the identification of standards

Standard	RT	1	2	3	4	6	7	9	10	11	12	13	14	15	16	17	18	19
AK II	2.46	2.405	2.42	2.439		2.446	2.446			2.434	2.542	2.501		2.546	2.689			
2,4-DNT		2.877	2.903	2.92	2.93	2.931		2.939	2.94	2.937	2.968	3.007		3.057		3.209	3.394	
MC	3.71															3.882		3.426
Nn-DPA	3.98	4.075	4.135	4.171	4.183	4.187	3.995	4.199	4.2		4.25				4.718		4.089	
4n-DPA	4.24	4.339	4.441	4.2460	4.479	4.482	4.188	4.449	4.493	4.474	4.542	4.307	4.335	4.391	5.061			
		4.644																
DPA	4.94	5.059	5.143	5.19	5.203	5.209	5.206	5.218	5.217	5.068	5.284	5.361	5.412	5.478	5.941			
EC	7.002																	6.281
2n-DPA	7.44	7.663	7.631	7.494	7.926	7.947	7.938	7.954	7.955		8.074	7.779		7.982	8.854			
				7.912														
DBP												8.203	8.263	8.411	9.365		7.324	7.369

## 7.2 GCMS of select propellant samples

Three samples were investigated using GCMS, to establish whether an established method could give an indication of the identity of any mass spectrometry peaks found in the LDI analysis. The purpose of these experiments allowed for a limited range of samples. Sample 2 yielded several peaks on the chromatogram seen in Figure 7.1. Figure 7.2 and Figure 7.3, the chromatograms for samples 4 and 6 respectively showed much fewer components being detected. Using the peak library associated with the instrument, the possible identities of each peak are listed in Table 7.3, Table 7.4 and Table 7.5 respectively. Some of the peaks represented compounds not common to propellants and thus were not listed, often these were the highest probability peak sources. It is observed that both Sample 2 and Sample 6 are suspected double base propellants, as they both displayed peaks that could represent nitroglycerin, however, this was the second most probable compound to be represented by this information, with a low 12-15% probability. Also, it is of interest that some of the components do not match up with the information found during the HPLC analysis discussed above, which brought the quality of the information into question.

In the analysis of sample 2 via HPLC it was found to contain AK II, 2,4-DNT, Nn-DPA, 4n-DPA, DPA and 2n-DPA, of those components only DPA and 2n-DPA were found using GCMS. However other components were found using GCMS, including DBP and MC. The final suspected compound, diphenyl phthalate, is not one of the standards that were being investigated, but as a phthalate, is thought to act in a similar manner to dibutyl phthalate. Diphenyl phthalate is a plasticizer used in the 1950s [221, 222].

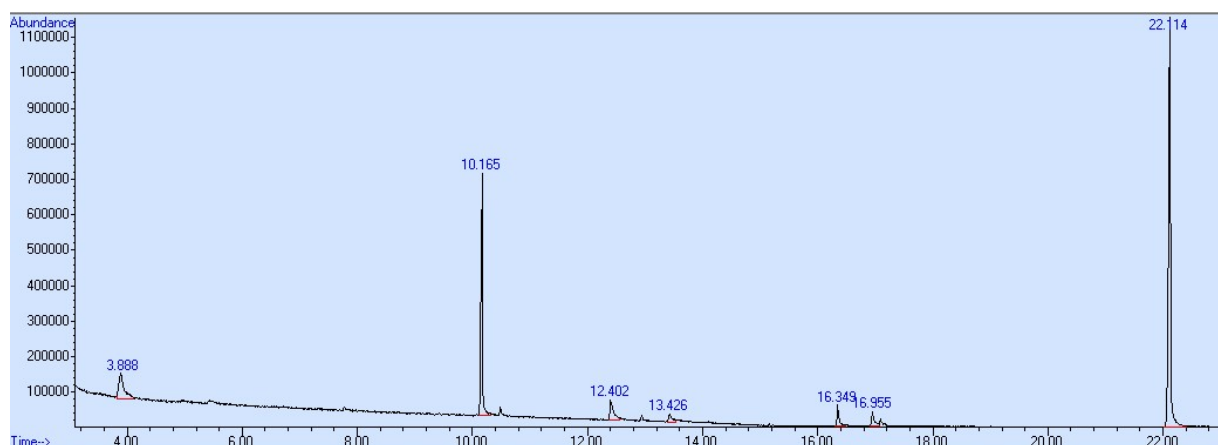


Figure 7.1: Gas Chromatogram of FSSA Sample 2

Table 7.3: List of possible propellant components for FSSA Sample 2

RT (min)	Suspected compound	% Probability	Strongest Mass Peaks (m/z)
10.172	Nitroglycerin	14.9	46
13.426	DPA	9.87	169
16.356	MC	61.5	120, 148, 268
16.947	DBP	14.2	149
17.092	2n-DPA	59.0	167, 214
22.114	Diphenyl phthalate	79.7	225

The analysis of sample 4 yielded much less information, with only one peak representing 2,4-DNT, this was also found in the HPLC analysis along with Nn-DPA, 4n-DPA, DPA and 2n-DPA. GCMS was significantly less informative in this case.

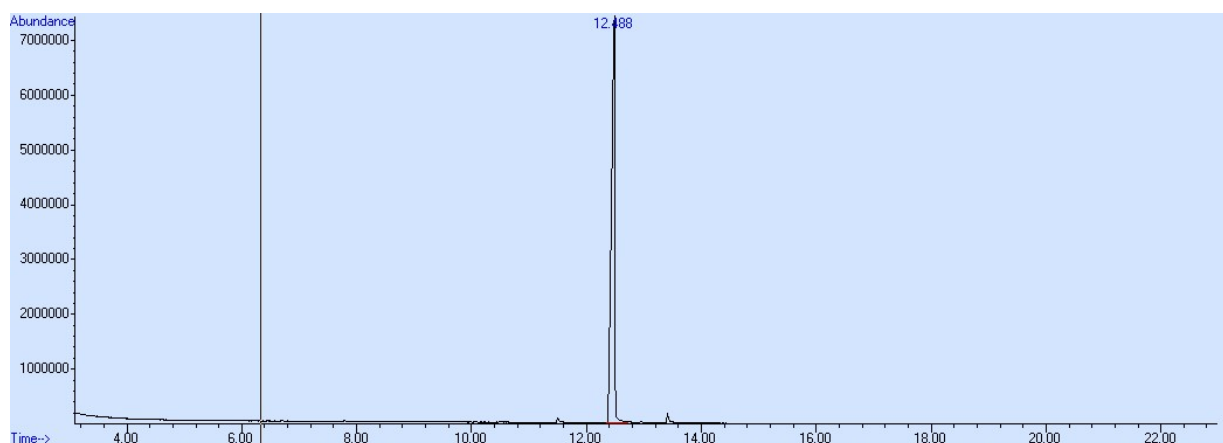


Figure 7.2: Gas Chromatogram of FSSA Sample 4

Table 7.4: List of possible propellant components for FSSA Sample 4

RT (min)	Suspected compound	% Probability	Strongest Mass Peaks (m/z)
12.488	2,4 DNT	91.5	165

Sample 6 showed the potential Nitroglycerin peak along with 2,4-DNT and DPA which were also detected in the HPLC analysis, along with Nn-DPA, 4n-DPA, and 2n-DPA. The GCMS also has a peak for DBP which was not found using HPLC.

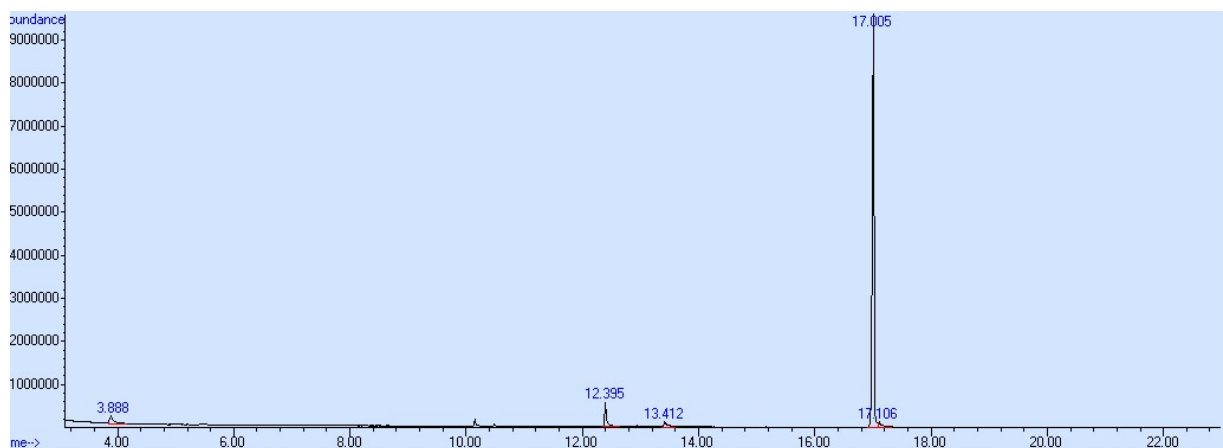


Figure 7.3: Gas Chromatogram of FSSA Sample 6

Table 7.5: List of possible propellant components for FSSA Sample 6

RT (min)	Suspected compound	% Probability	Strongest Mass Peaks (m/z)
10.151	Nitroglycerin	12.9	46
12.395	2,4-DNT	91.2	165
13.412	DPA	20.7	169
17.005	DBP	28.5	149

The GCMS analysis was a time-consuming process, much more so than the LDI process, analysis and library information was found for only three samples initially and upon inspection provided some information but few peaks which coincided with those found in the LDI spectra discussed below. The differences in these peaks is most likely due to the soft ionization used in LDI not fragmenting the samples as much as in GCMS, therefore the peaks will be vastly different. The information did not support that found in the HPLC analysis, some components were detected with both methods, but there was not a lot of agreement between the two methods. This GCMS method was only effective for one of the samples, indicating that the method would need to be optimized on a sample to sample basis. Overall, this analysis was deemed to be time consuming and did not provide enough appropriate information to support the LDI experiments to warrant further investigation into the samples. Therefore, further research focussed on using LDI analysis in the differentiation of the samples.

### 7.3 Mid to Far IR of select propellant samples

The data from this analysis is presented in the form of overlaid spectra of all samples to be differentiated per group. Further to this certain segments of these spectra have been enlarged to better highlight small differences and shallow peaks and shoulders. As some of these peaks were so

minor the software was not able to identify and label them, so they have been manually highlighted where possible.

### *FSSA Samples*

The FSSA samples were first investigated in solid form, by looking at one of the larger pellets directly on the diamond surface. As with early investigations of this study <sup>[58]</sup> the light did not penetrate the sample due to the abnormal shape and coatings. However, a secondary sample was also investigated, sample 11, the cordite has a more transparent appearance and was able to produce a spectrum, although it was only mildly different to the blank and provided much less information than the solutions.

The samples from FSSA were observed in the same spectrum to differentiate any important peaks. It can be seen from Figure 7.4 that as there are so many spectra it is difficult to identify any differences.

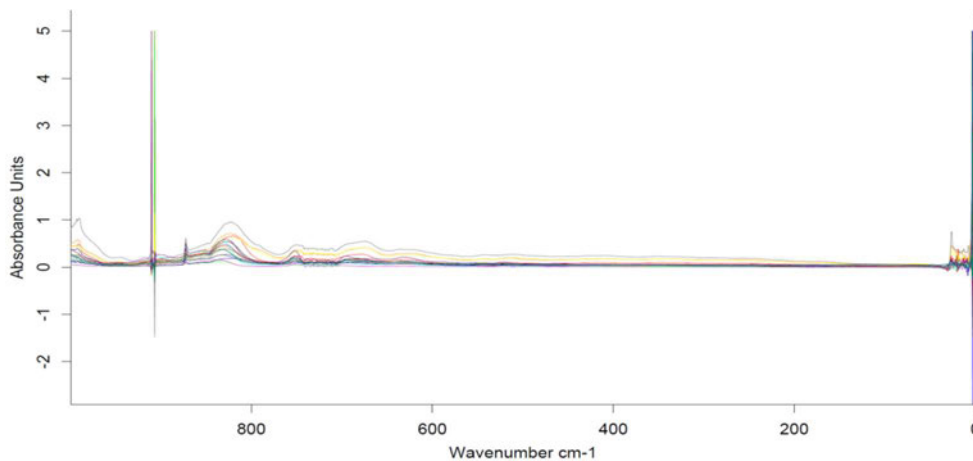


Figure 7.4: Mid-far IR spectrum of 18 FSSA propellant samples

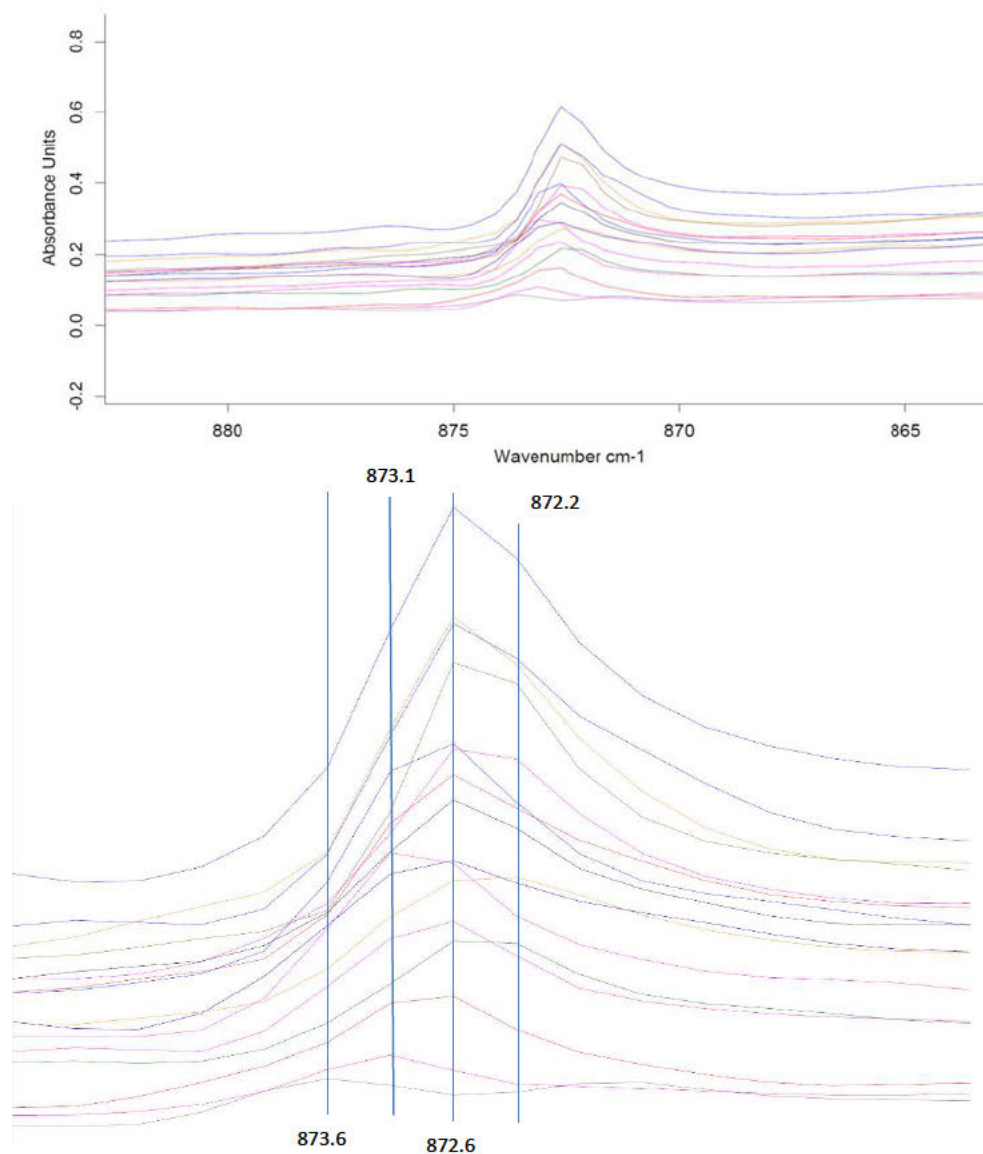


Figure 7.5: IR spectrum of 18 FSSA samples: 875-870  $\text{cm}^{-1}$

Figure 7.5 gives the zoomed region of a single peak 875-870  $\text{cm}^{-1}$ , there are five different peak-types that can be identified. Sample 15 (grey) presents the only peak at 873.6  $\text{cm}^{-1}$  and can therefore be easily differentiated from the other samples. There are three other points at 873.1  $\text{cm}^{-1}$ , 872.6  $\text{cm}^{-1}$  and 872.2  $\text{cm}^{-1}$ . Samples 3, 4, 6, 14, 17 and 19 have points at 873  $\text{cm}^{-1}$ , of these 3, 4, 6, 17 and 19 continue to a point at 872.6  $\text{cm}^{-1}$ , leaving sample 14 (pink second to bottom) as the only one with a narrower peak at 873.1  $\text{cm}^{-1}$ . Samples 1, 10, 11 and 16 have peaks across 872.6  $\text{cm}^{-1}$  to 872.2  $\text{cm}^{-1}$  leaving samples 2, 7, 8, 9, 12, 13 and 18 as the only samples with narrow peaks at 873.1  $\text{cm}^{-1}$ . From this single peak sample 14 and 15 can be completely differentiated, and all other samples can be narrowed into smaller groups.

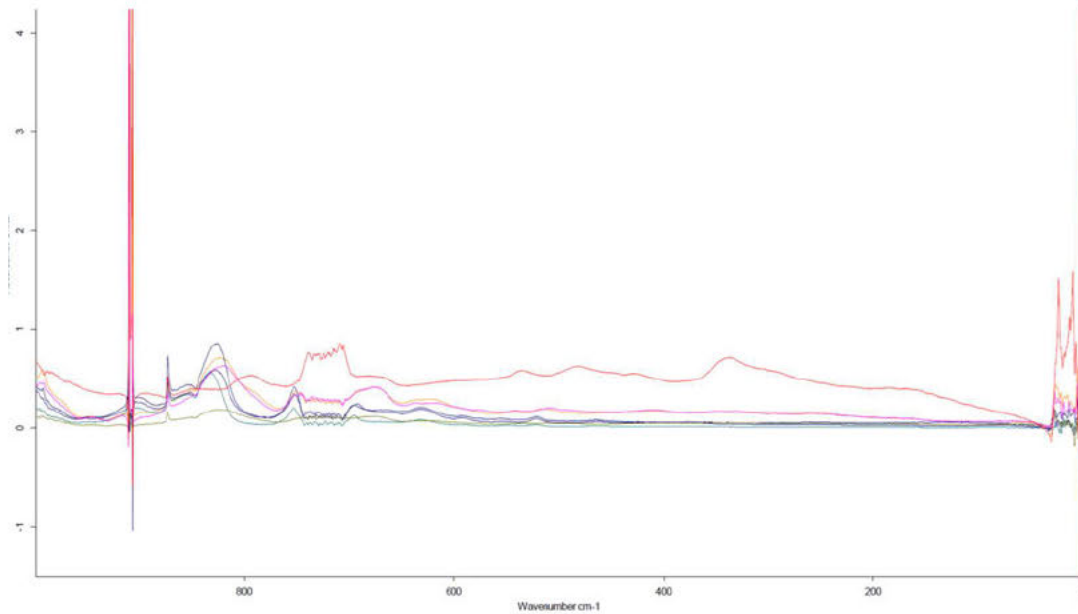


Figure 7.6: IR spectrum of FSSA samples 2, 7, 8, 9, 12, 13 and 18

Figure 7.6 shows the spectrum of the samples with a narrow peak at  $872.6\text{ cm}^{-1}$ , sample 8, in red, can be clearly differentiated, as it is completely different in shape, this can be seen again in Figure 7.7.

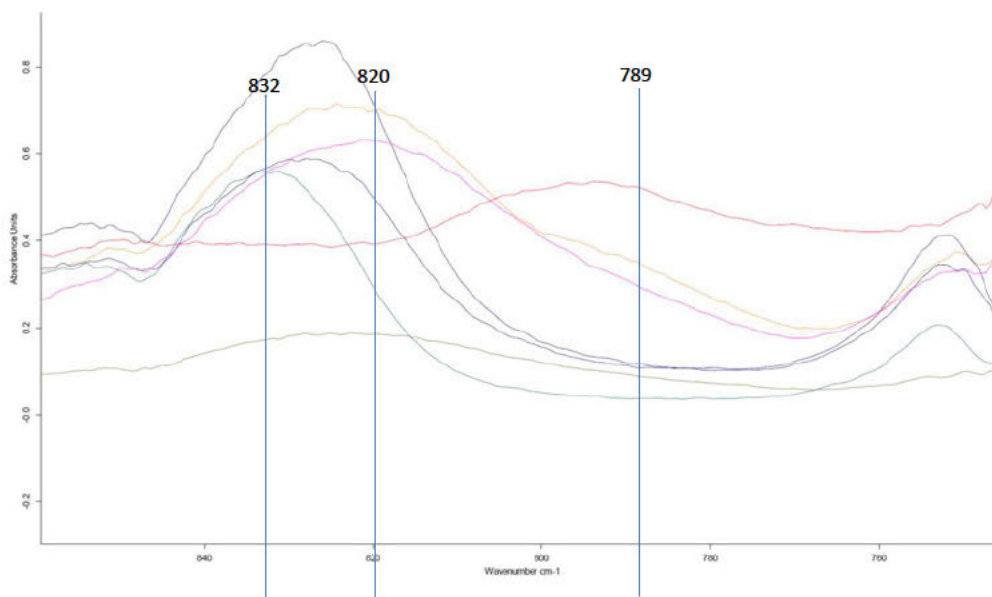


Figure 7.7: IR spectrum of FSSA samples 2, 7, 8, 9, 12, 13 and 18:  $900\text{-}650\text{ cm}^{-1}$

Samples 12 and 18 (pink and orange) both have a broad peak around  $820\text{ cm}^{-1}$ , sample 18 (orange) has a shoulder at  $789\text{ cm}^{-1}$ , whereas sample 12 does not. The teal spectrum is sample 13 which is the only one with a peak around  $832\text{ cm}^{-1}$ .



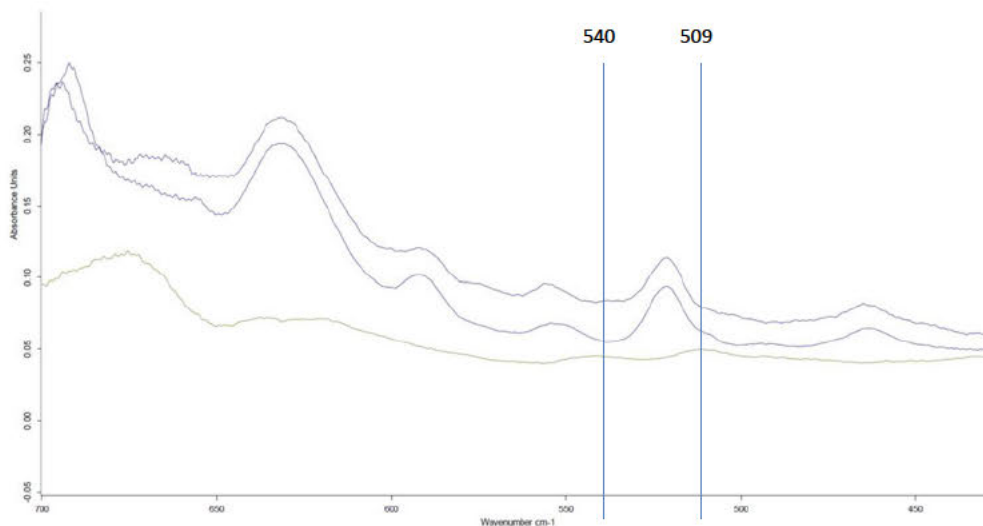


Figure 7.8: IR spectrum of FSSA samples 2, 7 and 9: 700-400  $\text{cm}^{-1}$

The spectra of the final three samples are similar, therefore a different area of the spectrum is investigated in Figure 7.8. Sample 9 (green) can be differentiated from samples 2 and 7 by the peaks at  $540 \text{ cm}^{-1}$  and  $509 \text{ cm}^{-1}$  which are not present in samples 2 and 7, which cannot be differentiated from each other, as seen in Figure 7.9.

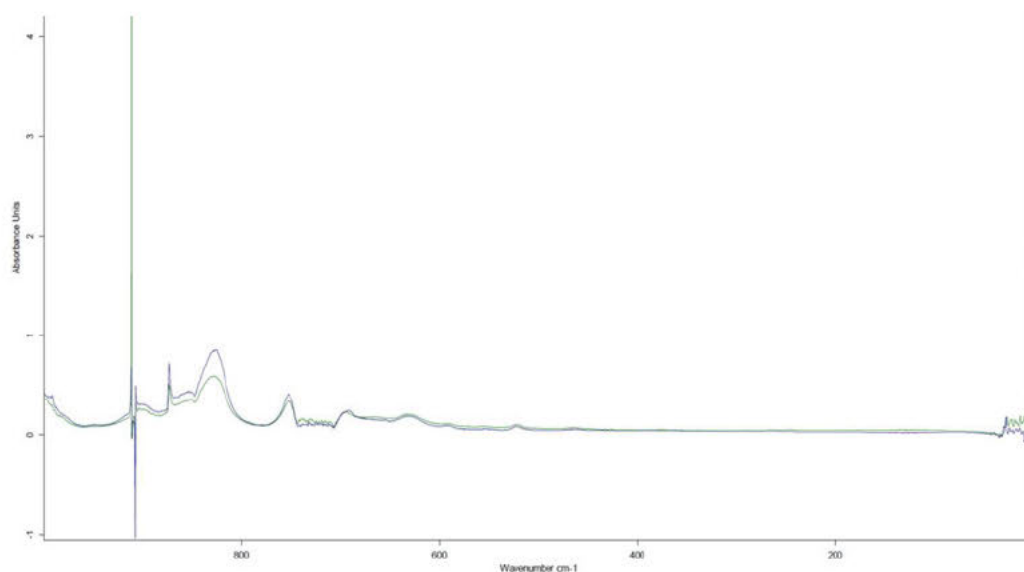


Figure 7.9: IR spectrum of FSSA samples 2 and 7

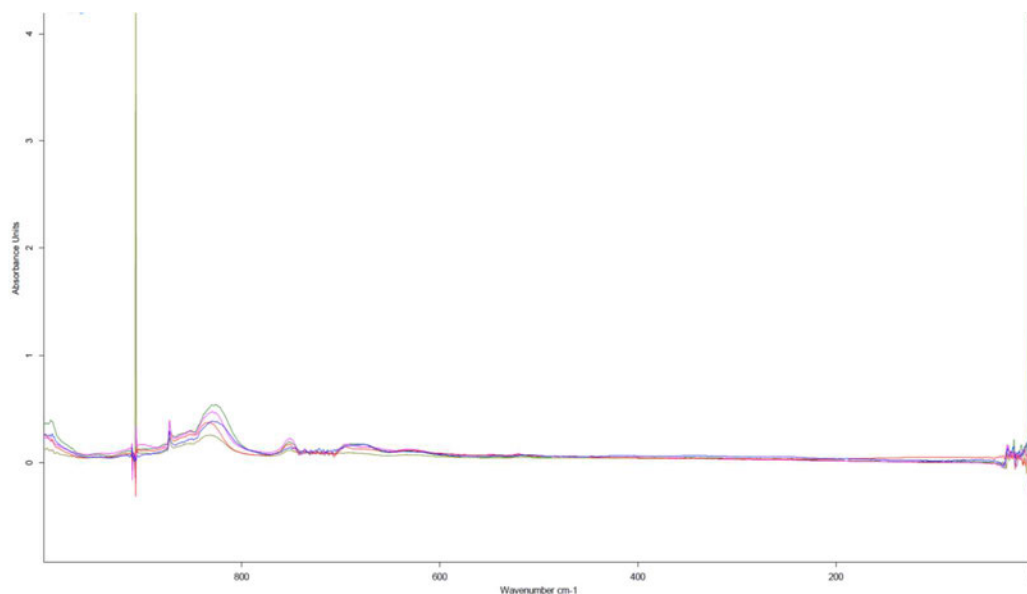


Figure 7.10: IR spectrum of FSSA samples 3, 4, 6, 17 and 19

The spectra of samples 3, 4, 6, 17 and 19 are displayed in Figure 7.10, and zoomed in to specific peaks in Figure 7.11 and Figure 7.12.

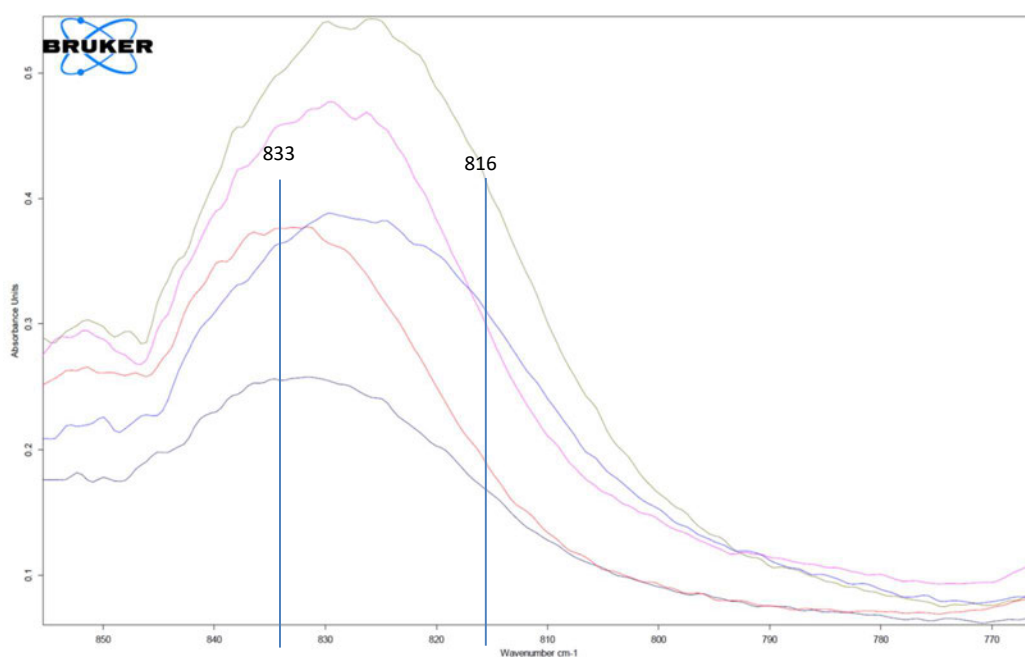


Figure 7.11: IR spectrum of FSSA samples 3, 4, 6, 17 and 19: 860-760  $\text{cm}^{-1}$

It can be seen in Figure 7.11 that samples 3 and 17 (orange and navy) both peak at  $833 \text{ cm}^{-1}$ , sample 4 (blue) also has a peak close to that at  $830 \text{ cm}^{-1}$  but also has a broadening shoulder at  $816 \text{ cm}^{-1}$ . Sample 6 (pink) has a narrow peak at  $830 \text{ cm}^{-1}$  and sample 19 (green) has a broad peak between  $830$  and  $825 \text{ cm}^{-1}$ .

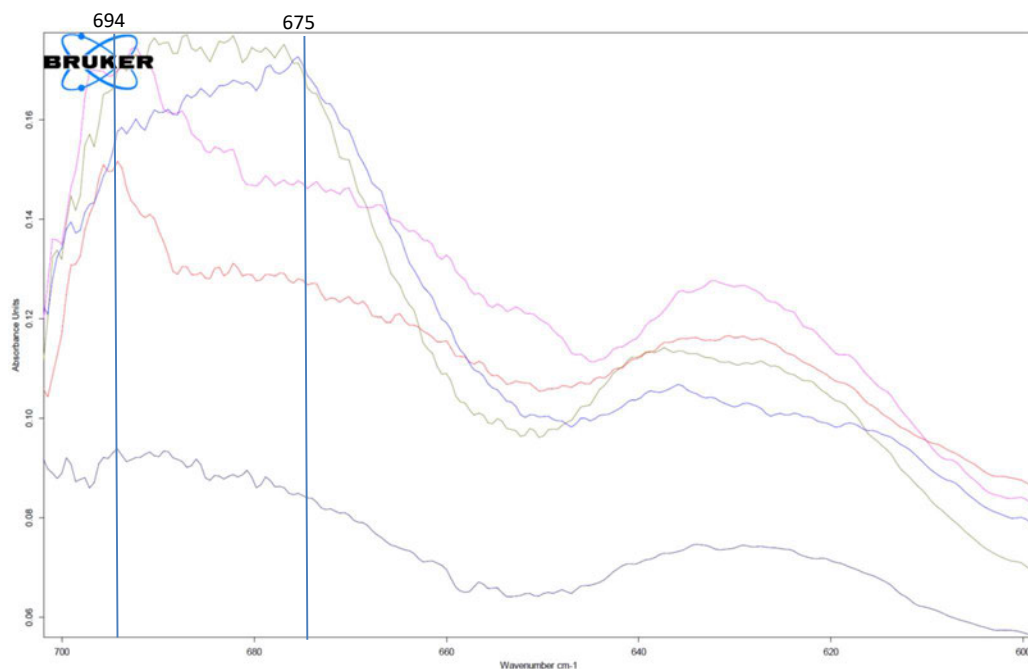


Figure 7.12: IR spectrum of FSSA samples 3, 4, 6, 17 and 19: 700-600  $\text{cm}^{-1}$

In Figure 7.12 more differentiation can occur, samples 3 (orange) and 6 (pink) peak around  $694 \text{ cm}^{-1}$ , sample 4 (blue) at  $675 \text{ cm}^{-1}$ , and 19 (green) presents a broad peak between  $694$  and  $675 \text{ cm}^{-1}$ , while sample 17 (navy) has almost no peak in this area. The final group of samples, 1, 10, 11 and 16, are displayed in Figure 7.13 and Figure 7.14, it can be seen from the enlarged segment in Figure 7.14 that there are four distinct peak positions. Sample 1 (red) peaks at  $831 \text{ cm}^{-1}$ , sample 11 (pink) at  $827 \text{ cm}^{-1}$ , sample 10 (blue) at  $823 \text{ cm}^{-1}$  with a shoulder at  $791 \text{ cm}^{-1}$ , and sample 16 (navy) at  $819 \text{ cm}^{-1}$ .

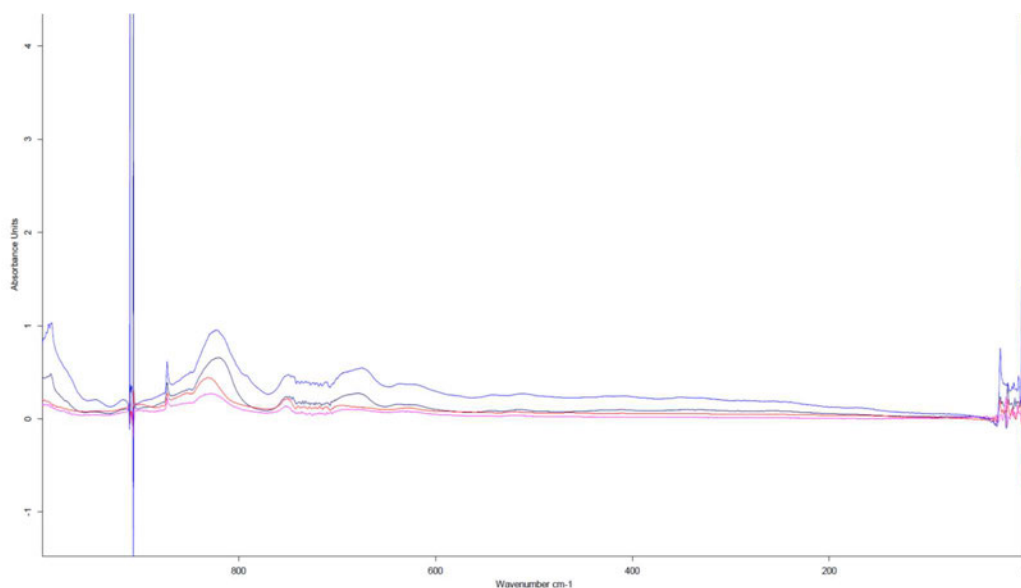


Figure 7.13: IR spectrum of FSSA samples 1, 10, 11 and 16

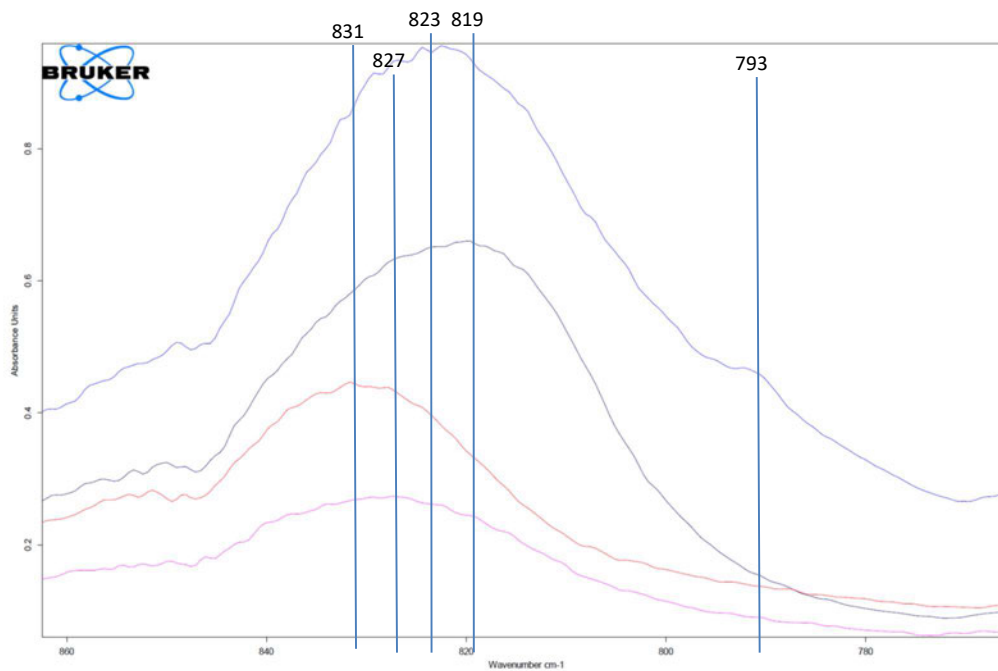


Figure 7.14: IR spectrum of FSSA samples 1, 10, 11 and 16: 860-760  $\text{cm}^{-1}$

Each FSSA samples was differentiated via Mid-Far IR except for samples 2 and 7, these samples are both 0.22 calibre propellants which look very similar and therefore most likely have similar makeup.

### Victoria Police Samples

The Victoria Police samples labelled 91, 100, 103, 119, 126, and 146 are world war II era samples, the spectra of which can be seen in Figure 7.15, Figure 7.16, Figure 7.17 and Figure 7.18. The data for sample 147 was lost and therefore this sample is not included in the analysis. Two main distinctions can be made from the overall spectrum, sample 103 (orange) and sample 91 (teal) have stronger and better-defined peaks and sample 119 (blue) does not follow the same trends. Figure 7.16 shows that at  $872.6 \text{ cm}^{-1}$  samples 91, 100 (black) 103 and 146 (red) peak, sample 126 (green) peaks at  $873.1 \text{ cm}^{-1}$ , and this is the same point where sample 119 has a valley. Another point of difference occurs between  $830$  and  $810 \text{ cm}^{-1}$ . Samples 91 and 103 have broad peaks in the spectrum around  $816 \text{ cm}^{-1}$ , whereas samples 100, 126 and 146 have broad peaks around  $826 \text{ cm}^{-1}$  and sample 119 has no peak at all. There are some differences in the Mid-far IR spectra of these samples but not enough to differentiate all samples. This may be due to a similarity in propellants developed in this era.

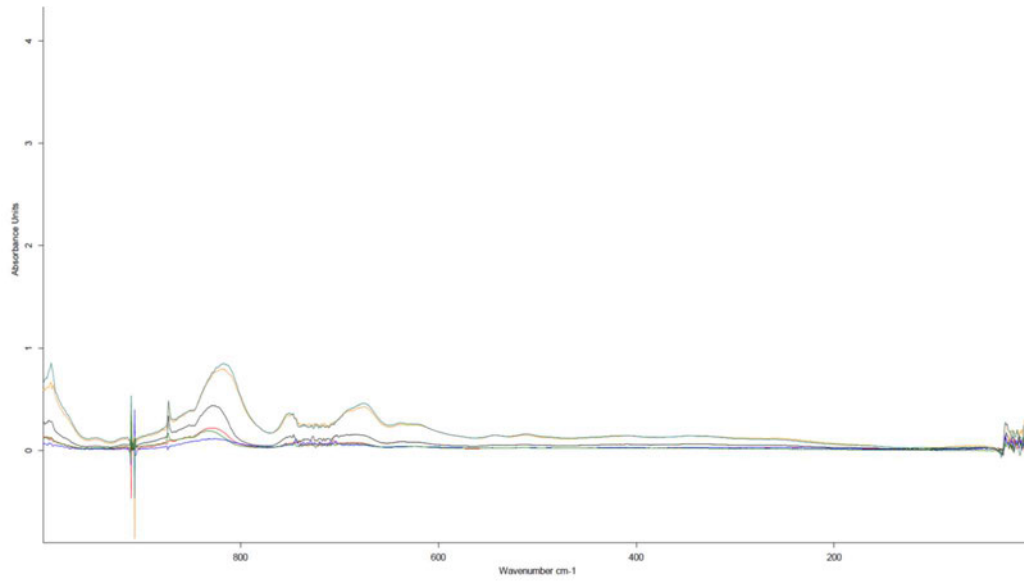


Figure 7.15: IR spectrum of Victoria Police samples 91, 100, 103, 119, 126 and 146

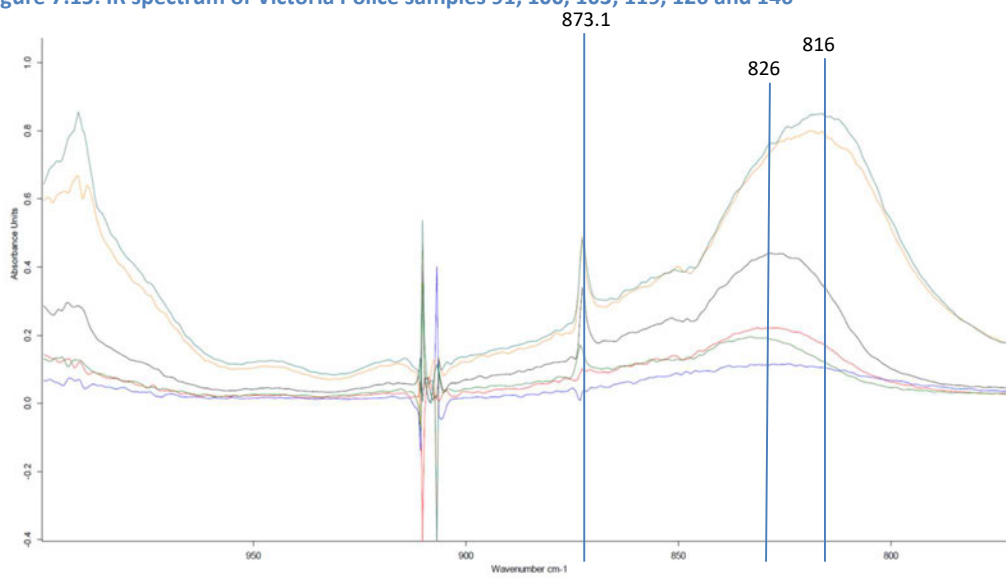


Figure 7.16: IR spectrum of Victoria Police samples 91, 100, 103, 119, 126 and 146: 1000-750  $\text{cm}^{-1}$

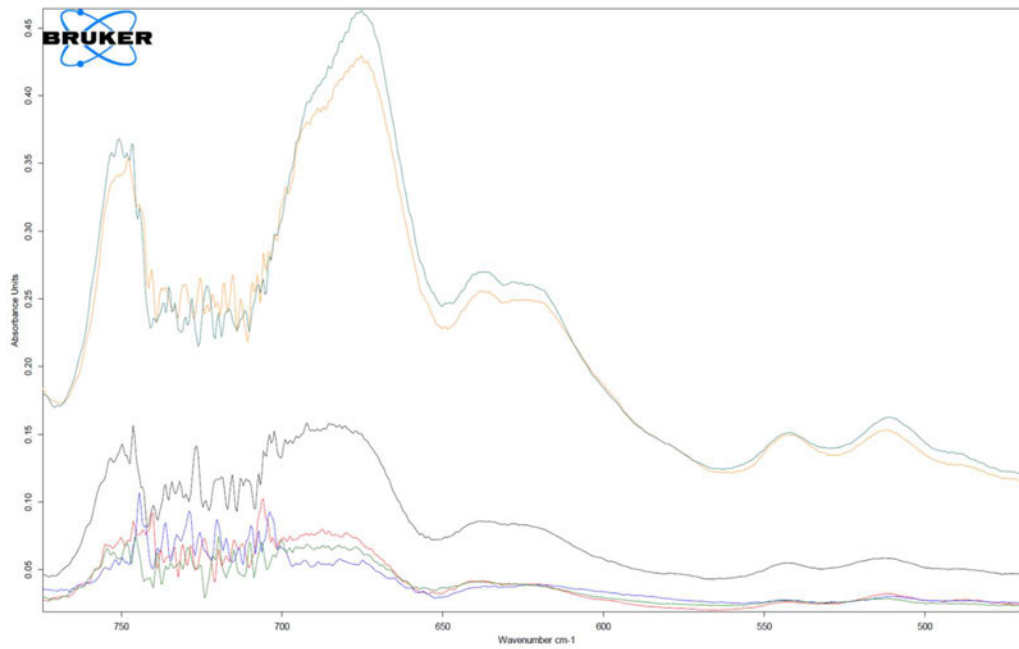


Figure 7.17: IR spectrum of Victoria Police samples 91, 100, 103, 119, 126 and 146: 780-450  $\text{cm}^{-1}$

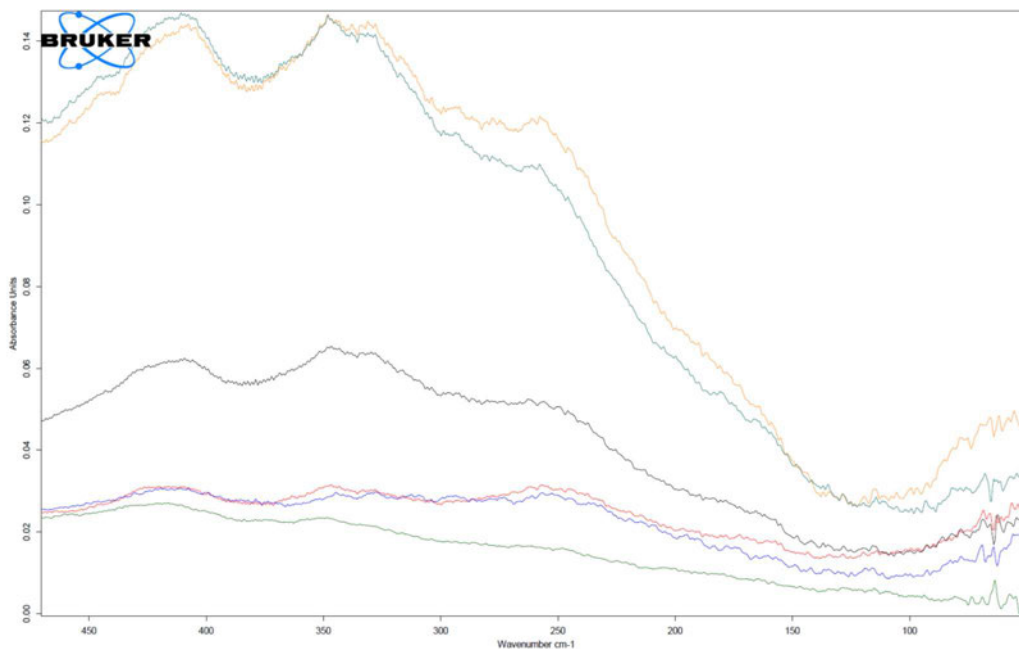


Figure 7.18: IR spectrum of Victoria Police samples 91, 100, 103, 119, 126 and 146: 460-50  $\text{cm}^{-1}$

The Winchester 760 ball samples, 253, 256, 274, 279 and 285, are displayed in Figure 7.19, Figure 7.20, Figure 7.21 and Figure 7.22 below. These samples are the same brand and type and only differ by batch number, the samples appear similar except when dissolved, sample 253 is darker and more dissolved than the others. On first inspection the biggest difference between samples is a higher absorption of sample 256 (green). Figure 7.21 produces a clear peak for sample 274 (teal) at  $618 \text{ cm}^{-1}$  and more defined peaks throughout the spectrum for both sample 256 and sample 279 (black). The other samples had similar peaks but were much weaker and less defined.

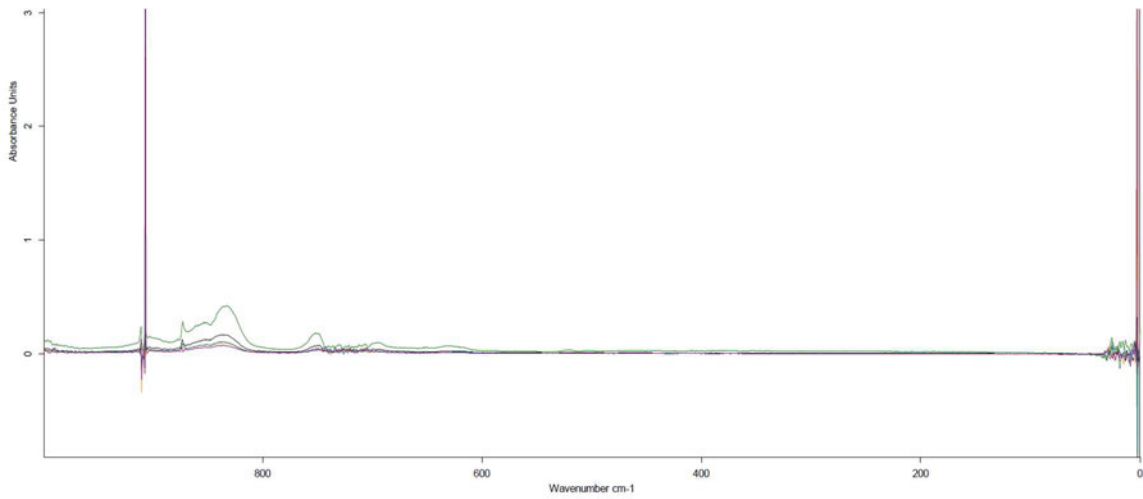


Figure 7.19: IR spectrum of Victoria Police samples 253, 256, 274, 279 and 285

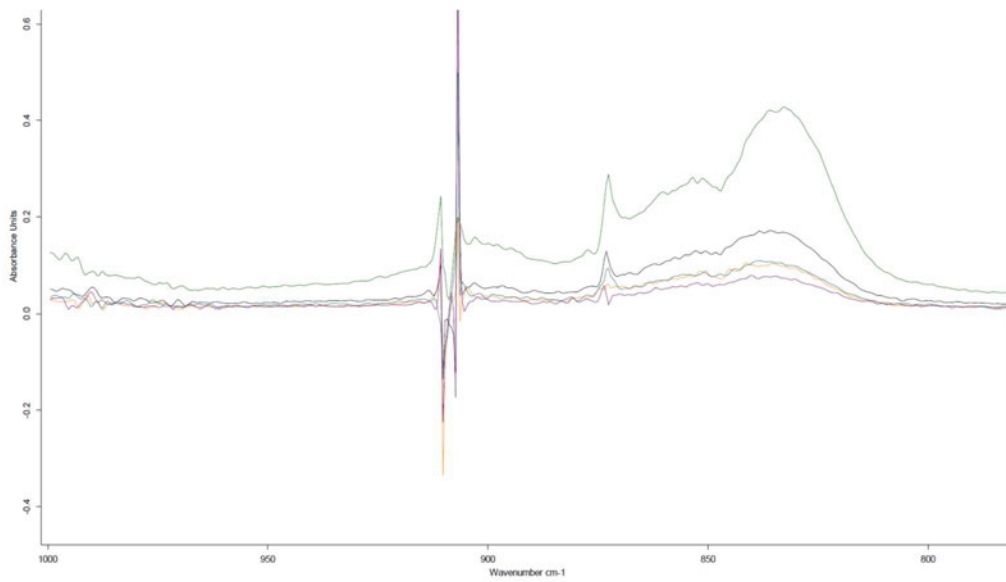


Figure 7.20: IR spectrum of Victoria Police samples 253, 256, 274, 279 and 285: 1000-780 cm<sup>-1</sup>

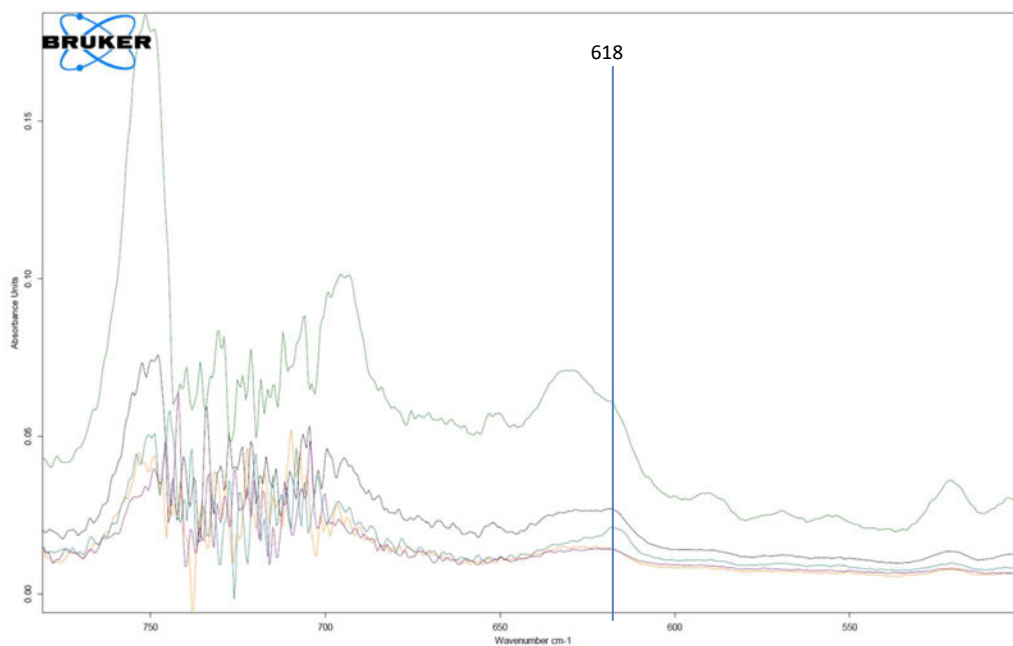


Figure 7.21: IR spectrum of Victoria Police samples 253, 256, 274, 279 and 285 780-400  $\text{cm}^{-1}$

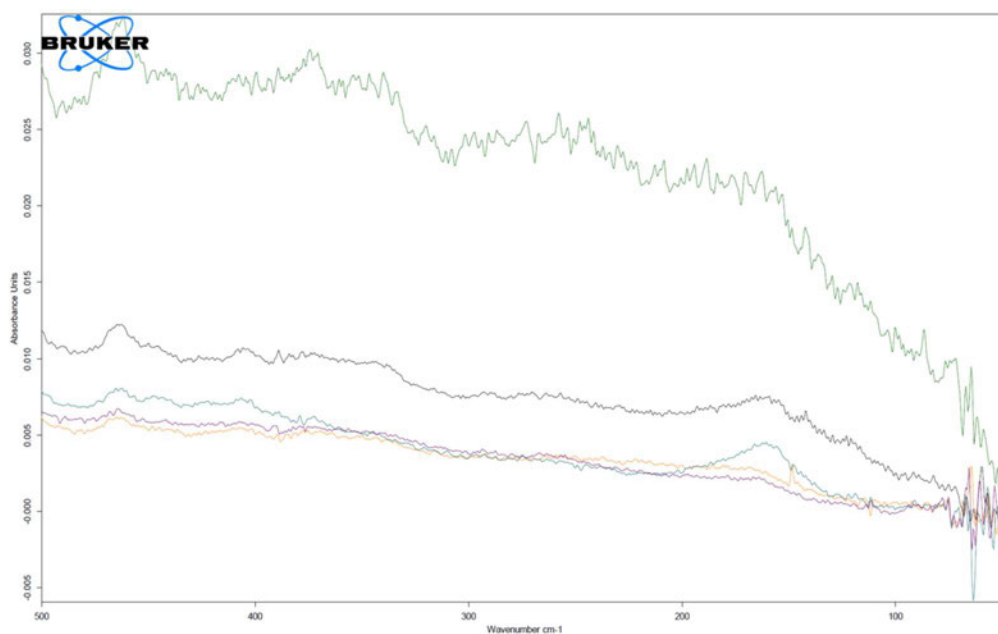


Figure 7.22: IR spectrum of Victoria Police samples 253, 256, 274, 279 and 285 500-50  $\text{cm}^{-1}$

The Hercules samples 303, 304 and 305 are displayed in Figure 7.23, Figure 7.24, Figure 7.25, Figure 7.26 and Figure 7.27. These three samples produced very similar spectra sample 303 (red) has slightly higher absorbance than the other two and Figure 7.24 shows a slightly shifted peak. Sample 305 (black) peaks at  $829.9 \text{ cm}^{-1}$ , sample 304 (blue) peaks at  $828.0 \text{ cm}^{-1}$  and sample 303 peaks at  $825.2 \text{ cm}^{-1}$ . Otherwise the other peaks only differ in terms of intensity of absorbance. This indicates that the three propellants have similar composition, differing slightly in one peak.



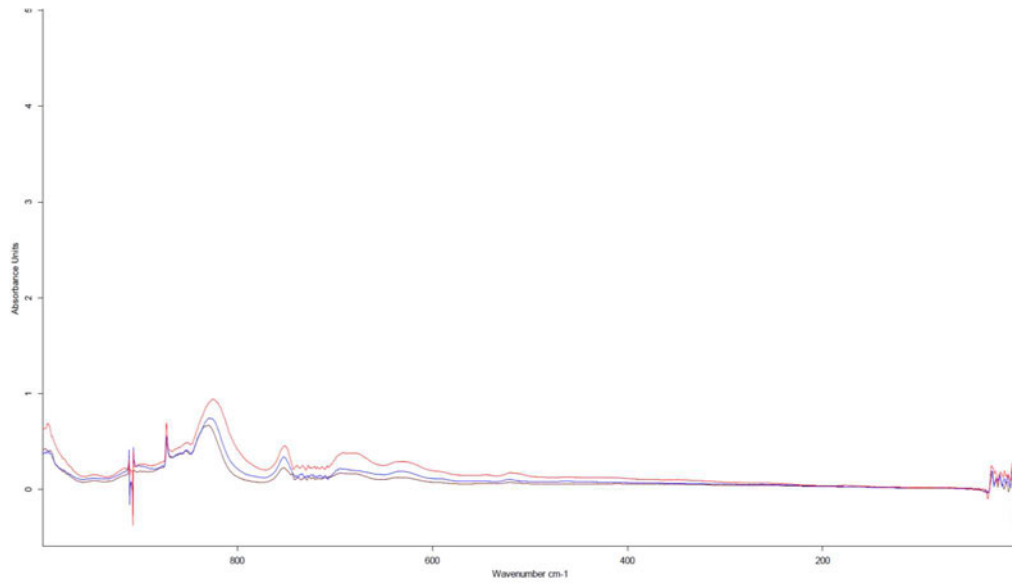


Figure 7.23: IR spectrum of Victoria Police samples 303, 304 and 305

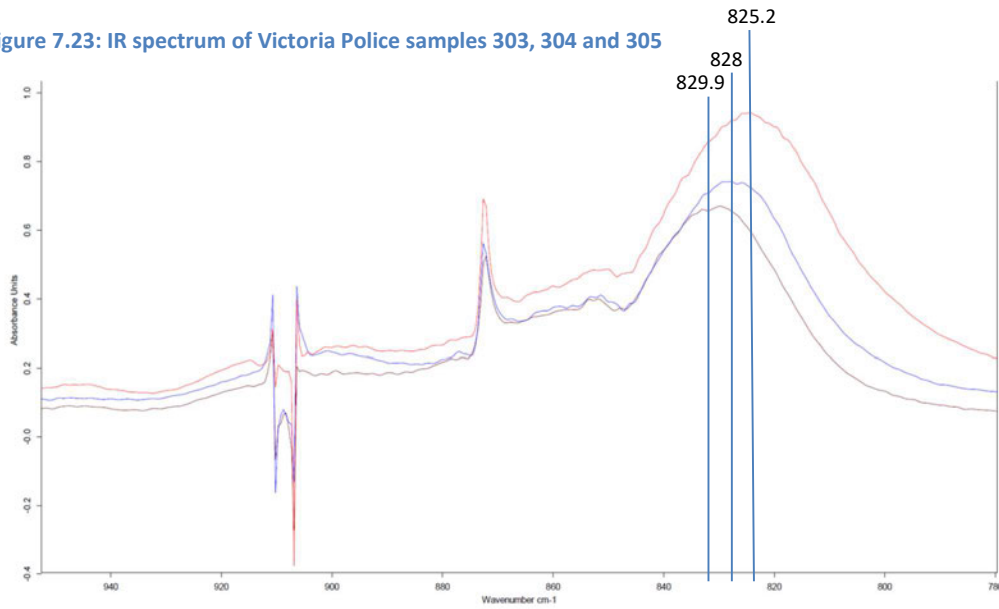


Figure 7.24: IR spectrum of Victoria Police samples 303, 304 and 305: 960-780 cm<sup>-1</sup>

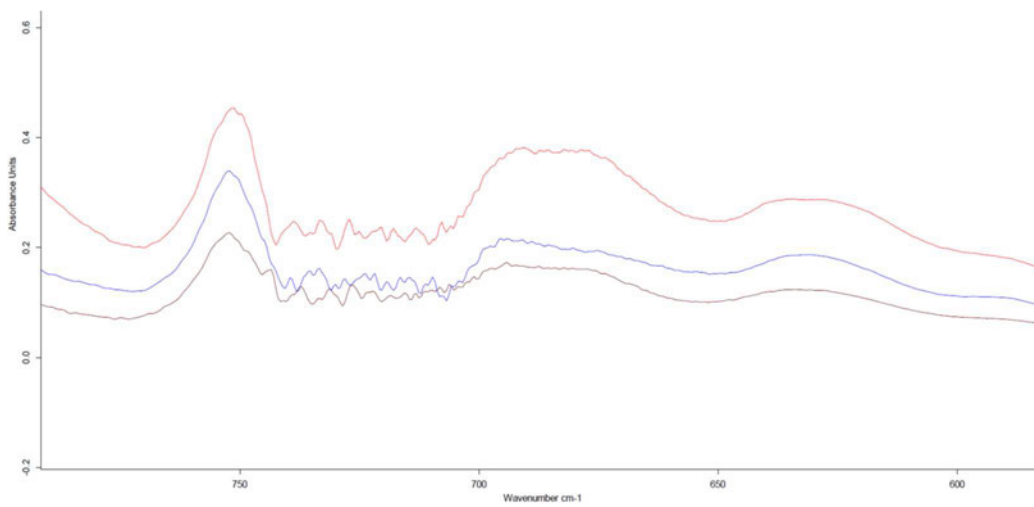


Figure 7.25: IR spectrum of Victoria Police samples 303, 304 and 305: 800-550 cm<sup>-1</sup>

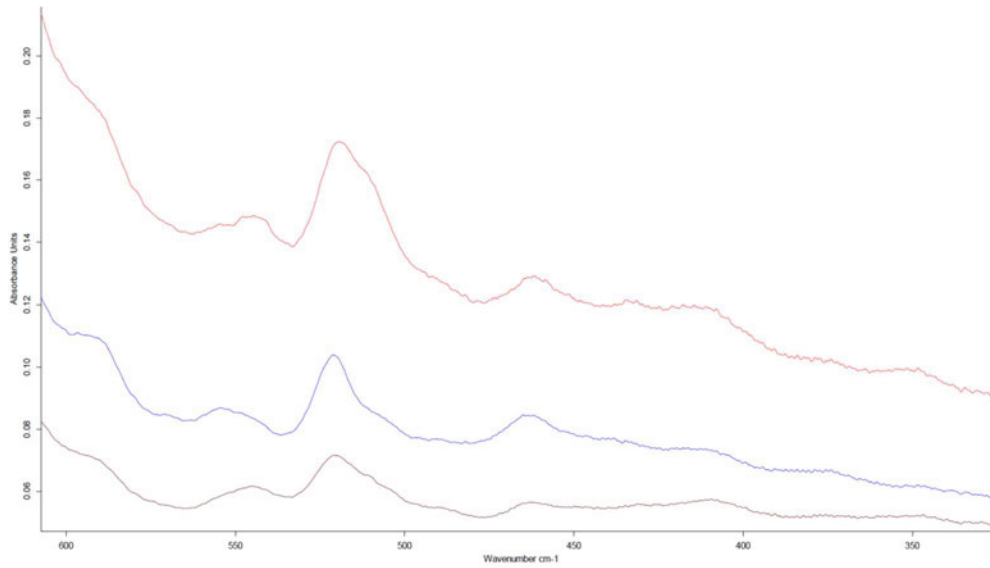


Figure 7.26: IR spectrum of Victoria Police samples 303, 304 and 305: 600-300  $\text{cm}^{-1}$

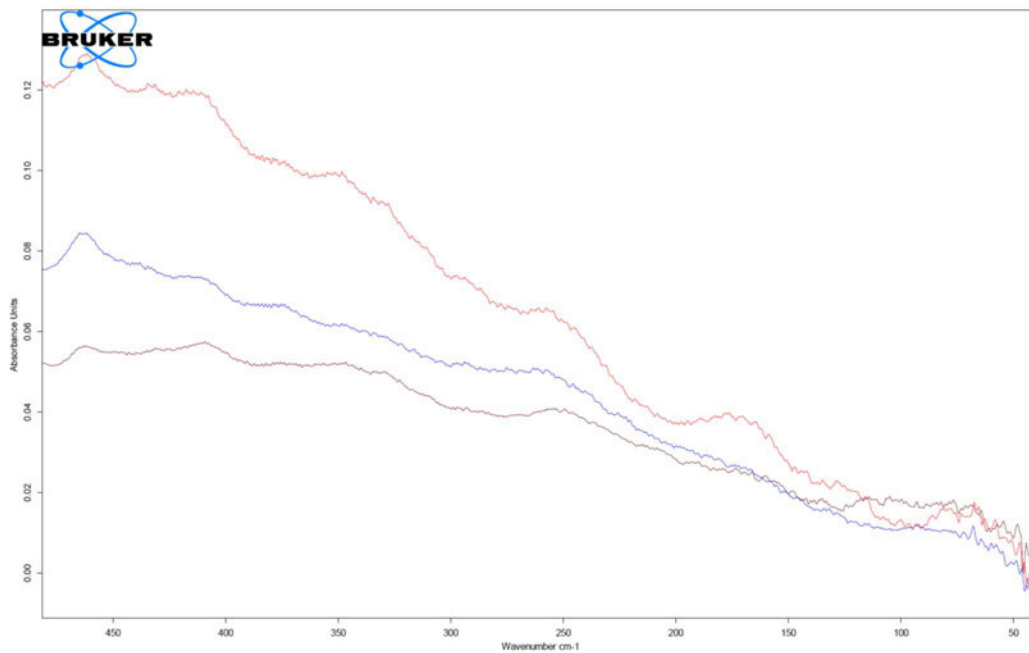


Figure 7.27: IR spectrum of Victoria Police samples 303, 304 and 305: 500-50  $\text{cm}^{-1}$

## 7.4 LDI of all propellant samples

### *FSSA Samples*

Alcohols proved to be effective solvents, although not fully solvating the propellants, the analysis of both the solvent and the solids residual provided a comprehensive idea of each propellant analysed. In terms of differentiation this was achieved using only the methanol samples. An overview of all peaks found for each sample can be seen in Table 7.6 and Table 7.7. Sample 19 was not included in Table 7.7

as there was minimal solid to use and yielded no peaks. Between Table 7.6 and Table 7.7 all eighteen samples analysed using methanol were able to be differentiated using peaks found from both forms. Some of the clear points of differentiation, which have been highlighted with orange, in Table 7.6 are as simple as sample 8 containing peaks at 345 and 390 m/z when no others do and sample 13 being the only example with a peak at 591 m/z. Sample 15 has the only peaks at 131, 301 and 331 m/z, sample 17 which is the sole sample with a peak at 307 m/z and sample 19 which is the only one to contain a peak at 133 m/z and 551 m/z are the other simple differentiations. Other distinctions are more complex, such as that of samples 1, 9 and 12; these three are the only samples to contain a peak at 138 m/z but can be differentiated as only sample 1 also contains a peak at 369 m/z, both 1 and 9 contain a peak at 717 m/z, sample 12 contains neither. Similarly samples 2, 6 and 11 are connected, whereby sample 2 contains peaks at 340, 380 and 467 m/z, sample 6 also contains peaks at 340 and 380 m/z, but none at 467 m/z. Sample 6 contains another peak at 424 m/z as well, and sample 11 is the only other sample with a peak at 380 m/z but has peaks at none of the other places mentioned in this set. The third set combines samples 3, 16 and 18. Sample 3 shows peaks at 137 and 701 m/z, but not at 409 m/z. Sample 16 has peaks at 137 and 409 m/z but not at 701 m/z and sample 18 has all three of the aforementioned peaks. Sample 4 is the only sample where peaks at 393, 475 and 701 m/z are seen together. In a similar fashion sample 10 combines 393, 410 and 424 m/z, peaks that are seen in other samples, but not strongly in the same spectrum. Unfortunately, both sample 3 and sample 14 show no individual peaks, sample 7 has more peaks but all of them are common, with most other samples also having these peaks. Sample 14 has very few peaks at all. These results are mirrored by those of the analysis done on the immiscible solids leftover from the solvation process, seen in Table 7.7. The peaks of interest here are highlighted in green, this analysis had less discriminating power than the previous table. It can be seen; however, the following samples are the only ones to contain specific peaks. Sample 1 has a peak at 317 m/z, sample 2 with a peak at 341 m/z and sample 6 contains 194 m/z. Sample 8 contains three specific peaks at 264 m/z, 345 m/z and 390 m/z, samples 10, 12 and 16 contain peaks at 323, 253 and 164 m/z respectively and sample 17 has peaks at 104 and 263 m/z. Sample 18 is the only sample that gave a spectrum from the solids and contained distinguishing peaks, these usable peaks have mass to charge ratios of 162 and 292. Sample 11 is the only other sample analysed from solids that presented more than one usable peak.

Although the peaks have not yet been able to be identified, the samples can be differentiated using LDI, a much quicker analysis method. In the time that three GCMS samples were done, all eighteen samples were analysed using LDI.

Table 7.6: Peaks (m/z) from samples solvation in methanol - liquids

1	2	3	4	6	7	8	9	10	11	12	13	14	15	16	17	18	19	
													131.997					
		137.868									150			137.887		137.882	132.896	
				249.275					250									
											267.312						267.317	
													301.339					
															307.358			
317.309								317.339		317.352								
													331.483					
	341.301			340														
						345.646												
	353.5			353.515					353.535				353.548					
369.482	min			369.5														
	380			381.568					381.592				381.604					
						390.475												
			393.575															
409.54								410	410		393.61		393.616		393.623			
	413.54		413.557		413.535		413.573	413.601		413.59	413.593	413.587	413.599	409.613	410	409.597	410	
														413	413.605	415	413.591	
								421.535										
			425		424.474			425	424.52			424.515						
429.517		429.542	429.535					429.553	429.578		429.569		429.571	429.581	429.592	429.59	429.577	429.573
	435			437.744	437.469	min												
	449.637		449.657		449.635		Min	449.702	449.682	450	449.669		449.703	499.712	449.708	449.701	449.693	
		452.52																
465.604			465.626			min	465.644	465.674		465.665		465.663	465.676	465.686	465.683	465.671	465.669	
	467.483										467.546						467.673	
	479		475.611	475.612	475.587				475.645									
	485												483.516					
491.556	min	491.583		491.578	497.553		491.597		491.614									
		516.511		min									516.548					
						545												
	553.578	553.6	553.595	553.589	553.573	min		553.652	553.63								551.624	
569.514	569.519	569.548	569.544	569.536	569.527		569.563	570	569.582									
											591.43							
			685.242					685.308	685.283				685.309					
701.127	min	701	701.221	701.222		min	701.182		701.272				700			701.204	701.2	
717.092		717.127					717.416											

Table 7.7: Table of significant and minimal peaks (m/z) from solvation in methanol - solids

1	2	3	4	6	7	8	9	10	11	12	13	14	15	16	17	18		
Residual	Residual	Residual	Residual	Residual	Solid	Residual	Residual	Residual	Residual	Residual	Solid	Residual	Solid	Solid	Solid	Residual	Residual	Solid
										112.795						103.871		
123.915										123.85						112.844		
								131.95				132.118	131.919			123.877		
		137.631			137							137.874	137.785			137.874		137.804
139.912									139.877	139.84							139.884	
																154.901		154.822
																163.9		161.823
				194.1183														
			212.919					212.886										212.89
												252.871						
								264.301									263.05	
																		291.926
301.361	301.366						min			min		min						
317.358												min						
											323.451							
	341.359																	
								345.463										
	353.565			353.56														
	380			381.618														
								390.487										
393.622		393.63	min			min			393.541	min		min						
410			409.578															min
413.603	413.613	413.614	min	413.607		413.616	min	413.525	413.523	413.54		413.542						
429.585	429.596	429.595	429.536	425		min		429.511	429.497	min		429.52			429.574	429.534		
449.704	449.716	449.718	min	449.711		449.718	449.694	min	449.62	min		449.637				min		
465.678	467.566	465.689	465.66					465.599	min			465.607				465.623		
												634.41						
	685.331			685.33		685.336	min		min	min		min						
701.221		701.236	min	700		min			min	min		min						
																823.198		

## DST Group Samples

The samples provided by the DST Group had a smaller sample size, lower relative age and came with some knowledge of their contents; therefore, a more component specific analysis was investigated using these samples. The individual standards were analysed in both methanol and ethanol due to a theory that some of the LDI peaks found may be products of fragments that had methyl or ethyl adducts provided by the solvent. The following tables show the strongest peaks from each analysis in order from the highest to lowest usable signal strengths. It can be seen from Table 7.8 to

Table 7.19 that many of the tables contain blank columns, this is an indication that no significant or usable spectra/peaks were yielded for that analysis/solvation combinations. It is also clear from these tables that the best method for the analysis of the common compounds of propellants was positive mode LDI of samples solvated with methanol as this was the experimental alternative that most consistently provided spectra for most of the standard samples. It can also be seen that many of the peaks seen throughout the samples are shared, this could be attributed to the similarities in the structures, especially when comparing DPA in its many derivatives.

Table 7.8: Major LDI peaks (m/z) for DPA

Molar Mass (g.mol <sup>-1</sup> )	Methanol positive	Methanol negative	Ethanol positive	Ethanol negative
169.227	336.2		323.2	78.9
	112.9		156.1	72.0
	323.2			96.0
	396.2			325.2
				311.2

Table 7.9: Major LDI peaks (m/z) for 2n-DPA

Molar Mass (g.mol <sup>-1</sup> )	Methanol positive	Methanol negative	Ethanol positive	Ethanol negative
214.224	197.1	360.8		213.1
	74.2	362.8		96.0
	214.1	596.6		72.0
	237.1	594.6		225.9
	300.8	598.6		
		314.8		

Table 7.10: Major LDI peaks (m/z) for 4n-DPA

Molar Mass (g.mol <sup>-1</sup> )	Methanol positive	Methanol negative	Ethanol positive	Ethanol negative
214.224	185.1	213.1	185.1	213.1
	207.1	489.1	199.1	425.2
	199.1	425.2	184.1	214.1
	184.1	214.1	198.1	441.2
	237.1		207.1	
	198.1		395.2	
			237.1	

Table 7.11: Major LDI peaks (m/z) for Nn-DPA

Molar Mass (g.mol <sup>-1</sup> )	Methanol positive	Methanol negative	Ethanol positive	Ethanol negative
198.225	424.2	213.1	336.2	258.1
	425.3	258.1	476.3	213.1
	336.2	214.1	462.2	311.2
	335.2	170.9	335.2	325.2
		172.9	424.2	242.1

Table 7.12: Major LDI peaks (m/z) for Akardite II

Molar Mass (g.mol <sup>-1</sup> )	Methanol positive	Methanol negative	Ethanol positive	Ethanol negative
226.7	112.9			
	114.9			
	156.9			
	96.9			
	140.9			

Table 7.13: Major LDI peaks (m/z) for 2,4 DNT

Molar Mass (g.mol <sup>-1</sup> )	Methanol positive	Methanol negative	Ethanol positive	Ethanol negative
182.134	125.0			
	81.0			
	140.9			
	96.9			

Table 7.14: Major LDI peaks (m/z) for 2,6 DNT

Molar Mass (g.mol <sup>-1</sup> )	Methanol positive	Methanol negative	Ethanol positive	Ethanol negative
182.134	112.9			
	114.9			
	156.9			
	96.9			
	119.9			
	140.9			

Table 7.15: Major MALDI peaks (m/z) for MC

Molar Mass (g.mol <sup>-1</sup> )	Methanol positive	Methanol negative	Ethanol positive	Ethanol negative
241.65	156.9		140.9	
	112.9		97.1	
	140.9		156.9	
	114.9		112.9	

Table 7.16: Major LDI peaks (m/z) for EC

Molar Mass (g.mol <sup>-1</sup> )	Methanol positive	Methanol negative	Ethanol positive	Ethanol negative
268.36	267.2	360.8		72.0
	250.8	362.8		96.0
	206.8	596.6		84.0
	112.9	594.6		108.0
	156.8			

Table 7.17: Major LDI peaks (m/z) for DBP

Molar Mass (g.mol <sup>-1</sup> )	Methanol positive	Methanol negative	Ethanol positive	Ethanol negative
278.34			97.1	226.0
			112.	72.0
			74.2	96.0
			114.9	147.0



Table 7.18: Major LDI peaks (m/z) for NC

Molar Mass (g.mol <sup>-1</sup> )	Methanol positive	Methanol negative	Ethanol positive	Ethanol negative
605.252	74.2		208.1	72.0
	124.9		104.5	301.1
	140.9		71.6	84.0
	81.0		95.5	96.0
			836.6	

Table 7.19: Major LDI peaks (m/z) of NG

Molar Mass (g.mol <sup>-1</sup> )	Methanol positive	Methanol negative	Ethanol positive	Ethanol negative
227.0865	140.9			226.0
	156.9			210.0
	124.9			61.9
				250.0

There were few peak differences seen between samples solvated with methanol as opposed to those solvated with ethanol, with the dominant peaks remaining quite consistent. Therefore, the likelihood of methyl and ethyl adduction is low.

The negative samples provided some interesting results for Nitroglycerin, the peak at 226 m/z in ethanol could have been of great use and high importance, showing the loss of a proton. This peak was, however, also found in the spectra for AK II and DBP and, therefore, loses its impact.

Table 7.20: Major LDI peaks for DST Group propellants

Sample A peaks (m/z)		Sample B peaks (m/z)		Sample C peaks (m/z)		Sample D peaks (m/z)	
Methanol	Ethanol	Methanol	Ethanol	Methanol	Ethanol	Methanol	Ethanol
112.9	156.9	156.9	323.2	424.2	156.9	156.9	413.3
156.9	393.3	112.9	429.3	516.3	256.3	112.9	96.9
114.9	409.3	114.9	156.9	206.1	112.9	140.9	140.9
96.9	429.3	140.9	140.9	440.2	140.9	96.9	423.3
140.9	140.9	96.9	413.3	156.9	96.9	156.1	124.9
119.9	413.3	156.1	156.1	373.2	114.9	323.2	81.0
212.8	103.9	323.2	409.3	265.1	158.9	114.9	112.9
158.9	119.9		112.9	454.2	228.3	424.2	156.9
274.8	112.9		96.9	140.9	250.8	265.1	99.0
150.9							

Many of the peaks seen for the propellants in Table 7.20 correspond to those seen in the tables for the individual components above. These include peaks such as 112 m/z, 156 m/z and 140.9 m/z; however, these peaks are present in several the standards and most of the propellant samples this means that they may be common products. They may also be the result of fragments or adducts, or even adducts of fragments, that are shared by all the samples. There are many more common peaks than there are differentiable peaks, interestingly many of them occur in both the methanol and ethanol solutions, this supports the idea that the peaks are not representative of methyl and ethyl adduction caused by the different solvents being used. The samples can, again, all be differentiated due to the number of peaks and their presence and absence in different samples. Samples B and D show no individual peaks for solvation in methanol but have at least one peak that is different when solvated in ethanol. Sample B has a peak at 413.3 m/z in ethanol and Sample D has peaks at 81.0, 99.0, 124.9 and 423.3 m/z in ethanol. Sample C is clearly the most diverse of all with several uncommon peaks for both solvation methods, 206.1, 373.2, 440.2, 454.4 and 516.3 m/z in methanol, as well as 158.9, 228.3, 250.8 and 256.3 m/z in ethanol. Like Sample C, Sample A has several differentiable peaks in methanol, coming in at 150.9, 158.9, 212.8 and 274.8 m/z. It only has two peaks that are different in ethanol, 103.9 and 393.3 m/z are the only ones that are different. This also differentiates it from the others and supports the use of both ethanol and methanol in the solvation of propellant samples.

In reference to the information provided about these propellants A is the only one described as including EC, there is 1 peak common to EC and A, however this peak can be found in many of the other components. Sample B and D were both defined as containing graphite, they share a peak in methanol at 323.2 m/z, which is not seen in any of the standard spectra nor in the other samples. This is encouraging especially as there is a collection of peaks around 320 seen in the spectrum of graphite and codeine in part one (Figure 3.8) which may be mistaken for codeine. Samples C and D were the double base propellants in this experiment, they too, share a peak not seen in the other samples at 424.2 m/z. This peak is not however, seen in nitroglycerin, but it the major peak of Nn-DPA.

While each sample can be differentiated clearly from the other based on these peaks, the identification of what has produced these peaks remains elusive.

### *Victoria Police samples*

Of the world war II era samples only two were able to be analysed, the samples were difficult to analyse were set on the plate with an impenetrable structure. This may be due to a higher

concentration of sample being dissolved in the solvent. Spectra for all the Winchester 760 samples were obtained, and it can be seen in Figure 6.2 that these were not as heavily solvated and clear. This might mean that the same solvation cannot be performed between LDI and Mid-Far IR analysis and that LDI requires less solvation of samples. It is also clear that not all samples behave and react the same way, making a universal solvation method for propellants difficult.

The spectra for the world war two samples that were analysed, 119 and 146 are summarised below. They are clearly differentiated, similarly to in the IR analysis. Again, there is little information for sample 119, the peaks at 23 and 39 m/z are most likely sodium and potassium ions and 571 m/z is a contaminant seen in most spectra. The peak at 111 m/z is interesting in that it has not been seen in other spectra. There are many more peaks for 146 the most interesting of which is at 177 m/z as again it has not been seen in the previous spectra.

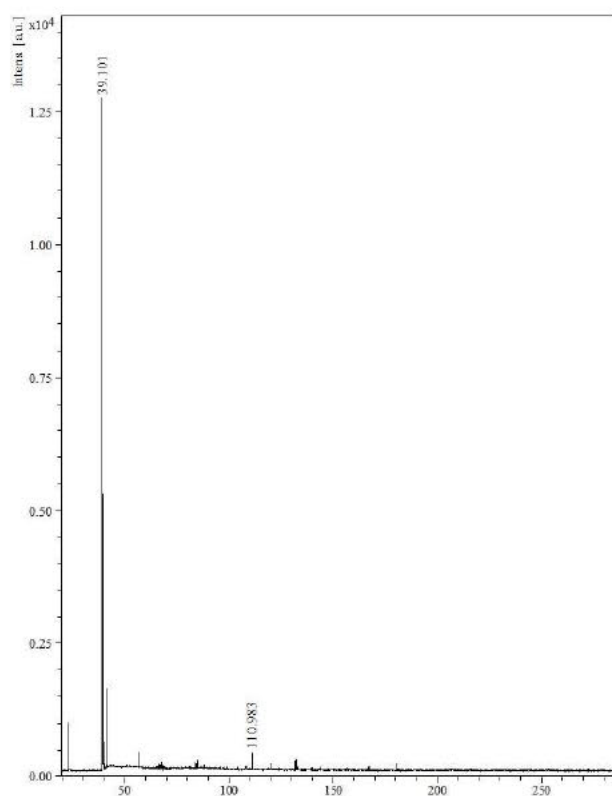


Table 7.21: Major LDI peaks of Victoria Police sample 119

119	
m/z	intensity
23.217	946.816
39.101	11843.521
41.095	1407.115
110.983	363.138
571.500	313.983

Figure 7.28: LDI spectrum of Victoria Police sample 119

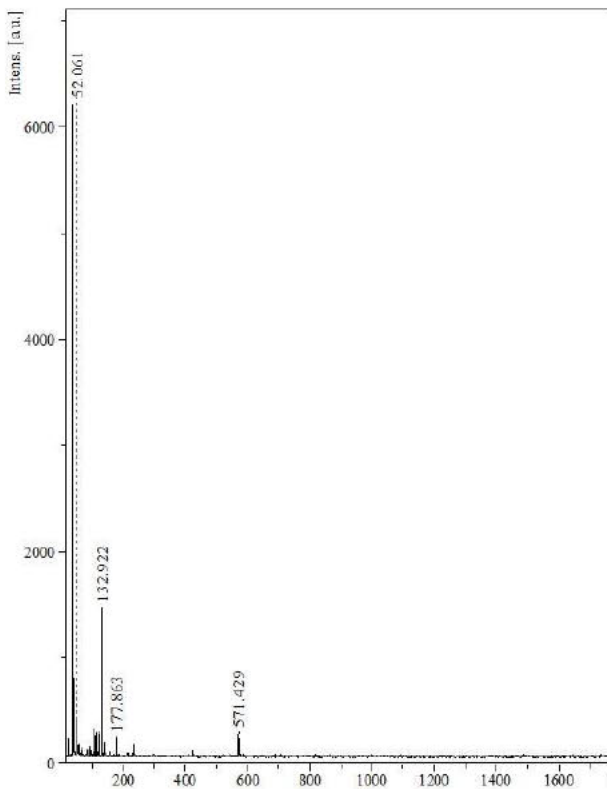


Table 7.22: Major LDI peaks of Victoria Police sample 146

146	
m/z	intensity
39.111	5494.066
41.112	613.490
52.061	269.366
103.953	310.113
112.910	253.962
122.936	250.830
123.941	228.333
132.922	1368.844
177.863	209.009
571.429	199.921

Figure 7.29: LDI spectrum of Victoria Police sample 146

The samples of the Winchester 760 ball propellant were all able to be analysed and can be seen below, these all appear very different and their peak values are summarised in Table 7.23 and sorted by greatest peak intensity. Some points of interest within the spectra include that sample 253 is the only spectrum containing a peak at 105 m/z, sample 256 contains peaks at both 214 and 317 m/z. Sample 274 contains the only peak at 124 m/z, a peak at 125 m/z is seen in sample 274 and 279 and a number of other times throughout this study. Sample 215 is the only one that does not contain a peak at 212m/z. These spectra can all be differentiated, despite many similarities, this was not achieved using Mid-Far IR.

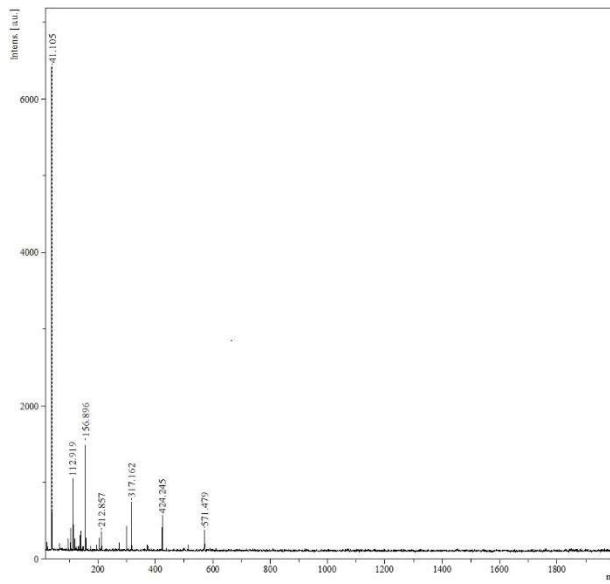


Figure 7.30: LDI spectrum of Victoria Police sample 253

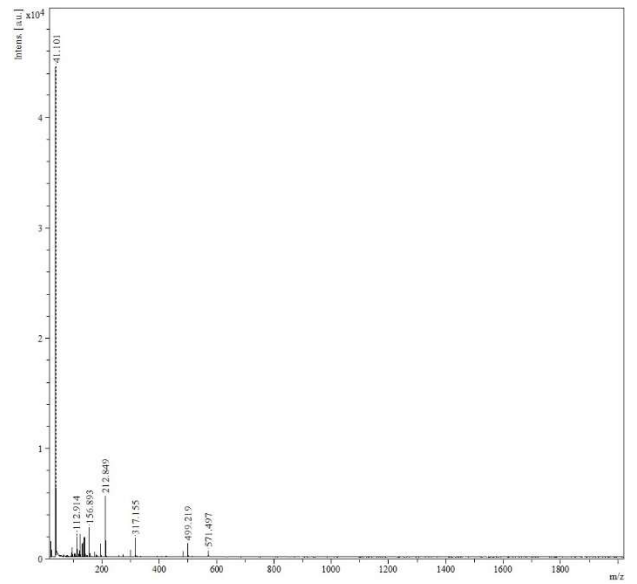


Figure 7.31: LDI spectrum of Victoria Police sample 256

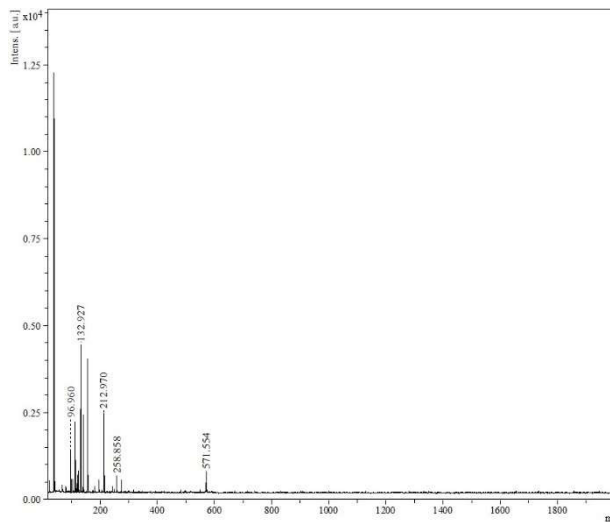


Figure 7.32: LDI spectrum of Victoria Police sample 274

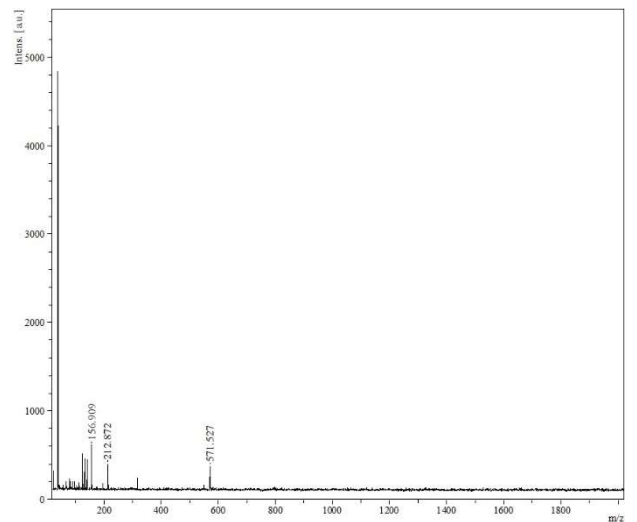


Figure 7.33: LDI spectrum of Victoria Police sample 279

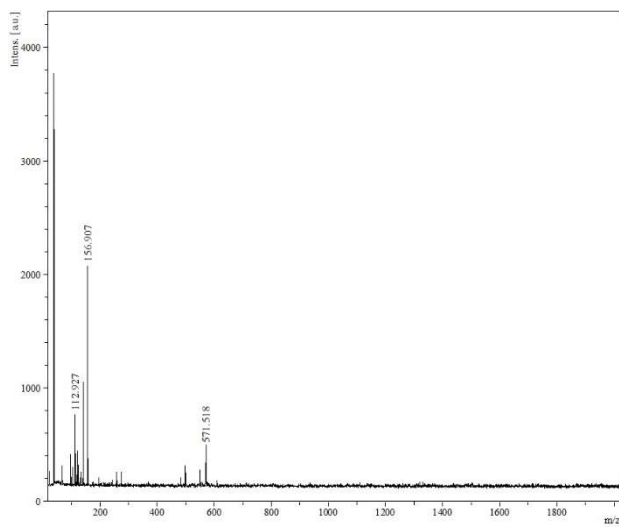


Figure 7.34: LDI spectrum of Victoria Police sample 285

Table 7.23: Peak summary of LDI samples Winchester 760 ball propellant

#253 m/z	#256 m/z	#274 m/z	#279 m/z	#285 m/z
39.11	39.10	39.14	39.12	39.12
156.90	212.85	132.93	156.91	156.91
112.92	41.10	156.90	124.96	140.93
317.16	156.89	140.93	132.93	112.93
41.10	123.93	212.97	140.93	96.96
424.24	112.91	112.92	41.11	114.92
114.92	139.92	96.96	212.87	571.52
301.18	214.85	114.92	571.53	120.95
105.11	317.16	41.13		158.91
140.92	23.22	124.95		571.91
212.86	132.92	120.95		
571.48	196.87	158.90		
	499.22	214.96		
	140.92	571.55		
	96.95	258.86		
	114.91	124.02		
	301.17	104.98		
	483.24	274.84		
	174.89	571.21		
	571.50			
	107.96			
	141.91			
	158.90			

The Hercules samples are summarised below in Figure 7.35, Figure 7.36, and Figure 7.37 the peaks of which are sorted by intensity in Table 7.24. The green dot propellant, sample 303, was tested both as a solution and from a solid green grain of propellant. The solution did not yield any information, but a spectrum was obtained from the grain. The two samples containing a taggant, sample 303 and 305, were extremely similar, sample 305 contained one extra peak at 137 m/z. This is very interesting as these samples seem to only differ in the taggant colour. Although these spectra do not contain many peaks therefore there is not a lot of information to be analysed. Sample 304 is greatly different in spectrum and easily differentiated from the other two Hercules samples.

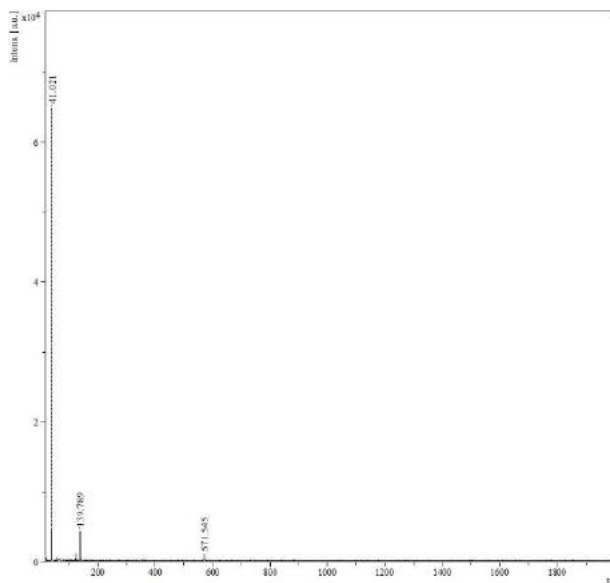


Figure 7.35: LDI spectrum of Victoria Police sample 303 solid

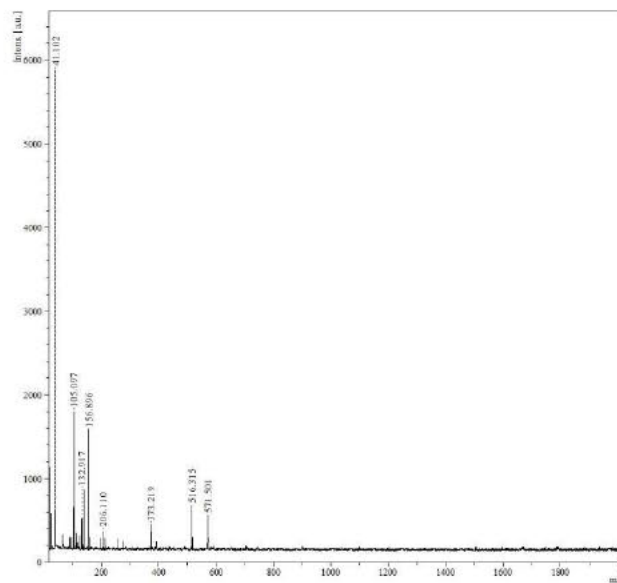


Figure 7.36: LDI spectrum of Victoria Police sample 304

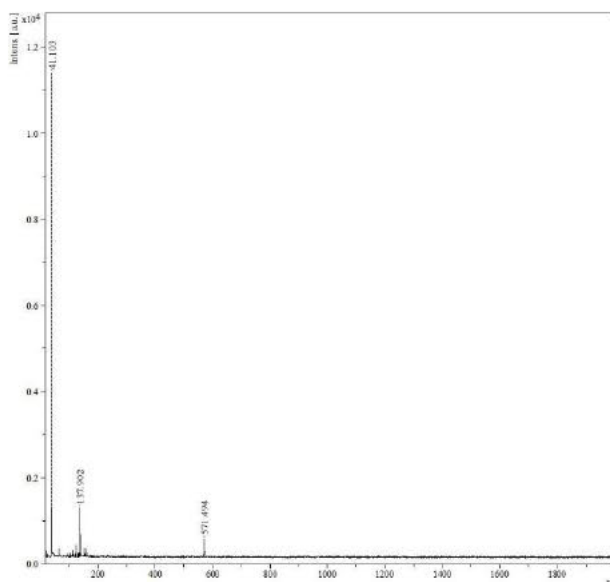


Figure 7.37: LDI spectrum of Victoria Police sample 305

Table 7.24: Peak summary of LDI samples Hercules

303 m/z	304 m/z	305 m/z
39.030	39.114	39.112
41.021	105.097	137.902
139.789	156.896	41.103
123.806	23.226	139.922
571.545	140.925	571.494
571.200	516.315	123.940
	41.102	571.916
	571.501	
	373.219	
	132.917	
	571.909	
	206.110	

## 8 Conclusions

The propellants in question were varying in age, content and origin. Many of these had little known about them, so proven methods of analysis were used first to establish any information to cross reference when using LDI. The HPLC was able to identify many of the stabilizers and their derivatives present in the original propellants provided. Further analysis by GCMS was undertaken to provide information about mass spectra peaks, however the information from the GCMS did not correlate very well with that of the HPLC. Also, as the ionization methods used for GCMS are harsh there was a lot of fragmentation of the peaks, as opposed to the molecular and adducted ions seen in LDI spectra. This meant that the masses found in the GCMS were not similar to those in LDI and therefore could not be used for identification purposes.

Mid to Far IR was undertaken at the Australian Synchrotron, using the Synchrotron light and applied to the FSSA and Victoria Police samples. Of the 18 FSSA samples all but two were able to be differentiated based on peak positions, as Mid-Far IR is not used for identification of peaks, more looking at the spectrum overall. A comparison of different Victoria Police sample groups was made within each group. The world war 2 era samples showed many similarities, only a few of these samples could be distinguished from each other, There were minor differences for two of the Winchester 760 ball samples, which was interesting. It was theorised that these would be indistinguishable, as they are all the same propellant from different batches. The Hercules samples were all different, at one peak, but the same throughout the rest of the spectrum.

The complexity of propellant samples proved to be a large challenge for this type of analysis, initial LDI experimentation, provided information that was difficult to understand, when focus was on identifying peaks. Reference samples of the common propellant ingredients was not able to connect any peaks to specific samples components. Optimum sample preparation was established for the FSSA samples and differentiation of samples rather than peak identification was the new purpose. Simple alcohols such as methanol and ethanol were effective solvents, providing a balance of solubility and range of peaks. Differentiation of the FSSA samples was achieved with little knowledge of peak representation, by analysing both the solvents and residual samples. The DST group samples were also differentiated, only some of the Victoria Police samples were able to be analysed. The solvation method used for the analysis via IR resulted in samples that were too concentrated for LDI analysis for some samples. All the Winchester samples presented different spectra, which could be differentiated. The Hercules samples were also all differentiated, however only 2 world war II era samples were analysable.



The mid-far IR and LDI analysis together provided complimentary information, although it is clear that the different analyses cannot always be performed using the same solutions. LDI provides quicker and simpler differentiation of samples and requires lower concentration samples. While IR is a simple analysis technique it needs to be highlighted that this IR source, from the synchrotron, is a very powerful and not easily accessible

Peak identification may be achieved with much more prior knowledge of samples and knowledge of any interactions that may occur between components, this may be done using a synthesised model sample, which would include a range of components.

# Overall Conclusions and Future Work

Overall conclusions about the project were made throughout this thesis. Included among these is the fact that of the tapes used, carbon tape is the least useful, its removal from the plate is difficult and provides a lot of interference from multiple carbon peaks. Copper tape was found to provide some assistance, providing the most spectra from fibre samples, although, with enough optimisation, regular double-sided tape could provide a less expensive alternative.

For the analysis of codeine there was success using LDI analysis methods. Among the number of alternative matrices investigated binary matrices were interesting and provided some useful spectra, but there was far too much potential for matrix interference with the drug samples being examined. Nanoparticles proved to be the most useful. The nanoparticles are retained throughout the vacuum process on the fibre samples during analysis and that they work best when they are applied to the fibres after the sample. A 1:2 ratio of nanoparticle: analyte is enough to assist in the analysis process but not smother the sample.

Gold nanoparticles were chosen due to the ease of functionalisation associated with them, especially with thiol compounds. Bare gold nanoparticles proved to be as good a starting point, as predicted, providing good on-plate analysis, with quick preparation and a potential for in-sample calibration. Phenethyl mercaptan nanoclusters, however, were the most useful matrices used for on-plate analysis, with much lower background peaks than the bare nanoparticles. This is a positive despite the much longer preparation time, higher chance for error during synthesis and the difficulty associated with using a non-aqueous base.

Fibre analysis proved much more difficult and the paper itself seemed to deter desorption and ionization, however, functionalised gold nanoparticles were successful in this analysis. 4-mercaptobenzoic acid was the best attachment option, providing the least background peaks and strongest sample intensity using the lowest laser fluence.

4-mercaptobenzoic acid functionalised nanoclusters were investigated, but unsuccessful. It is suspected that this lack of success was due to a lack of experience in nanoscience and synthesis of such compounds. Future work could be done to optimise this synthesis for better analysis from fibres.

Overall analysis of codeine was successful, and the method could be expanded to the analysis of a much larger range of drugs and classes, as well as real samples. Future work for this project would include expansion to other drugs, oral fluid-based samples, with all the contaminants associated with this. Other optimisation would be in synthesis of a 4-mercaptobenzoic acid-based nanocluster to

provide a better signal to noise ratio. The use of gold as an internal standard would also be useful for expansion to quantitative analysis. This would eventually result in analysis of oral fluid being more prevalent than by blood or urine for short term investigations. Finally, the evolution of portable mass spectrometry devices would make this a technique that could be performed on site. LDI is such a rapid and specific technique that delays would be greatly minimised in cases of false positive immunoassay results.

Propellant analysis is much more difficult, because it is a complex mixture, its spectra contain many more peaks and thus are much more difficult to differentiate and clarify. Preparation at low concentrations with methanol and ethanol and analysis of positive ions was the most successful. These results allowed the differentiation of most of the samples provided, the samples that were too concentrated with sample were found to crystallise and not allow penetration of the laser.

The differentiation of samples was compared to analysis with Mid-far IR spectroscopy. Again, this technique was able to differentiate most samples and gave insight to different sample groups. The analysis was performed using light from the Australian synchrotron, which allows for much more sensitive and specific analysis, which would not be possible on a standard device. LDI has a much quicker turnover of results and allows for application of all samples simultaneously.

Although differentiation of samples was successful identifying the source of peaks and the sample contents was very difficult. Many of the common additives contained many of the same peaks, due to similarities in the structures. Future work in this part of the study should be aimed at peak identification and understanding sample differences. A simple model sample could be created to establish a clear spectrum to compare samples to. The use of modelling software was mentioned in some examples of propellant analysis and would greatly reduce time to analyse data and provide a better understanding of sample differences. Another option for future would be finding an appropriate alternative matrix. Something with no interference in the low mass range of the spectrum. The nanoclusters used in part one may provide clearer spectra with better signal to noise ratios and may allow for analysis of a greater range of samples. Once this process has been optimised and the peaks understood, it could be expanded further to include burnt samples of propellants and eventually GSR samples. These could be collected using copper tape and analysed in solid form if an appropriate alternative matrix is found.

As an instrument to be used in forensic applications LDI has a variety of advantages, samples can be simply and quickly prepared for analysis and may be easily retained for future analysis. The technique is high throughput, a lot of samples can be analysed quite quickly and the spectra

produced are very sample specific. There are however limitations, specifically bulk and price of the instrument, coupled with a know-how associated with analysis. These issues may become less significant with the progression of technology. Other analysis techniques of analysis have become more compact and accessible over time and the same may happen with LDI.

# Bibliography

1. Harvey, D.J., *MASS SPECTROMETRY | Matrix-Assisted Laser Desorption/Ionization*, in *Encyclopedia of Analytical Science*, P. Worsfold, A. Townshend, and C. Poole, Editors. 2005, Elsevier: Oxford. p. 386-397.
2. Peterson, D.S., *Matrix-free methods for laser desorption/ionization mass spectrometry*. *Mass Spectrometry Reviews*, 2007. **26**(1): p. 19-34.
3. Doroshenko, V.M., Laiko, V. V., Taranenko, N. I., Berkout, V. D., Lee, H. S., *Recent developments in atmospheric pressure MALDI mass spectrometry*. *International Journal of Mass Spectrometry*, 2002. **221**(1): p. 39-58.
4. Hillenkamp, F., Karas, M., *The MALDI Process and Method*, in *MALDI MS: A Practical Guide to Instrumentation, Methods and Applications*, F. Hillenkamp and J. Peter-Katalinic, Editors. 2007, Wiley-VCH Verlag GmbH & co.: Weinham.
5. Laboratory, N.H.M.F. *National High Magnetic Field Laboratory: Matrix Assisted Laser Desorption Ionization (MALDI)*. 2011 [cited 2011 18/10/2011]; Available from: [http://www.magnet.fsu.edu/education/tutorials/tools/ionization\\_maldi.html](http://www.magnet.fsu.edu/education/tutorials/tools/ionization_maldi.html).
6. Dreisewerd, K., *The Desorption Process in MALDI*. *Chemical Reviews*, 2003. **103**(2): p. 395-426.
7. Zenobi, R., Knochenmuss, R., *Ion formation in MALDI mass spectrometry*. *Mass Spectrometry Reviews*, 1998. **17**(5): p. 337-366.
8. Guilhaus, M., *Special feature: Tutorial. Principles and instrumentation in time-of-flight mass spectrometry. Physical and instrumental concepts*. *Journal of Mass Spectrometry*, 1995. **30**(11): p. 1519-1532.
9. Guilhaus, M., *MASS SPECTROMETRY | Time-of-Flight*, in *Encyclopedia of Analytical Science (Second Edition)*, W. Editors-in-Chief: Paul, T. Alan, and P. Colin, Editors. 2005, Elsevier: Oxford. p. 412-423.
10. O'Connor, P.B., Hillenkamp, F., *MALDI Mass Spectrometry and Instrumentation*, in *MALDI MS: A Practical Guide to Instrumentation, Methods and Applications*, F. Hillenkamp and J. Peter-Katalinic, Editors. 2007, Wiley-VCH Verlag GmbH & co.: Weinham.
11. Goheen, S.C., et al., *Mass Spectrometry of Low Molecular Mass Solids by Matrix-assisted Laser Desorption/Ionization*. *Journal of Mass Spectrometry*, 1997. **32**(8): p. 820-828.
12. Mamyrin, B.A., Karatev, V. I., Schmikk, D. B., Zagulin, B. A., *The mass reflectron, a new non-magnetic time-of-flight mass spectrometer with high resolution*. *Sov. Physics JETP*, 1973. **37**: p. 45-48.
13. Henkelman, R.M., Ottensmeyer, F. P., *An electrostatic mirror*. *Journal of Physics E Scientific Instruments*, 1974. **7**(3): p. 176-178.
14. Standing, K.G., Ens, W., *Time of Flight Mass Spectrometers*, in *Encyclopedia of Spectroscopy and Spectrometry*, C.L. Editor-in-Chief: John, Editor. 1999, Elsevier: Oxford. p. 2360-2365.
15. Lee, K.J., et al., *Simple fabrication of micro time-of-flight mass spectrometer using a carbon nanotube ionizer*. *Sensors and Actuators B: Chemical*, 2017. **243**(Supplement C): p. 394-402.
16. Bergman, N., D. Shevchenko, and J. Bergquist, *Approaches for the analysis of low molecular weight compounds with laser desorption/ionization techniques and mass spectrometry*. *Analytical and Bioanalytical Chemistry*, 2014. **406**(1): p. 49-61.
17. Karas, M. and F. Hillenkamp, *Laser desorption ionization of proteins with molecular masses exceeding 10,000 daltons*. *Analytical Chemistry*, 1988. **60**(20): p. 2299-2301.
18. Beavis, R.C., B.T. Chait, and H.M. Fales, *Cinnamic acid derivatives as matrices for ultraviolet laser desorption mass spectrometry of proteins*. *Rapid Communications in Mass Spectrometry*, 1989. **3**(12): p. 432-435.

19. Beavis, R.C., B.T. Chait, and K.G. Standing, *Matrix-assisted laser-desorption mass spectrometry using 355 nm radiation*. Rapid Communications in Mass Spectrometry, 1989. **3**(12): p. 436-439.
20. Hatsis, P., et al., *Quantitative analysis of small pharmaceutical drugs using a high repetition rate laser matrix-assisted laser/desorption ionization source*. Rapid Communications in Mass Spectrometry, 2003. **17**(20): p. 2303-2309.
21. Beavis, R.C., T. Chaudhary, and B.T. Chait,  *$\alpha$ -Cyano-4-hydroxycinnamic acid as a matrix for matrix-assisted laser desorption mass spectrometry*. Organic Mass Spectrometry, 1992. **27**(2): p. 156-158.
22. Strupat, K., M. Karas, and F. Hillenkamp, *2,5-Dihydroxybenzoic acid: a new matrix for laser desorption—ionization mass spectrometry*. International Journal of Mass Spectrometry and Ion Processes, 1991. **111**(Supplement C): p. 89-102.
23. Kawasaki, H., et al., *Layer-by-layer self-assembled multilayer films of gold nanoparticles for surface-assisted laser desorption/ionization mass spectrometry*. Anal Chem, 2008. **80**(19): p. 7524-33.
24. Kaufmann, R., *Matrix-assisted laser desorption ionization (MALDI) mass spectrometry: a novel analytical tool in molecular biology and biotechnology*. Journal of Biotechnology, 1995. **41**(2-3): p. 155-175.
25. Petkovski, E., Keyser-Tracqui, C., Hienne, R., Ludes, B., *SNPs and MALDI-TOF MS: Tools for DNA Typing in Forensic Paternity Testing and Anthropology*. Journal of Forensic Sciences, 2005. **50**(3): p. 1-7.
26. Kumooka, Y., *Classification of OPP adhesive tapes according to MALDI mass spectra of adhesives*. Forensic Science International, 2010. **197**(1-3): p. 75-79.
27. Matthews, B., Walker, G. S., Kobus, H., Pigou, P., Bird, C., Smith, G., *The analysis of dyes in ball point pen inks on single paper fibres using laser desorption ionisation time of flight mass spectrometry (LDI-TOFMS)*. Forensic Science International, 2011. **209**(1-3): p. e26-e30.
28. Van Bocxlaer, J.F., *Recent trends in analytical procedures in forensic toxicology*. Therapeutic Drug Monitoring, 2005. **27**(6): p. 752-755.
29. Minakata, K., et al., *MALDI-TOF mass spectrometric determination of four pyrrolidino cathinones in human blood*. 2014. **32**(1): p. 169-175.
30. Pihlainen, K., et al., *Analysis of amphetamines and fentanyl by atmospheric pressure desorption/ionization on silicon mass spectrometry and matrix-assisted laser desorption/ionization mass spectrometry and its application to forensic analysis of drug seizures*. Journal of Mass Spectrometry, 2005. **40**(4): p. 539-545.
31. Beckey, H.D. and H.R. Schulten, *Field Desorption Mass Spectrometry*. Angewandte Chemie International Edition in English, 1975. **14**(6): p. 403-415.
32. Harvey, D.J., *MASS SPECTROMETRY | Ionization Methods Overview*, in *Encyclopedia of Analytical Science (Second Edition)*, W. Editors-in-Chief: Paul, T. Alan, and P. Colin, Editors. 2005, Elsevier: Oxford. p. 350-359.
33. Williams, P., *SECONDARY ION MASS-SPECTROMETRY*. Annual Review of Materials Science, 1985. **15**: p. 517-548.
34. Barber, M., et al., *Fast atom bombardment of solids (F.A.B.): a new ion source for mass spectrometry*. Journal of the Chemical Society, Chemical Communications, 1981. **0**(7): p. 325-327.
35. Grim, D., J. Siegel, and J. Allison, *Evaluation of Desorption/Ionization Mass Spectrometric Methods in the Forensic Applications of the Analysis of Inks on Paper*. 2001.
36. Hillenkamp, F., et al., *A high-sensitivity laser microprobe mass analyzer*. Applied physics, 1975. **8**(4): p. 341-348.
37. Hillenkamp, F., et al., *Laser microprobe mass analysis of organic materials*. Nature, 1975. **256**(5513): p. 119-120.

38. Karas, M., D. Bachmann, and F. Hillenkamp, *Influence of the wavelength in high-irradiance ultraviolet laser desorption mass spectrometry of organic molecules*. *Analytical Chemistry*, 1985. **57**(14): p. 2935-2939.
39. Tanaka, K., et al., *Protein and polymer analyses up to m/z 100 000 by laser ionization time-of-flight mass spectrometry*. *Rapid Communications in Mass Spectrometry*, 1988. **2**(8): p. 151-153.
40. Bruins, A.P., *MASS SPECTROMETRY | Atmospheric Pressure Ionization Techniques*, in *Encyclopedia of Analytical Science (Second Edition)*, W. Editors-in-Chief: Paul, T. Alan, and P. Colin, Editors. 2005, Elsevier: Oxford. p. 366-373.
41. Weston, D.J., et al., *Direct Analysis of Pharmaceutical Drug Formulations Using Ion Mobility Spectrometry/Quadrupole-Time-of-Flight Mass Spectrometry Combined with Desorption Electrospray Ionization*. *Analytical Chemistry*, 2005. **77**(23): p. 7572-7580.
42. Talaty, N., et al., *Fabric analysis by ambient mass spectrometry for explosives and drugs*. *Analyst*, 2008. **133**(11): p. 1532-1540.
43. Shariatgorji, M., N. Amini, and L.L. Ilag, *Silicon nitride nanoparticles for surface-assisted laser desorption/ionization of small molecules*. *Journal of Nanoparticle Research*, 2009. **11**(6): p. 1509-1512.
44. Laiko, V.V., M.A. Baldwin, and A.L. Burlingame, *Atmospheric Pressure Matrix-Assisted Laser Desorption/Ionization Mass Spectrometry*. *Analytical Chemistry*, 2000. **72**(4): p. 652-657.
45. Zhang, J., et al., *Graphite-Coated Paper as Substrate for High Sensitivity Analysis in Ambient Surface-Assisted Laser Desorption/Ionization Mass Spectrometry*. *Analytical Chemistry*, 2012. **84**(7): p. 3296-3301.
46. Eiceman, G.A., D. Young, and G.B. Smith, *Mobility spectrometry of amino acids and peptides with matrix assisted laser desorption and ionization in air at ambient pressure*. *Microchemical Journal*, 2005. **81**(1): p. 108-116.
47. Cornett, D.S., et al., *MALDI imaging mass spectrometry: molecular snapshots of biochemical systems*. *Nat Meth*, 2007. **4**(10): p. 828-833.
48. Shanta, S.R., et al., *A new combination MALDI matrix for small molecule analysis: application to imaging mass spectrometry for drugs and metabolites*. *Analyst*, 2012. **137**(24): p. 5757-5762.
49. Wang, C.-C., et al., *Critical factors determining the quantification capability of matrix-assisted laser desorption/ionization–time-of-flight mass spectrometry*. *Philosophical Transactions of the Royal Society A: Mathematical, Physical and Engineering Sciences*, 2016. **374**(2079).
50. Szájli, E., Fehér, T., Medzihradzsky, K. F., *Investigating the Quantitative Nature of MALDI-TOF MS*. *Molecular & Cellular Proteomics*, 2008. **7**(12): p. 2410-2418.
51. Ho, Y.-C., et al., *Nanoparticle-assisted MALDI-TOF MS combined with seed-layer surface preparation for quantification of small molecules*. *Analytica Chimica Acta*, 2011. **697**(1): p. 1-7.
52. Duncan, M.W., H. Roder, and S.W. Hunsucker, *Quantitative matrix-assisted laser desorption/ionization mass spectrometry*. *Briefings in Functional Genomics & Proteomics*, 2008. **7**(5): p. 355-370.
53. Duncan, M.W., H. Roder, and S.W. Hunsucker, *Quantitative matrix-assisted laser desorption/ionization mass spectrometry*. *Briefings in Functional Genomics*, 2008. **7**(5): p. 355-370.
54. Kang, M.-J., A. Tholey, and E. Heinzle, *Quantitation of low molecular mass substrates and products of enzyme catalyzed reactions using matrix-assisted laser desorption/ionization time-of-flight mass spectrometry*. *Rapid Communications in Mass Spectrometry*, 2000. **14**(21): p. 1972-1978.
55. Han, G., et al., *MIL-101(Cr) as matrix for sensitive detection of quercetin by matrix-assisted laser desorption/ionization mass spectrometry*. *Talanta*, 2017. **164**: p. 355-361.

56. Duan, J., et al., *CHCA-Modified Au Nanoparticles for Laser Desorption Ionization Mass Spectrometric Analysis of Peptides*. Journal of the American Society for Mass Spectrometry, 2009. **20**(8): p. 1530-1539.
57. Guo, Z., et al., *A Method for the Analysis of Low-Mass Molecules by MALDI-TOF Mass Spectrometry*. Analytical Chemistry, 2002. **74**(7): p. 1637-1641.
58. West, R., *Surface Assisted Laser Desorption Ionisation for the analysis of drugs and propellants in solid form*, in *School of Chemical and Physical Sciences*. 2011, Flinders University: Adelaide.
59. Guild, G.E., Lenehan, C. E., Walker, G. S., *Surface-assisted laser desorption ionisation time-of-flight mass spectrometry with an activated carbon surface for the rapid detection of underivatised steroids*. International Journal of Mass Spectrometry, 2010. **294**(1): p. 16-22.
60. Dattelbaum, A.M., Hicks, R K, Shelley, J, Koppisch, A T, Iyer, S, *Surface assisted laser desorption–ionization mass spectrometry on patterned nanoporous silica thin films*. Microporous and Mesoporous Materials, 2008. **114**(1-3): p. 193-200.
61. Wei, J., J.M. Buriak, and G. Siuzdak, *Desorption-ionization mass spectrometry on porous silicon*. Nature, 1999. **399**(6733): p. 243-246.
62. Lowe, R.D., et al., *Rapid drug detection in oral samples by porous silicon assisted laser desorption/ionization mass spectrometry*. Rapid Communications in Mass Spectrometry, 2009. **23**(22): p. 3543-3548.
63. Pihlainen, K., Grigoras, K., Franssila, S., Ketola, R., Kotiaho, T., Kostianen, R., *Analysis of amphetamines and fentanyl by atmospheric pressure desorption/ionization on silicon mass spectrometry and matrix-assisted laser desorption/ionization mass spectrometry and its application to forensic analysis of drug seizures*. Journal of Mass Spectrometry, 2005. **40**(4): p. 539-545.
64. Kinumi, T., et al., *Matrix-assisted laser desorption/ionization time-of-flight mass spectrometry using an inorganic particle matrix for small molecule analysis*. Journal of Mass Spectrometry, 2000. **35**(3): p. 417-422.
65. Chen, Y.-C. and M.-F. Tsai, *Using surfactants to enhance the analyte signals in activated carbon, surface-assisted laser desorption/ionization (SALDI) mass spectrometry*. Journal of Mass Spectrometry, 2000. **35**(11): p. 1278-1284.
66. Dale, M.J., R. Knochenmuss, and R. Zenobi, *Graphite/Liquid Mixed Matrices for Laser Desorption/Ionization Mass Spectrometry*. Analytical Chemistry, 1996. **68**(19): p. 3321-3329.
67. Sunner, J., E. Dratz, and Y.-C. Chen, *Graphite surface-assisted laser desorption/ionization time-of-flight mass spectrometry of peptides and proteins from liquid solutions*. Analytical Chemistry, 1995. **67**(23): p. 4335-4342.
68. Zhang, H., S. Cha, and E.S. Yeung, *Colloidal Graphite-Assisted Laser Desorption/Ionization MS and MSn of Small Molecules. 2. Direct Profiling and MS Imaging of Small Metabolites from Fruits*. Analytical Chemistry, 2007. **79**(17): p. 6575-6584.
69. Han, M. and J. Sunner, *An activated carbon substrate surface for laser desorption mass spectrometry*. Journal of the American Society for Mass Spectrometry, 2000. **11**(7): p. 644-649.
70. Black, C., et al., *The use of pencil lead as a matrix and calibrant for matrix-assisted laser desorption/ionisation*. 2006. **20**(7): p. 1053-1060.
71. Gusev, A.I., et al., *Improvement of signal reproducibility and matrix/comatrix effects in MALDI analysis*. Analytical Chemistry, 1995. **67**(6): p. 1034-1041.
72. Billeci, T.M. and J.T. Stults, *Tryptic mapping of recombinant proteins by matrix-assisted laser desorption/ionization mass spectrometry*. Analytical Chemistry, 1993. **65**(13): p. 1709-1716.
73. Rosinke, B., et al., *Matrix-assisted laser desorption/ionization mass spectrometry (MALDI-MS) of membrane proteins and non-covalent complexes*. Journal of Mass Spectrometry, 1995. **30**(10): p. 1462-1468.



74. Pfenninger, A., et al., *Matrix optimization for matrix-assisted laser desorption/ionization mass spectrometry of oligosaccharides from human milk*. Journal of Mass Spectrometry, 1999. **34**(2): p. 98-104.
75. Fratelli, M., et al., *Identification by redox proteomics of glutathionylated proteins in oxidatively stressed human T lymphocytes*. Proceedings of the National Academy of Sciences, 2002. **99**(6): p. 3505-3510.
76. Laugesen, S. and P. Roepstorff, *Combination of two matrices results in improved performance of maldi ms for peptide mass mapping and protein analysis*. Journal of the American Society for Mass Spectrometry, 2003. **14**(9): p. 992-1002.
77. Guo, Z. and L. He, *A binary matrix for background suppression in MALDI-MS of small molecules*. Analytical and Bioanalytical Chemistry, 2007. **387**(5): p. 1939-1944.
78. Hameed, S., et al., *Nanoparticle-assisted Laser Desorption/ionization (nano-PALDI)-based Imaging Mass Spectrometry (IMS) and its Application to Brain Sciences, in Nanomedicine and the Nervous System*. 2012, Science Publishers. p. 97-118.
79. Wu, W., Q. He, and C. Jiang, *Magnetic Iron Oxide Nanoparticles: Synthesis and Surface Functionalization Strategies*. Nanoscale Research Letters, 2008. **3**(11): p. 397-415.
80. Heiligtag, F.J. and M. Niederberger, *The fascinating world of nanoparticle research*. Materials Today, 2013. **16**(7): p. 262-271.
81. Murph, S.E.H., G.K. Larsen, and K.J. Coopersmith, *Anisotropic and Shape-Selective Nanomaterials: Structure-Property Relationships*. 2017: Springer International Publishing.
82. Hulla, J.E., S.C. Sahu, and A.W. Hayes, *Nanotechnology: History and future*. Human & Experimental Toxicology, 2015. **34**(12): p. 1318-1321.
83. Henglein, A., *Small-particle research: physicochemical properties of extremely small colloidal metal and semiconductor particles*. Chemical Reviews, 1989. **89**(8): p. 1861-1873.
84. Su, C.-L. and W.-L. Tseng, *Gold Nanoparticles as Assisted Matrix for Determining Neutral Small Carbohydrates through Laser Desorption/Ionization Time-of-Flight Mass Spectrometry*. Analytical Chemistry, 2007. **79**(4): p. 1626-1633.
85. Huang, Y.-F. and H.-T. Chang, *Analysis of Adenosine Triphosphate and Glutathione through Gold Nanoparticles Assisted Laser Desorption/Ionization Mass Spectrometry*. Analytical Chemistry, 2007. **79**(13): p. 4852-4859.
86. Lin, P.-C., et al., *Functionalized Magnetic Nanoparticles for Small-Molecule Isolation, Identification, and Quantification*. Analytical Chemistry, 2007. **79**(9): p. 3401-3408.
87. Daniel, M.-C. and D. Astruc, *Gold Nanoparticles: Assembly, Supramolecular Chemistry, Quantum-Size-Related Properties, and Applications toward Biology, Catalysis, and Nanotechnology*. Chemical Reviews, 2004. **104**(1): p. 293-346.
88. Link, S. and M.A. El-Sayed, *Size and Temperature Dependence of the Plasmon Absorption of Colloidal Gold Nanoparticles*. The Journal of Physical Chemistry B, 1999. **103**(21): p. 4212-4217.
89. Rainer, M., M.N. Qureshi, and G.K. Bonn, *Matrix-free and material-enhanced laser desorption/ionization mass spectrometry for the analysis of low molecular weight compounds*. Analytical and Bioanalytical Chemistry, 2011. **400**(8): p. 2281-2288.
90. Arakawa, R. and H. Kawasaki, *Functionalized nanoparticles and nanostructured surfaces for surface-assisted laser desorption/ionization mass spectrometry*. Anal Sci, 2010. **26**(12): p. 1229-40.
91. Taira, S., et al., *Manganese oxide nanoparticle-assisted laser desorption/ionization mass spectrometry for medical applications*. Science and Technology of Advanced Materials, 2009. **10**(3): p. 034602.
92. Castellana, E.T. and D.H. Russell, *Tailoring Nanoparticle Surface Chemistry to Enhance Laser Desorption Ionization of Peptides and Proteins*. Nano Letters, 2007. **7**(10): p. 3023-3025.
93. Taira, S., et al., *Oligonucleotide analysis by nanoparticle-assisted laser desorption/ionization mass spectrometry*. Analyst, 2012. **137**(9): p. 2006-2010.

94. Kusano, M., et al., *Laser Desorption/Ionization Mass Spectrometry (LDI-MS) of Lipids with Iron Oxide Nanoparticle-Coated Targets*. Mass spectrometry (Tokyo, Japan), 2014. **3**(1): p. A0026-A0026.
95. Komori, H., et al., *Nanoparticle-assisted laser desorption/ionization using sinapic acid-modified iron oxide nanoparticles for mass spectrometry analysis*. Analyst, 2015. **140**(24): p. 8134-8137.
96. Yan, B., et al., *Laser desorption/ionization mass spectrometry analysis of monolayer-protected gold nanoparticles*. Analytical and Bioanalytical Chemistry, 2010. **396**(3): p. 1025-1035.
97. Wen, X., S. Dagan, and V.H. Wysocki, *Small-molecule analysis with silicon-nanoparticle-assisted laser desorption/ionization mass spectrometry*. Anal Chem, 2007. **79**(2): p. 434-44.
98. Taira, S., et al., *Nanotrap and Mass Analysis of Aromatic Molecules by Phenyl Group-Modified Nanoparticle*. Analytical Chemistry, 2011. **83**(4): p. 1370-1374.
99. Qian, H., et al., *Quantum Sized Gold Nanoclusters with Atomic Precision*. Accounts of Chemical Research, 2012. **45**(9): p. 1470-1479.
100. Faraday, M., *The Bakerian Lecture: Experimental Relations of Gold (and Other Metals) to Light*. Philosophical Transactions of the Royal Society of London, 1857. **147**: p. 145-181.
101. Jin, R., *Quantum sized, thiolate-protected gold nanoclusters*. Nanoscale, 2010. **2**(3): p. 343-362.
102. Haiss, W., et al., *Determination of Size and Concentration of Gold Nanoparticles from UV-Vis Spectra*. Analytical Chemistry, 2007. **79**(11): p. 4215-4221.
103. Zhou, J., et al., *Functionalized gold nanoparticles: Synthesis, structure and colloid stability*. Journal of Colloid and Interface Science, 2009. **331**(2): p. 251-262.
104. Amendola, V. and M. Meneghetti, *Size Evaluation of Gold Nanoparticles by UV-vis Spectroscopy*. The Journal of Physical Chemistry C, 2009. **113**(11): p. 4277-4285.
105. Pilolli, R., et al., *Thermally annealed gold nanoparticles for surface-assisted laser desorption ionisation-mass spectrometry of low molecular weight analytes*. Anal Bioanal Chem, 2012. **404**(6-7): p. 1703-11.
106. James, T., et al., *A one-step etching method to produce gold nanoparticle coated silicon microwells and microchannels*. Anal Bioanal Chem, 2010. **398**(7-8): p. 2949-54.
107. Yonezawa, T. and T. Kunitake, *Practical preparation of anionic mercapto ligand-stabilized gold nanoparticles and their immobilization*. Colloids and Surfaces A: Physicochemical and Engineering Aspects, 1999. **149**(1): p. 193-199.
108. Lin, Y.-H. and W.-L. Tseng, *A Sample Preparation Method for Gold Nanoparticle-Assisted Laser Desorption/Ionization Time-of-Flight Mass Spectrometry*, in *Nanoproteomics: Methods and Protocols*, S.A. Toms and R.J. Weil, Editors. 2011, Humana Press: Totowa, NJ. p. 167-172.
109. Castellana, E.T., S.D. Sherrod, and D.H. Russell, *Nanoparticles for Selective Laser Desorption/Ionization in Mass Spectrometry*. JALA: Journal of the Association for Laboratory Automation, 2008. **13**(6): p. 330-334.
110. Lemire, J.A., J.J. Harrison, and R.J. Turner, *Antimicrobial activity of metals: mechanisms, molecular targets and applications*. Nat Rev Micro, 2013. **11**(6): p. 371-384.
111. Ayers, P.W., *The physical basis of the hard/soft acid/base principle*. Faraday Discussions, 2007. **135**(0): p. 161-190.
112. Brust, M., et al., *Synthesis of Thiol-Derivatized Gold Nanoparticles in a 2-Phase Liquid-Liquid System*. Vol. 7. 1994.
113. Shalom, D., et al., *Synthesis of thiol functionalized gold nanoparticles using a continuous flow microfluidic reactor*. Materials Letters, 2007. **61**(4): p. 1146-1150.
114. Ackerson, C.J., P.D. Jadzinsky, and R.D. Kornberg, *Thiolate Ligands for Synthesis of Water-Soluble Gold Clusters*. Journal of the American Chemical Society, 2005. **127**(18): p. 6550-6551.

115. Ackerson, C.J., et al., *Synthesis and Bioconjugation of 2 and 3 nm-Diameter Gold Nanoparticles*. *Bioconjugate Chemistry*, 2010. **21**(2): p. 214-218.
116. Tvedte, L.M. and C.J. Ackerson, *Size-Focusing Synthesis of Gold Nanoclusters with p-Mercaptobenzoic Acid*. *The Journal of Physical Chemistry A*, 2014. **118**(37): p. 8124-8128.
117. Johnson, S.R., S.D. Evans, and R. Brydson, *Influence of a Terminal Functionality on the Physical Properties of Surfactant-Stabilized Gold Nanoparticles*. *Langmuir*, 1998. **14**(23): p. 6639-6647.
118. Wu, Z., J. Suhan, and R. Jin, *One-pot synthesis of atomically monodisperse, thiol-functionalized Au<sub>25</sub> nanoclusters*. *Journal of Materials Chemistry*, 2009. **19**(5): p. 622-626.
119. Wu, Z., J. Chen, and R. Jin, *One-Pot Synthesis of Au<sub>25</sub>(SG)<sub>18</sub> 2- and 4-nm Gold Nanoparticles and Comparison of Their Size-Dependent Properties*. *Advanced Functional Materials*, 2011. **21**(1): p. 177-183.
120. Chevrier, D.M., et al., *Sensitivity of Structural and Electronic Properties of Gold–Thiolate Nanoclusters to the Atomic Composition: A Comparative X-ray Study of Au<sub>19</sub>(SR)<sub>13</sub> and Au<sub>25</sub>(SR)<sub>18</sub>*. *The Journal of Physical Chemistry C*, 2012. **116**(47): p. 25137-25142.
121. Jin, R., et al., *Size Focusing: A Methodology for Synthesizing Atomically Precise Gold Nanoclusters*. *The Journal of Physical Chemistry Letters*, 2010. **1**(19): p. 2903-2910.
122. Dass, A., et al., *Nanoparticle MALDI-TOF Mass Spectrometry without Fragmentation: Au<sub>25</sub>(SCH<sub>2</sub>CH<sub>2</sub>Ph)<sub>18</sub> and Mixed Monolayer Au<sub>25</sub>(SCH<sub>2</sub>CH<sub>2</sub>Ph)<sub>18-x</sub>(L)<sub>x</sub>*. *Journal of the American Chemical Society*, 2008. **130**(18): p. 5940-5946.
123. Dass, A., et al., *Mass Spectrometrically Detected Statistical Aspects of Ligand Populations in Mixed Monolayer Au<sub>25</sub>L<sub>18</sub> Nanoparticles*. *The Journal of Physical Chemistry C*, 2008. **112**(51): p. 20276-20283.
124. Schaaff, T.G., *Laser Desorption and Matrix-Assisted Laser Desorption/Ionization Mass Spectrometry of 29-kDa Au:SR Cluster Compounds*. *Analytical Chemistry*, 2004. **76**(21): p. 6187-6196.
125. Kouchi, H., H. Kawasaki, and R. Arakawa, *A new matrix of MALDI-TOF MS for the analysis of thiolate-protected gold clusters*. *Analytical Methods*, 2012. **4**(11): p. 3600-3603.
126. Barrett, C., Good, C., Moore, C., *Comparison of point-of-collection screening of drugs of abuse in oral fluid with a laboratory-based urine screen*. *Forensic Science International*, 2001. **122**(2-3): p. 163-166.
127. Tsai, J.S.-C., *Immunoassays for the Detection of Cannabis Abuse*, in *Forensic Science and Medicine: Marijuana and the Cannabinoids*, M.A. Elsohly, Editor., Human Press Inc.: Totowa, New Jersey.
128. Verstraete, A.G., *Oral fluid testing for driving under the influence of drugs: history, recent progress and remaining challenges*. *Forensic Science International*, 2005. **150**(2-3): p. 143-150.
129. O'Neal, C.L., et al., *Correlation of Saliva Codeine Concentrations with Plasma Concentrations after Oral Codeine Administration*. *Journal of Analytical Toxicology*, 1999. **23**(6): p. 452-459.
130. Kim, I., et al., *Plasma and Oral Fluid Pharmacokinetics and Pharmacodynamics after Oral Codeine Administration*. *Clinical Chemistry*, 2002. **48**(9): p. 1486-1496.
131. Jaffee, W.B., et al., *Is this urine really negative? A systematic review of tampering methods in urine drug screening and testing*. *Journal of Substance Abuse Treatment*, 2007. **33**(1): p. 33-42.
132. DOLAN, K., D. ROUEN, and J. KIMBER, *An overview of the use of urine, hair, sweat and saliva to detect drug use*. 2004. **23**(2): p. 213-217.
133. Kidwell, D.A., J.C. Holland, and S. Athanasis, *Testing for drugs of abuse in saliva and sweat*. *Journal of Chromatography B: Biomedical Sciences and Applications*, 1998. **713**(1): p. 111-135.
134. Crouch, D.J., *Oral fluid collection: The neglected variable in oral fluid testing*. *Forensic Science International*, 2005. **150**(2): p. 165-173.

135. Toennes, S.W., et al., *Driving under the influence of drugs — evaluation of analytical data of drugs in oral fluid, serum and urine, and correlation with impairment symptoms*. Forensic Science International, 2005. **152**(2): p. 149-155.
136. Drummer, O.H., *Review: Pharmacokinetics of illicit drugs in oral fluid*. Forensic Science International, 2005. **150**(2): p. 133-142.
137. Verstraete, A.G., *Oral fluid testing for driving under the influence of drugs: history, recent progress and remaining challenges*. Forensic Science International, 2005. **150**(2): p. 143-150.
138. DrugtestAustralia. *Workplace drug testing for mining and industry*. 2011 [cited 2011 22/09/2011]; Available from: [www.drugtestaustralia.com.au/products/saliva-testing/](http://www.drugtestaustralia.com.au/products/saliva-testing/).
139. Criminology, A.I.o. *Illicit Drug Types*. 12/4/2011 [cited 2013 24/4/2013]; Available from: [http://www.aic.gov.au/crime\\_types/drugs\\_alcohol/drug\\_types.htm](http://www.aic.gov.au/crime_types/drugs_alcohol/drug_types.htm).
140. SouthAustralianGovernmentSAHealth. *Drug and Alcohol Services South Australia*. 2009 [cited 2011 22/09/2011]; Available from: <http://www.dassa.gov.au/site/page.cfm?u=131>.
141. Drummer, O.H., *Drug testing in oral fluid*. The Clinical biochemist. Reviews / Australian Association of Clinical Biochemists, 2006. **27**(3): p. 147-159.
142. Bedford, K. *Opiate Chemistry and Metabolism XII - Biotech - C - Opiate Chemistry*. 2008 [cited 2012; Available from: [nzic.org.nz/ChemProcesses/biotech/12C.pdf](http://nzic.org.nz/ChemProcesses/biotech/12C.pdf)].
143. Speckl, I.M., et al., *Opiate Detection in Saliva and Urine—A Prospective Comparison by Gas Chromatography–Mass Spectrometry*. Clinical Toxicology, 1999. **37**(4): p. 441-445.
144. Musharraf, S.G., M. Ameer, and A. Ali, *MALDI-MS analysis and theoretical evaluation of olanzapine as a UV laser desorption ionization (LDI) matrix*. Journal of Pharmaceutical and Biomedical Analysis, 2017. **132**(Supplement C): p. 190-194.
145. Escobar, J.P., *Pablo Escobar: My Father*. 2016: Ebury Publishing.
146. McDermott, S. and J. Power, *Drug Smuggling Using Clothing Impregnated with Cocaine*. Vol. 50. 2005. 1423-5.
147. Washton, A.M. and J.E. Zweben, *Treating Alcohol and Drug Problems in Psychotherapy Practice: Doing What Works*. 2008: Guilford Press.
148. Anzenbacher, P. and U.M. Zanger, *Metabolism of Drugs and Other Xenobiotics*. 2012: Wiley.
149. Allen, K.R., *Screening for drugs of abuse: which matrix, oral fluid or urine?* 2011. **48**(6): p. 531-541.
150. Greene, S.L., F. Kerr, and G. Braitberg, *Review article: Amphetamines and related drugs of abuse*. Emergency Medicine Australasia, 2008. **20**(5): p. 391-402.
151. WEISS, B. and V.G. LATIES, *ENHANCEMENT OF HUMAN PERFORMANCE BY CAFFEINE AND THE AMPHETAMINES*. 1962. **14**(1): p. 1-36.
152. Heal, D.J., et al., *Amphetamine, past and present – a pharmacological and clinical perspective*. Journal of Psychopharmacology (Oxford, England), 2013. **27**(6): p. 479-496.
153. Bedford, K.R., et al., *The illicit preparation of morphine and heroin from pharmaceutical products containing codeine: 'homebake' laboratories in New Zealand*. Forensic Science International, 1987. **34**(3): p. 197-204.
154. Brady, J., *A simple technique for making very fine, durable dissecting needles by sharpening tungsten wire electrolytically*. Bull World Health Organ, 1965. **32**(1): p. 143-4.
155. Mangos, D.N., T. Nakanishi, and D.A. Lewis, *A simple method for the quantification of molecular decorations on silica particles*. Science and Technology of Advanced Materials, 2014. **15**(1): p. 015002.
156. Yonezawa, T., et al., *Detailed investigation on the possibility of nanoparticles of various metal elements for surface-assisted laser desorption/ionization mass spectrometry*. Anal Sci, 2009. **25**(3): p. 339-46.
157. Agrawal, J.P., *High Energy Materials: Propellants, Explosives and Pyrotechnics*. 2010, Weinheim: Wiley VTC.
158. Heard, B.J., *Handbook of Firearms and Ballistics: Examining and Interpreting Forensic Evidence*. 2008, West Sussex: John Wiley & Sons.

159. Davis, T.L., *The chemistry of powder and explosives*. 1943: Angriff Press.
160. Heramb, R.M., McCord, B. R., *The Manufacture of smokeless powders and their forensic analysis: A brief review*. Forensic Science Communications, 2002. **4**(2).
161. Lindblom, T., *Reactions in the System Nitro-cellulose/ Diphenylamine with Special Reference to the Formation of a Stabilizing Product Bonded to Nitro-cellulose*. 2004: Acta Universitatis Upsaliensis.
162. Thredgold, L., *Development of efficient methodology for the extraction and detection of propellants, stabilizers and their derivatives*, in *School of Chemical and Physical Sciences*. 2010, Flinders University: Adelaide. p. 54.
163. Laza, D., Nys, B., De Kinder, J., Mesmaeker, A. K. D., Moucheron, C., *Development of a quantitative LC-MS/MS method for the analysis of common propellant powder stabilizers in gunshot residue*. Journal of Forensic Sciences, 2007. **52**(4): p. 842-850.
164. Damse, R.S. and A. Singh, *Studies on the high-energy gun propellant formulations based on 1,5-diazido-3-nitrazapentane*. Journal of Hazardous Materials, 2009. **172**(2): p. 1699-1702.
165. Wallace, J.S., *Chemical Analysis of Firearms, Ammunition, and Gunshot Residue*. 2008: CRC Press.
166. Dalby, O., D. Butler, and J.W. Birkett, *Analysis of Gunshot Residue and Associated Materials—A Review*. Journal of Forensic Sciences, 2010. **55**(4): p. 924-943.
167. Bernal Morales, E. and A.L. Revilla Vázquez, *Simultaneous determination of inorganic and organic gunshot residues by capillary electrophoresis*. Journal of Chromatography A, 2004. **1061**(2): p. 225-233.
168. Brożek-Mucha, Z., *Comparison of cartridge case and airborne GSR—a study of the elemental composition and morphology by means of SEM-EDX*. X-Ray Spectrometry, 2007. **36**(6): p. 398-407.
169. S.Basu, *Formation of Gunshot Residues*. Journal of Forensic Sciences, 1982. **27**(1): p. 72-91.
170. J. Andrasko, A.C.M., *Detection of Gunshot Residues on Hands by Scanning Electron Microscopy*. Journal of Forensic Sciences, 1977. **22**(2): p. 279-287.
171. Brozek-Mucha, Z. and A. Jankowicz, *Evaluation of the possibility of differentiation between various types of ammunition by means of GSR examination with SEM-EDX method*. Forensic Science International, 2001. **123**(1): p. 39-47.
172. Schwoeble, A.J. and D.L. Exline, *Current Methods in Forensic Gunshot Residue Analysis*. 2010: Taylor & Francis.
173. Saverio Romolo, F. and P. Margot, *Identification of gunshot residue: a critical review*. Forensic Science International, 2001. **119**(2): p. 195-211.
174. Pun, K.-M. and A. Gallusser, *Macroscopic observation of the morphological characteristics of the ammunition gunpowder*. Forensic Science International, 2008. **175**(2-3): p. 179-185.
175. Speers, S.J., et al., *Evaluation of improved methods for the recovery and detection of organic and inorganic cartridge discharge residues*. Journal of Chromatography A, 1994. **674**(1-2): p. 319-327.
176. Northrop, D.M., *Gunshot Residue Analysis by Micellar Electrokinetic Capillary Electrophoresis: Assessment for Application to Casework. Part I*. Journal of Forensic Sciences, 2001. **46**(3): p. 549-559.
177. Northrop, D.M., *Gunshot Residue Analysis by Micellar Electrokinetic Capillary Electrophoresis: Assessment for Application to Casework. Part II*. Journal of Forensic Sciences, 2001. **46**(3): p. 560-572.
178. Mahoney, C.M., G. Gillen, and A.J. Fahey, *Characterization of gunpowder samples using time-of-flight secondary ion mass spectrometry (TOF-SIMS)*. Forensic Science International, 2006. **158**(1): p. 39-51.
179. Coumbaros, J., et al., *Characterisation of 0.22 caliber rimfire gunshot residues by time-of-flight secondary ion mass spectrometry (TOF-SIMS): a preliminary study*. Forensic Science International, 2001. **119**(1): p. 72-81.

180. Koons, R.D., *Analysis of gunshot primer residue collection swabs by inductively coupled plasma-mass spectrometry*. Journal of Forensic Sciences, 1998. **43**(4): p. 748-754.
181. R. D. Koons, D.G.H., C. A. Peters, *Determination of barium in gunshot residue collection swabs using inductively coupled plasma-atomic emission spectrometry*. Journal of Forensic Sciences, 1988. **33**(1): p. 35-41.
182. Zeichner, A., et al., *Application of lead isotope analysis in shooting incident investigations*. Forensic Science International, 2006. **158**(1): p. 52-64.
183. Steffen, S., et al., *Chemometric classification of gunshot residues based on energy dispersive X-ray microanalysis and inductively coupled plasma analysis with mass-spectrometric detection*. Spectrochimica Acta Part B: Atomic Spectroscopy, 2007. **62**(9): p. 1028-1036.
184. Krishnan, S.S., *Firing distance determination by atomic absorption spectrophotometry*. Journal of Forensic Sciences, 1974. **19**(2): p. 351-356.
185. Ravreby, M., *Analysis of long-range bullet entrance holes by atomic absorption spectrophotometry and scanning electron microscopy*. J Forensic Sci, 1982. **27**(1): p. 92-112.
186. Reed, G.E., P.J. McGuire, and A. Boehm, *Analysis of gunshot residue test results in 112 suicides*. J Forensic Sci, 1990. **35**(1): p. 62-8.
187. Rudzitis, E. and M. Wahlgren, *Firearm residue detection by instrumental neutron activation analysis*. J Forensic Sci, 1975. **20**(1): p. 119-24.
188. K. K. S. Pillay, W.A.J., H. A. Fox, *New method for the collection and analysis of gunshot residues as forensic evidence*. Journal of Forensic Sciences, 1974. **19**(1): p. 768-783.
189. Capannesi, G. and A.F. Sedda, *Bullet identification: a case of a fatal hunting accident resolved by comparison of lead shot using instrumental neutron activation analysis*. J Forensic Sci, 1992. **37**(2): p. 657-62.
190. Xu, X., A.M. van de Craats, and P.C. de Bruyn, *Highly sensitive screening method for nitroaromatic, nitramine and nitrate ester explosives by high performance liquid chromatography-atmospheric pressure ionization-mass spectrometry (HPLC-API-MS) in forensic applications*. J Forensic Sci, 2004. **49**(6): p. 1171-80.
191. Zeichner, A., et al., *Vacuum collection of gunpowder residues from clothing worn by shooting suspects, and their analysis by GC/TEA, IMS, and GC/MS*. J Forensic Sci, 2003. **48**(5): p. 961-72.
192. Zeichner, A. and B. Eldar, *A novel method for extraction and analysis of gunpowder residues on double-side adhesive coated stubs*. J Forensic Sci, 2004. **49**(6): p. 1194-206.
193. Espinoza, E.O.N. and J.I.J.A.c.a. Thornton, *Characterization of smokeless gunpowder by means of diphenylamine stabilizer and its nitrated derivatives*. 1994. **288**(1-2): p. 57-69.
194. Hopper, K.G. and B.R. McCord, *A comparison of smokeless powders and mixtures by capillary zone electrophoresis*. J Forensic Sci, 2005. **50**(2): p. 307-15.
195. Xie, J., et al., *Extraction and derivatization in single drop coupled to MALDI-FTICR-MS for selective determination of small molecule aldehydes in single puff smoke*. Analytica Chimica Acta, 2009. **638**(2): p. 198-201.
196. Jackson, S.N., S.M. Dutta, and K.K. Murray, *A nitrocellulose matrix for infrared matrix-assisted laser desorption/ionization of polycyclic aromatic hydrocarbons*. Rapid Communications in Mass Spectrometry, 2004. **18**(2): p. 228-230.
197. Liu, Y.H., et al., *Use of a nitrocellulose film substrate in matrix-assisted laser desorption/ionization mass spectrometry for DNA mapping and screening*. Anal Chem, 1995. **67**(19): p. 3482-90.
198. Luque-Garcia, J.L., et al., *Use of Nitrocellulose Membranes for Protein Characterization by Matrix-Assisted Laser Desorption/Ionization Mass Spectrometry*. Analytical Chemistry, 2006. **78**(14): p. 5102-5108.
199. Picariello, G., R. Romano, and F. Addeo, *Nitrocellulose Film Substrate Minimizes Fragmentation in Matrix-Assisted Laser Desorption Ionization Time-of-Flight Mass Spectrometry Analysis of Triacylglycerols*. Analytical Chemistry, 2010. **82**(13): p. 5783-5791.

200. Lennert, E. and C. Bridge, *Analysis and classification of smokeless powders by GC–MS and DART-TOFMS*. Forensic Science International, 2018. **292**: p. 11-22.
201. Perez, J.J., et al., *Classification of Smokeless Powders Using Laser Electrospray Mass Spectrometry and Offline Multivariate Statistical Analysis*. Analytical Chemistry, 2013. **85**(1): p. 296-302.
202. Wood, J.L., *Far-infrared spectroscopy*. Quarterly Reviews, Chemical Society, 1963. **17**(4): p. 362-381.
203. Smith, B.C., *Fundamentals of Fourier Transform Infrared Spectroscopy*. 2011: CRC Press.
204. *Infrared Spectroscopy*, in Kirk-Othmer Encyclopedia of Chemical Technology.
205. Oberg, K.A. and A.L. Fink, *A New Attenuated Total Reflectance Fourier Transform Infrared Spectroscopy Method for the Study of Proteins in Solution*. Analytical Biochemistry, 1998. **256**(1): p. 92-106.
206. Lindon, J.C., G.E. Tranter, and D. Koppenaal, *Encyclopedia of Spectroscopy and Spectrometry*. 2016: Elsevier Science.
207. Schuttlefield, J.D. and V.H. Grassian, *ATR–FTIR Spectroscopy in the Undergraduate Chemistry Laboratory. Part I: Fundamentals and Examples*. Journal of Chemical Education, 2008. **85**(2): p. 279.
208. Government, A.A. *The Australian Synchrotron*. 2018 25/09/2018]; Available from: [www.synchrotron.org.au](http://www.synchrotron.org.au).
209. Chen, Y., et al. *Spectroscopic characterization of explosives in the far-infrared region*. in *Defense and Security*. 2004. SPIE.
210. Fan, W.H., et al., *Far-Infrared Spectroscopic Characterization of Explosives for Security Applications Using Broadband Terahertz Time-Domain Spectroscopy*. 2007. **61**(6): p. 638-643.
211. Barber, J., et al., *Temperature-Dependent Far-Infrared Spectra of Single Crystals of High Explosives Using Terahertz Time-Domain Spectroscopy*. The Journal of Physical Chemistry A, 2005. **109**(15): p. 3501-3505.
212. Lo, T., et al., *The very far-infrared spectra of energetic materials and possible confusion materials using terahertz pulsed spectroscopy*. Vibrational Spectroscopy, 2006. **42**(2): p. 243-248.
213. Chalmers, J.M., H.G.M. Edwards, and M.D. Hargreaves, *Infrared and Raman Spectroscopy in Forensic Science*. 2012: Wiley.
214. Warlow, T., *Firearms, the Law, and Forensic Ballistics, Third Edition*. 2016: CRC Press.
215. Woodbridge, R.G., *The relation of cotton to explosives*. Journal of Chemical Education, 1930. **7**(8): p. 1832.
216. Winchester. *Winchester Smokeless Powders*. 27/09/2018]; Available from: <https://wwpowder.com/760-2/>.
217. Powder, A. *Alliant Powder - Safety Data Sheets*. 2018 27/09/2018]; Available from: <https://www.alliantpowder.com/resources/sds.aspx>.
218. Croft, S.A., Q.U.o.T.S.o. Physical, and C. Sciences, *The Analysis of Unfired Propellant Particles by Gas Chromatography-mass Spectrometry: A Forensic Approach*. 2008: Queensland University of Technology, Brisbane.
219. Muller, D., et al., *A Novel Method for the Analysis of Discharged Smokeless Powder Residues*. Journal of Forensic Sciences, 2007. **52**(1): p. 75-78.
220. Fryš, O., et al., *Method validation for the determination of propellant components by Soxhlet extraction and gas chromatography/mass spectrometry*. Journal of Separation Science, 2011. **34**(18): p. 2405-2410.
221. Grodzinski, J., *New Method for Determining Phthalate Esters in Propellants*. Analytical Chemistry, 1955. **27**(11): p. 1765-1767.
222. Wypych, G., *Handbook of Plasticizers*. 2004: ChemTec Publishing.